SUPPORTING INFORMATION

# Tuning the Electronic Properties of Homoleptic Silver(I) bis-BIAN Complexes Towards Efficient Electrocatalytic $CO_2$ Reduction

Dominik Krisch[1], He Sun[1], Kevinjeorjios Pellumbi[2,3], Kirill Faust[4], Ulf-Peter Apfel[2,3] and Wolfgang Schöfberger[1,*]

[1] *Institute of Organic Chemistry, Johannes Kepler University Linz, Altenberger Straße 69, 4040 Linz, Austria.*

[2] *Inorganic Chemistry I – Bioinorganic Chemistry, Ruhr University Bochum, Universitätsstraße 150, 44801 Bochum, Germany*

[3] *Department of Electrosynthesis, Fraunhofer Institute for Environmental, Energy and Safety Technology UMSICHT, Osterfelder Straße 3, 46047 Oberhausen, Germany*

[4] *Institute of Catalysis (INCA), Johannes Kepler University Linz, Altenberger Straße 69, 4040 Linz, Austria.*

## Content

## Synthesis

### Materials and Methods

All chemicals were purchased from Alfa Aesar, Strem, BLDpharm, Merck or Sigma-Aldrich and used without further purification unless otherwise noted. Anhydrous DCM, THF and ACN were obtained from a molar sieve MB-SPS-7, M. Braun inert gas-System GmbH (Garching, Germany) under argon atmosphere. All deuterated NMR solvents were purchased from Euriso-Top. Proton ($^{1}$H NMR), Carbon ($^{13}$C NMR) and Fluorine ($^{19}$F NMR) spectra were recorded on a Bruker DRX 500 MHz spectrometer equipped with a cryoprobe (TXI) and on a Bruker Advance 300 MHz NMR spectrometer. The chemical shifts are given in parts per million (ppm) on the delta scale (δ) and are referenced to the used deuterated solvent for $^{1}$H NMR and $^{13}$C NMR. High resolution mass spectra were obtained utilizing an Agilent 6520 Q-TOF mass spectrometer with an ESI source and an Agilent G1607A coaxial sprayer. UV-Vis absorption spectra were collected on a Varian CARY 300 Bio spectrophotometer from 200 to 900 nm. IR spectra were recorded on a Bruker ALPHA II FT IR instrument.

### Synthetic Procedures

*General procedure for the preparation of BIAN ligands*

BIAN ligands **L1**-**L4** and **L6** were synthesized *via* the methodology established by the group of Ragaini with modified workup procedures for **L3** and **L6** as described below [40]. In general, acenaphthenequinone and zinc(II) chloride (2.7 equiv.) were stirred in acetic acid (and toluene for **L1** and **L6**) at 80 °C under argon for 30 min. Subsequently, 2.2 equiv. of the respective aniline were added and the mixtures refluxed for 15 (**L2**, **L4**), 30 (**L3**) or 45 min (**L1**, **L6**) leading to the formation of BIAN ligated zinc(II) dichloride precipitate, which was collected *via* suction filtration. The residues were washed with cold HOAc and $Et_2O$ before being extracted with DCM and saturated aqueous potassium oxalate solution. Finally, the organic layers were dried over $Na_2SO_4$ and concentrated *in vacuo* to obtain the free BIAN ligands in yields comparable to the literature.

*1-Pyrene-BIAN (**L3**)*

According to the literature procedure [40] but with an adapted workup: Subsequently to extraction with aq. $K_2C_2O_4$ and evaporation, the dark residue was triturated with *n*-heptane/ethyl acetate (3:1) thrice to remove residual 1-aminopyrene. The solid was collected *via* suction filtration, washed with *n*-heptane/ethyl acetate (3:1) and dried *in vacuo* to obtain 1-pyrene-BIAN **L3** as dark red-purple powder in 68% yield (2.66 mmol, 1.54 g).

*4-Diethylamino-BIAN (**L6**)*

According to the literature procedure [40] but with an adapted workup: Subsequently to refluxing the reaction mixture in HOAc/toluene for 45 min it was cooled in a refrigerator for 1 h. The solution was decanted and the dark sticky residue triturated with $Et_2O$ and filtered five times. Afterwards it was dissolved in MeOH (blue color) and extracted with DCM and saturated aqueous $K_2C_2O_4$. The now purple organic phase was dried over $Na_2SO_4$, filtered and concentrated *in vacuo* to obtain 4-diethylamino-BIAN **L6** as dark purple solid in 66% yield (5.17 mmol, 2.46 g).

*3,4,5-Trimethoxy-BIAN (**L5**)*

Synthesized in analogy to a reported procedure [41] with modified workup: 3,5-bis-$CF_3$-BIAN zinc(II) dichloride complex (1.20 g, 1.58 mmol) was dissolved in 80 mL MeOH, 3,4,5-trimethoxyaniline (868 mg, 4.74 mmol, 3 eq.) added and the solution stirred at rt overnight, during which it turned from orange to red. Subsequently, the reaction mixture was evaporated to dryness, and the residue taken up in DCM and extracted with saturated aqueous $K_2C_2O_4$ solution. After concentration *in vacuo* the oily residue was triturated with *n*-heptane, the remaining solid dissolved in DCM, extracted five times with 0.1M HCl and finally washed with water. Afterwards it was dried over $Na_2SO_4$, filtered and concentrated *in vacuo* to obtain 3,4,5-trimethoxy-BIAN **L5** as red solid in 66% yield (1.04 mmol, 531 mg).

*General procedure for the preparation of $[Ag(I)(BIAN)_2]BF_4$ complexes **Ag1**-**Ag6***

Ag(I) bis-BIAN complexes were prepared in analogy to a literature procedure, where **Ag2** has been reported [39]. DCM solutions (10 mL) of $[Ag(I)(ACN)_4]BF_4$ (0.2 mmol) were treated with dropwise addition of BIAN ligand (0.4 mmol, 2 equiv.) in 20 mL DCM, leading to immediate color changes. The mixtures were stirred at room temperature under argon in the dark overnight, before the reaction volumes were reduced to ca. 5 mL under reduced pressure. Subsequently, *n*-pentane was added, the resulting

suspensions cooled for 1 h and the precipitated solids collected *via* suction filtration. After washing the residues with *n*-pentane they were dried *in vacuo* to obtain **Ag1**-**Ag6** as orange (**Ag1**, **Ag2**), red (**Ag4**, **Ag5**) or purple (**Ag3**, **Ag6**) powders in 85-98% yield (see Scheme 1).

**Characterization**

**L1.** $N^1$,$N^2$-bis(3,5-bis(trifluoromethyl)phenyl)acenaphthylene-1,2-diimine (3,5-bis-$CF_3$-BIAN) was synthesized according to the general procedure for the preparation of BIAN ligands and obtained as yellow solid.

$^1$H NMR (300 MHz, $CDCl_3$, 25 °C) δ / ppm: 6.87 (d, *J* = 7.2 Hz, 2 H, ArH), 7.50 (t, *J* = 7.8 Hz, 2 H, ArH), 7.62 (s, 4 H, ArH), 7.81 (s, 2 H, ArH), 8.04 (d, *J* = 8.2 Hz, 2 H, ArH)

$^{13}$C NMR (126 MHz, $CDCl_3$, 25 °C) δ / ppm: 118.5, 119.0 124.1, 127.6, 128.3, 130.6, 131.7, 133.3 (q, *J* = 33.7 Hz), 142.6, 152.4, 162.5

$^{19}$F NMR (470 MHz, $CDCl_3$, 25 °C) δ / ppm: -62.93 ($CF_3$)

UV-vis (ACN) $\lambda_{max}$ nm (log $\varepsilon$): 201 (4.65), 226 (4.71), 297 (3.95), 308 (3.95)

IR (25 °C) $\nu$ / $cm^{-1}$: 3100, 1669, 1649 1616, 1601, 1591, 1457, 1420, 1369, 1278, 1227, 1165, 1122, 1099, 1048, 1021, 999, 955, 917, 904, 881, 846, 831, 778, 725, 702, 681, 641, 603, 533, 513, 455, 440, 405

**L2.** $N^1$,$N^2$-bis(2,6-diisopropylphenyl)acenaphthylene-1,2-diimine (2,6-dipp-BIAN) was synthesized according to the general procedure for the preparation of BIAN ligands and obtained as orange solid.

$^1$H NMR (300 MHz, $CDCl_3$, 25 °C) δ / ppm: 0.97 (d, *J* = 6.9 Hz, 12 H, $CH_3$), 1.23 (d, *J* = 6.9 Hz, 12 H, $CH_3$), 3.03 (hept, *J* = 6.9 Hz, 4 H, CH), 6.63 (d, *J* = 7.2 Hz, 2 H, ArH), 7.21 – 7.30 (overlapping m, 6 H, ArH), 7.36 (t, *J* = 7.8 Hz, 2 H, ArH), 7.87 (d, *J* = 8.3 Hz, 2 H, ArH)

$^{13}$C NMR (75 MHz, $CDCl_3$, 25 °C) δ / ppm: 23.3, 23.6 28.8, 123.5, 123.6, 124.4, 128.0, 129.0, 129.7, 131.3, 135.6, 147.6, 161.1

UV-vis (ACN) $\lambda_{max}$ nm (log $\varepsilon$): 204 (4.99), 229 (4.97), 272 (3.94), 308 (3.93), 409 (2.96)

IR (25 °C) $\nu$ / $cm^{-1}$: 3065, 2960, 2927, 2867, 1667, 1653, 1641, 1591, 1487, 1465, 1455, 1428, 1383, 1362, 1347, 1325, 1274, 1249, 1223, 1192, 1180, 1159, 1115, 1089, 1060, 1043, 939, 924, 836, 809, 786, 749, 704, 659, 607, 593, 533, 464

**L3.** $N^1$,$N^2$-di(pyren-1-yl)acenaphthylene-1,2-diimine (1-pyrene-BIAN) was synthesized according to the respective modified procedure for the preparation of BIAN ligands and obtained as purple solid in 68% yield.

$^1$H NMR (500 MHz, $CDCl_3$, 25 °C) δ / ppm: 6.46 (d, $J$ = 7.4 Hz, 2 H, ArH), 7.11 (t, $J$ = 7.8 Hz, 2 H, ArH), 7.78 (d, $J$ = 8.3 Hz, 2 H, ArH), 7.90 (d, $J$ = 8.0 Hz, 2 H, ArH), 8.01 – 8.11 (m, 6 H, ArH), 8.16 (d, $J$ = 8.7 Hz, 4 H, ArH), 8.22 (d, $J$ = 7.5 Hz, 2 H, ArH), 8.33 (d, $J$ = 8.0 Hz, 2 H, ArH), 8.36 (d, $J$ = 9.1 Hz, 2 H, ArH)

$^{13}$C NMR (126 MHz, $CDCl_3$, 25 °C) δ / ppm: 116.2, 120.5, 123.3, 124.0, 125.0, 125.1, 125.4, 125.9, 126.4, 126.5, 127.3, 127.7, 127.9, 128.8, 128.9, 129.3, 131.3, 131.8, 142.1, 146.3, 162.5

UV-vis (DCM) $\lambda_{max}$ nm (log $\varepsilon$): 245 (5.28), 270 (4.92), 280 (4.97), 348 (4.91), 384 (4.35), 484 (4.04)

IR (25 °C) $\nu$ / cm$^{-1}$: 3040, 1731, 1665, 1632, 1593, 1499, 1486, 1460, 1431, 1392, 1357, 1325, 1280, 1245, 1231, 1212, 1177, 1150, 1136, 1103, 1072, 1056, 1029, 963, 949, 927, 899, 885, 838, 827, 791, 774, 766, 735, 721, 712, 679, 642, 619, 601, 581, 566, 544, 527, 512, 482, 461, 449, 414, 408

HRMS (ESI) $m/z$ calcd for $C_{44}H_{24}N_2$+H$^+$: 581.2012 [$M$+H]$^+$; found: 581.2011

**L4.** $N^1$,$N^2$-bis(4-methoxyphenyl)acenaphthylene-1,2-diimine (4-OMe-BIAN) was synthesized according to the general procedure for the preparation of BIAN ligands and obtained as red solid.

$^1$H NMR (300 MHz, $CDCl_3$, 25 °C) δ / ppm: 3.90 (s, 6 H, $CH_3$), 7.00 – 7.04 (m, 6 H, ArH), 7.08 – 7.11 (m, 4 H, ArH), 7.39 (dd, $J_1$ = 7.3 Hz, $J_2$ = 8.2 Hz, 2 H, ArH), 7.89 (d, $J$ = 8.2 Hz, 2 H, ArH)

$^{13}$C NMR (75 MHz, $CDCl_3$, 25 °C) δ / ppm: 55.6, 114.8, 119.9, 123.8, 127.7, 128.9, 129.0, 131.4, 145.1, 157.0, 161.7

UV-vis (ACN) $\lambda_{max}$ nm (log $\varepsilon$): 212 (4.64), 229 (4.83), 291 (4.08), 424 (3.63)

IR (25 °C) $\nu$ / cm$^{-1}$: 3043, 3033, 3003, 2972, 2949, 2939, 2913, 2840, 1642, 1599, 1579, 1499, 1484, 1463, 1441, 1434, 1414, 1286, 1272, 1231, 1178, 1165, 1108, 1088, 1028, 926, 833, 811, 786, 743, 718, 586, 544, 529, 502, 467, 418

**L5.** $N^1$,$N^2$-bis(3,4,5-trimethoxyphenyl)acenaphthylene-1,2-diimine (3,4,5-trimethoxy-BIAN) was synthesized according to the procedure for the preparation of BIAN ligand **L5** and obtained as red solid in 66% yield.

$^1$H NMR (300 MHz, $CDCl_3$, 25 °C) δ / ppm: 3.83 (s, 12 H, $CH_3$), 3.94 (s, 6 H, $CH_3$), 6.38 (s, 4 H, ArH), 7.09 (d, *J* = 7.2 Hz, 2 H, ArH), 7.45 (t, *J* = 7.8 Hz, 2 H, ArH), 7.94 (d, *J* = 8.3 Hz, 2 H, ArH)

$^{13}$C NMR (126 MHz, $CDCl_3$, 25 °C) δ / ppm: 56.3, 61.4, 95.5, 124.4, 128.0, 128.3, 129.3, 131.4, 134.8, 142.0, 147.9, 154.3, 161.9

UV-vis (ACN) $\lambda_{max}$ nm (log $\varepsilon$): 208 (4.91), 228 (4.94), 300 (3.94), 429 (3.43)

IR (25 °C) *v* / cm$^{-1}$: 3050, 3011, 2996, 2970, 2951, 2923, 2868, 2838, 1730, 1671, 1647, 1584, 1501, 1467, 1449, 1431, 1412, 1336, 1278, 1228, 1179, 1124, 1044, 1017, 1004, 988, 840, 819, 791, 774, 745, 729, 694, 685, 667, 648, 628, 611, 570, 545, 527, 495, 475, 465, 441, 428

HRMS (ESI) *m*/*z* calcd for $C_{30}H_{28}N_2O_6$+$H^+$: 513.2026 [*M*+H]$^+$; found: 513.2022

**L6.** $N^1$,$N^2$-bis(4-(*N*,*N*-diethylamino)phenyl)acenaphthylene-1,2-diimine (4-diethyl-amino-BIAN) was synthesized according to the respective modified procedure for the preparation of BIAN ligands and obtained as purple solid in 66% yield.

$^1$H NMR (500 MHz, $CDCl_3$, 25 °C) δ / ppm: 1.23 (t, *J* = 7.0 Hz, 12 H, $CH_3$), 3.42 (q, *J* = 7.0 Hz, 8 H, $CH_2$), 6.79 (d, *J* = 8.8 Hz, 4 H, ArH), 7.11 (d, *J* = 8.8 Hz, 4 H, ArH), 7.35 – 7.41 (m, 4 H, ArH), 7.85 (d, *J* = 7.8 Hz, 2 H, ArH)

$^{13}$C NMR (126 MHz, $CDCl_3$, 25 °C) δ / ppm: 12.8, 44.7, 112.8, 121.1, 123.2, 127.5, 128.4, 129.5, 131.4, 140.8, 141.4, 145.9, 160.5

UV-vis (ACN) $\lambda_{max}$ nm (log $\varepsilon$): 208 (4.82), 229 (4.88), 265 (4.63), 306 (4.27), 317 (4.25), 517 (4.09)

IR (25 °C) *v* / cm$^{-1}$: 3040, 2970, 2931, 2871, 1722, 1651, 1599, 1505, 1488, 1467, 1447, 1417, 1398, 1375, 1352, 1262, 1239, 1186, 1180, 1142, 1118, 1091, 1070, 1041, 1012, 932, 916, 829, 807, 782, 774, 727, 696, 685, 673, 657, 599, 581, 529, 519, 494, 486, 428, 418, 406

HRMS (ESI) *m*/*z* calcd for $C_{32}H_{34}N_4$+$H^+$: 475.2856 [*M*+H]$^+$; found: 475.2856

**Ag1.** [Ag(3,5-bis-$CF_3$-BIAN)$_2$]$BF_4$ was synthesized according to the general procedure for the preparation of [Ag(I)(BIAN)$_2$]$BF_4$ complexes and obtained as bright orange solid in 98% yield.

$^1$H NMR (500 MHz, DMSO-d6, 25 °C) δ / ppm: 6.84 (d, *J* = 7.2 Hz, 4 H, ArH), 7.87 (t, *J* = 8.0 Hz, 2 H, ArH), 7.79 (s, 8 H, ArH), 8.07 (s, 4 H, ArH), 8.29 (d, *J* = 8.2 Hz, 4 H, ArH)

$^{13}$C NMR (126 MHz, DMSO-d6, 25 °C) δ / ppm: 119.1, 120.3, 124.2, 126.9, 128.6, 129.8, 131.8 (q, *J* = 33.2 Hz), 141.8, 151.2, 162.2

$^{19}$F NMR (470 MHz, DMSO-d6, 25 °C) δ / ppm: -61.85 ($CF_3$), -148.23 ($^{10}BF_4^-$), -148.28 ($^{11}BF_4^-$)

UV-vis (THF) $\lambda_{max}$ nm (log $\varepsilon$): 229 (5.35), 297 (4.58)

IR (25 °C) $\nu$ / cm$^{-1}$: 3081, 1686, 1655, 1603, 1492, 1461, 1435, 1422, 1371, 1278, 1169, 1122, 1105, 1093, 1046, 1033, 998, 963, 928, 910, 889, 862, 846, 830, 776, 727, 703, 683, 644, 611, 594, 577, 537, 516, 468, 441, 412

HRMS (ESI) *m*/*z* calcd for $C_{56}H_{24}AgF_{24}N_4^+$: 1315.0669 [*M*-$BF_4^-$]$^+$; found: 1315.0667

**Ag2.** [Ag(2,6-dipp-BIAN)$_2$]$BF_4$ was synthesized according to the general procedure for the preparation of [Ag(I)(BIAN)$_2$]$BF_4$ complexes and obtained as orange solid in 90% yield.

$^1$H NMR (500 MHz, $CDCl_3$, 0 °C) δ / ppm: 0.33 (d, *J* = 4.8 Hz, 12 H, $CH_3$), 0.54 (d, *J* = 4.9 Hz, 12 H, $CH_3$), 0.92 (d, *J* = 4.9 Hz, 12 H, $CH_3$), 1.37 (d, *J* = 4.8 Hz, 12 H, $CH_3$), 2.42 (bs, 4 H, CH), 3.14 (bs, 4 H, CH), 5.93 (d, *J* = 7.5 Hz, 4 H, ArH), 7.17 (bs, 4 H, ArH), 7.39 (t, *J* = 7.9 Hz, 12 H, ArH), 8.05 (d, *J* = 8.3 Hz, 4 H, ArH)

$^{13}$C NMR (126 MHz, $CDCl_3$, 0 °C) δ / ppm: 22.5, 23.0, 23.6, 24.5, 29.0, 29.7, 125.0, 125.4, 125.9, 127.5, 128.7, 130.8, 131.9, 136.9, 137.1, 141.4, 145.6, 164.3

UV-vis (ACN) $\lambda_{max}$ nm (log $\varepsilon$): 204 (5.20), 229 (5.19), 308 (4.23), 412 (3.30)

IR (25 °C) $\nu$ / cm$^{-1}$: 3063, 2962, 2927, 2868, 1655, 1620, 1585, 1490, 1463, 1434, 1423, 1386, 1363, 1342, 1319, 1283, 1255, 1225, 1189, 1163, 1151, 1058, 940, 836, 799, 780, 759, 735, 714, 607, 583, 539, 519, 467, 447, 424, 403

HRMS (ESI) *m*/*z* calcd for $C_{72}H_{80}AgN_4^+$: 1107.5434 [*M*-$BF_4^-$]$^+$; found: 1107.5434

**Ag3.** [Ag(1-pyrene-BIAN)$_2$]$BF_4$ was synthesized according to the general procedure for the preparation of [Ag(I)(BIAN)$_2$]$BF_4$ complexes and obtained as dark purple solid in 97% yield.

$^1$H NMR (500 MHz, $CD_3CN$, 25 °C) δ / ppm: 5.85 (d, *J* = 7.4 Hz, 4 H, ArH), 6.89 (t, *J* = 7.9 Hz, 4 H, ArH), 7.51 – 7.59 (m, 16 H, ArH), 7.72 – 7.77 (m, 8 H, ArH), 7.87 (t, *J* = 7.5 Hz, 4 H, ArH), 7.93 – 7.97 (m, 4 H, ArH), 8.05 (d, *J* = 7.6 Hz, 4 H, ArH)

$^{13}$C NMR (126 MHz, $CD_3CN$, 25 °C) δ / ppm: 116.2, 119.9, 121.3, 123.9, 124.3, 124.5, 124.8, 125.2, 125.4, 126.2, 126.6, 126.8, 127.2, 127.7, 128.1, 129.0, 130.5, 130.8, 131.1, 142.0, 143.3, 162.6

UV-vis (ACN) $\lambda_{max}$ nm (log $\varepsilon$): 239 (5.35), 269 (5.02), 279 (5.06), 347 (5.01), 383 (4.45), 474 (4.11)

IR (25 °C) *v* / cm$^{-1}$: 3041, 1662, 1624, 1587, 1503, 1486, 1461, 1433, 1420, 1363, 1326, 1279, 1249, 1213, 1184, 1156, 1138, 1188, 1046, 1034, 972, 941, 895, 840, 830, 790, 774, 755, 727, 712, 692, 677, 652, 642, 585, 578, 552, 529, 519, 482, 465, 447, 418, 405

HRMS (ESI) *m*/*z* calcd for $C_{88}H_{48}AgN_4^+$: 1267.2930 [*M*-$BF_4^-$]$^+$; found: 1267.2929

**Ag4.** [Ag(4-OMe-BIAN)$_2$]$BF_4$ was synthesized according to the general procedure for the preparation of [Ag(I)(BIAN)$_2$]$BF_4$ complexes and obtained as red solid in 93% yield.

$^1$H NMR (500 MHz, $CDCl_3$, 25 °C) δ / ppm: 3.90 (s, 12 H, $CH_3$), 7.04 (d, *J* = 8.9 Hz, 8 H, ArH), 7.18 (d, *J* = 8.9 Hz, 8 H, ArH), 7.27 (d, overlapping, *J* = 8.0 Hz, 4 H, ArH) 7.50 (t, *J* = 8.0 Hz, 8 H, ArH), 8.03 (d, *J* = 8.2 Hz, 4 H, ArH)

$^{13}$C NMR (126 MHz, $CDCl_3$, 25 °C) δ / ppm: 55.9, 115.2, 121.6, 125.0, 127.2, 128.3, 131.0, 131.2, 141.8, 142.5, 158.7, 161.4

UV-vis (ACN) $\lambda_{max}$ nm (log $\varepsilon$): 212 (4.92), 229 (5.12), 292 (4.36), 422 (3.88)

IR (25 °C) *v* / cm$^{-1}$: 3061, 3005, 2962, 2942, 2913, 2839, 1660, 1619, 1597, 1584, 1501, 1464, 1441, 1420, 1359, 1295, 1278, 1242, 1209, 1180, 1169, 1150, 1105, 1051,

1023, 947, 932, 856, 830, 778, 721, 655, 640, 632, 611, 596, 562, 537, 519, 492, 465, 412

HRMS (ESI) *m*/*z* calcd for $C_{52}H_{40}AgN_4O_4^+$: 891.2100 [*M*-$BF_4^-$]$^+$; found: 891.2096

**Ag5.** [Ag(3,4,5-trimethoxy-BIAN)$_2$]$BF_4$ was synthesized according to the general procedure for the preparation of [Ag(I)(BIAN)$_2$]$BF_4$ complexes and obtained as dark red solid in 91% yield.

$^1$H NMR (500 MHz, $CDCl_3$, 25 °C) δ / ppm: 3.74 (s, 24 H, $CH_3$), 3.96 (s, 12 H, $CH_3$), 6.42 (s, 8 H, ArH), 6.90 (d, *J* = 5.1 Hz, 4 H, ArH), 7.46 (t, *J* = 7.8 Hz, 4 H, ArH), 8.00 (d, *J* = 8.2 Hz, 4 H, ArH)

$^{13}$C NMR (126 MHz, $CDCl_3$, 25 °C) δ / ppm: 56.3, 61.2, 96.2, 125.3, 127.2, 128.4, 130.8, 131.2, 135.8, 142.4, 146.1, 154.3, 162.5

UV-vis (ACN) $\lambda_{max}$ nm (log $\varepsilon$): 207 (5.12), 228 (5.17), 300 (4.22), 429 (3.72)

IR (25 °C) *v* / cm$^{-1}$: 3067, 2938, 2834, 1725, 1661, 1621, 1584, 1496, 1453, 1429, 1414, 1373, 1334, 1278, 1229, 1180, 1122, 1101, 1048, 1035, 988, 922, 897, 830, 775, 703, 682, 638, 626, 606, 580, 523, 479, 449, 404

HRMS (ESI) *m*/*z* calcd for $C_{60}H_{56}AgN_4O_{12}^+$: 1131.2945 [*M*-$BF_4^-$]$^+$; found: 1131.2948

**Ag6.** [Ag(4-diethylamino-BIAN)$_2$]$BF_4$ was synthesized according to the general procedure for the preparation of [Ag(I)(BIAN)$_2$]$BF_4$ complexes and obtained as dark purple solid in 85% yield.

$^1$H NMR (500 MHz, $CDCl_3$, 25 °C) δ / ppm: 1.22 (t, *J* = 7.0 Hz, 24 H, $CH_3$), 3.45 (bd, *J* = 7.0 Hz, 16 H, $CH_2$), 6.73 (bs, 8 H, ArH), 7.13 (d, *J* = 8.8 Hz, 8 H, ArH), 7.53 (t, *J* = 7.8 Hz, 4 H, ArH), 7.76 (bs, 4 H, ArH), 8.02 (d, *J* = 8.3 Hz, 4 H, ArH)

$^{13}$C NMR (126 MHz, $CDCl_3$, 25 °C) δ / ppm: 12.6, 45.2, 112.3, 123.5, 123.8, 128.1, 130.3, 131.2, 137.1, 141.5, 146.8, 158.3

UV-vis (ACN) $\lambda_{max}$ nm (log $\varepsilon$): 206 (5.05), 230 (5.09), 268 (4.86), 308 (4.51), 537 (4.38)

IR (25 °C) $\nu$ / $cm^{-1}$: 3069, 2968, 2929, 2894, 2869, 1593, 1507, 1470, 1452, 1431, 1401, 1378, 1350, 1264, 1179, 1146, 1091, 1044, 1008, 939, 814, 798, 774, 751, 722, 698, 680, 650, 632, 609, 589, 519, 482, 458, 449, 402

HRMS (ESI) *m*/*z* calcd for $C_{64}H_{68}AgN_8^+$: 1055.4618 [*M*-$BF_4^-$]$^+$; found: 1055.4618

# Spectral data BIAN ligands

## 3,5-bis-$CF_3$-BIAN (L1)

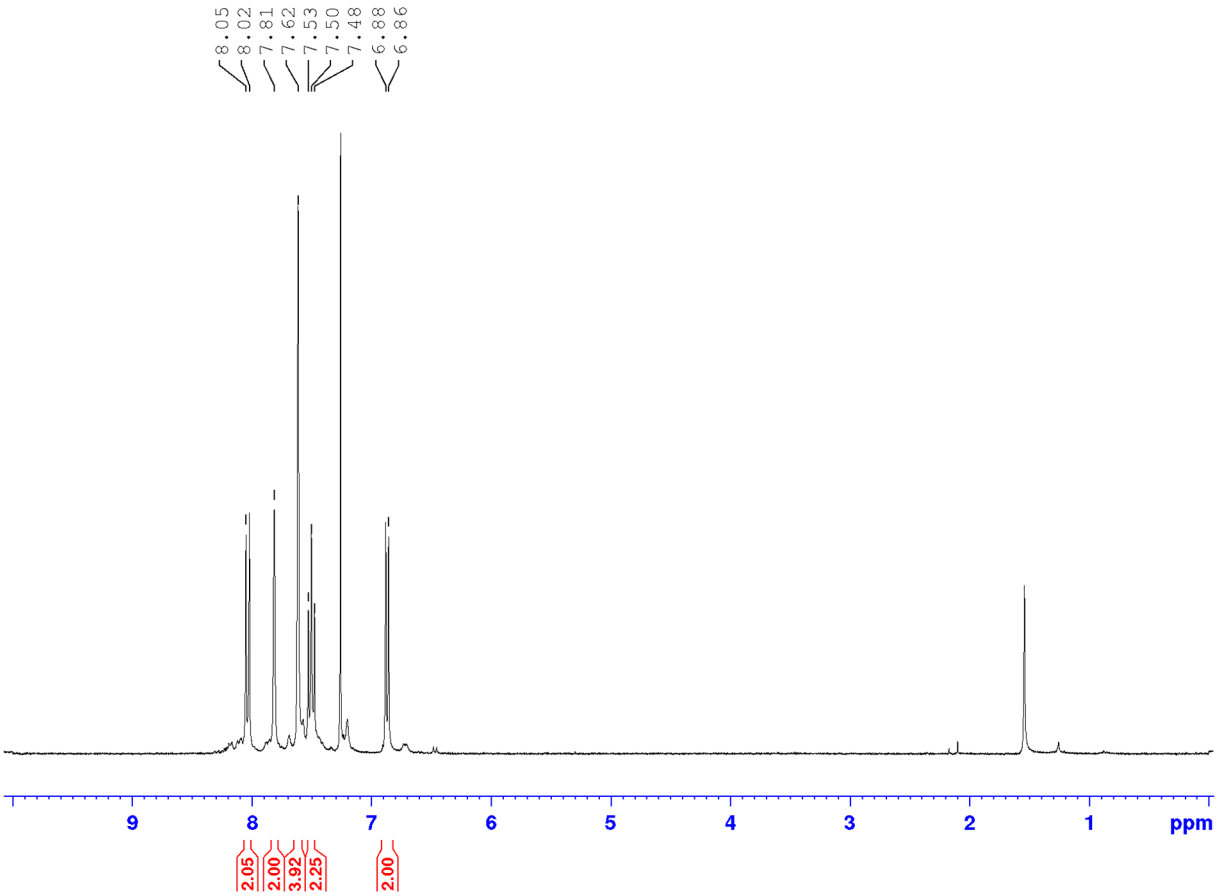


**Figure S1**: $^1$H NMR (300 MHz, $CDCl_3$, 25 °C) of $N^1$,$N^2$-bis(3,5-bis(trifluoromethyl)phenyl) acenaphthylene-1,2-diimine **L1**.

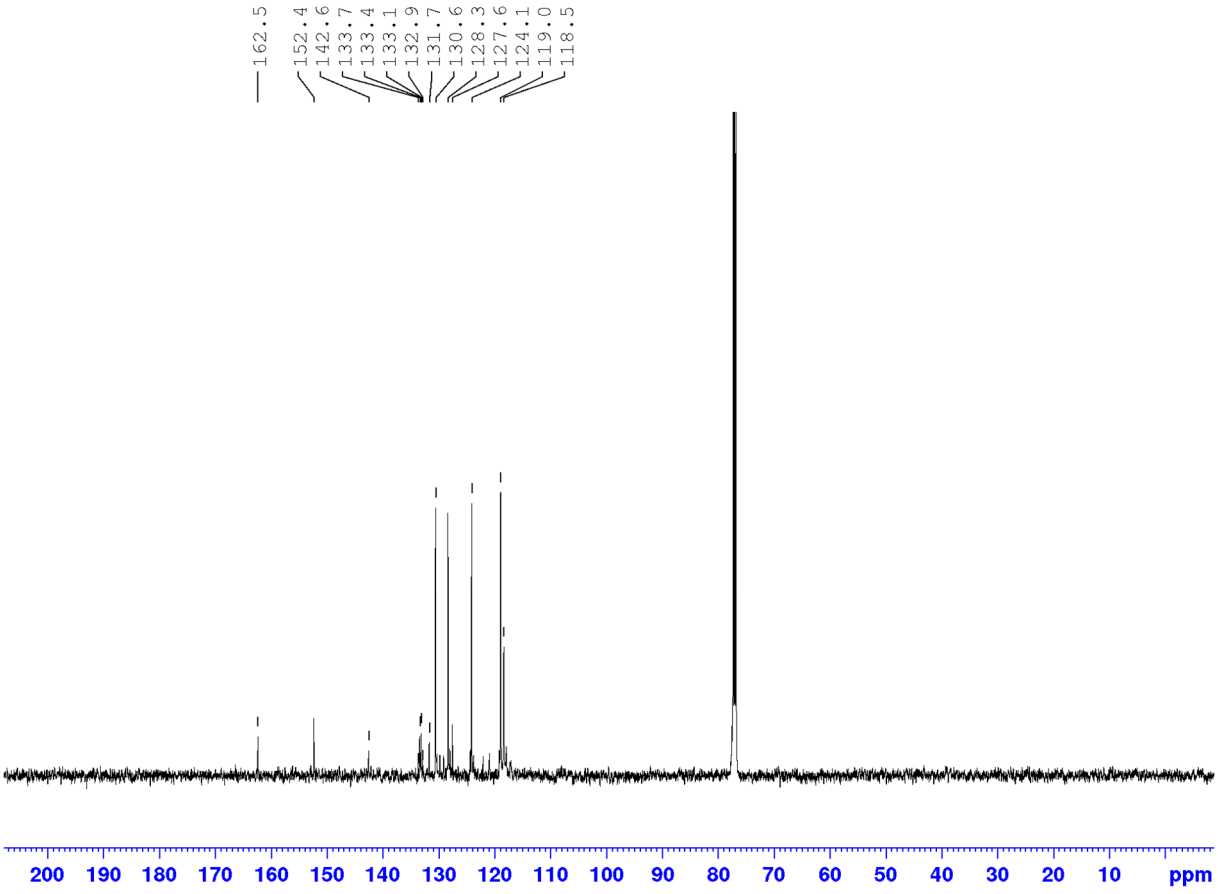


**Figure S2:** $^{13}C$ NMR (126 MHz, $CDCl_3$, 25 °C) of $N^1$,$N^2$-bis(3,5-bis(trifluoromethyl)phenyl) acenaphthylene-1,2-diimine **L1**.

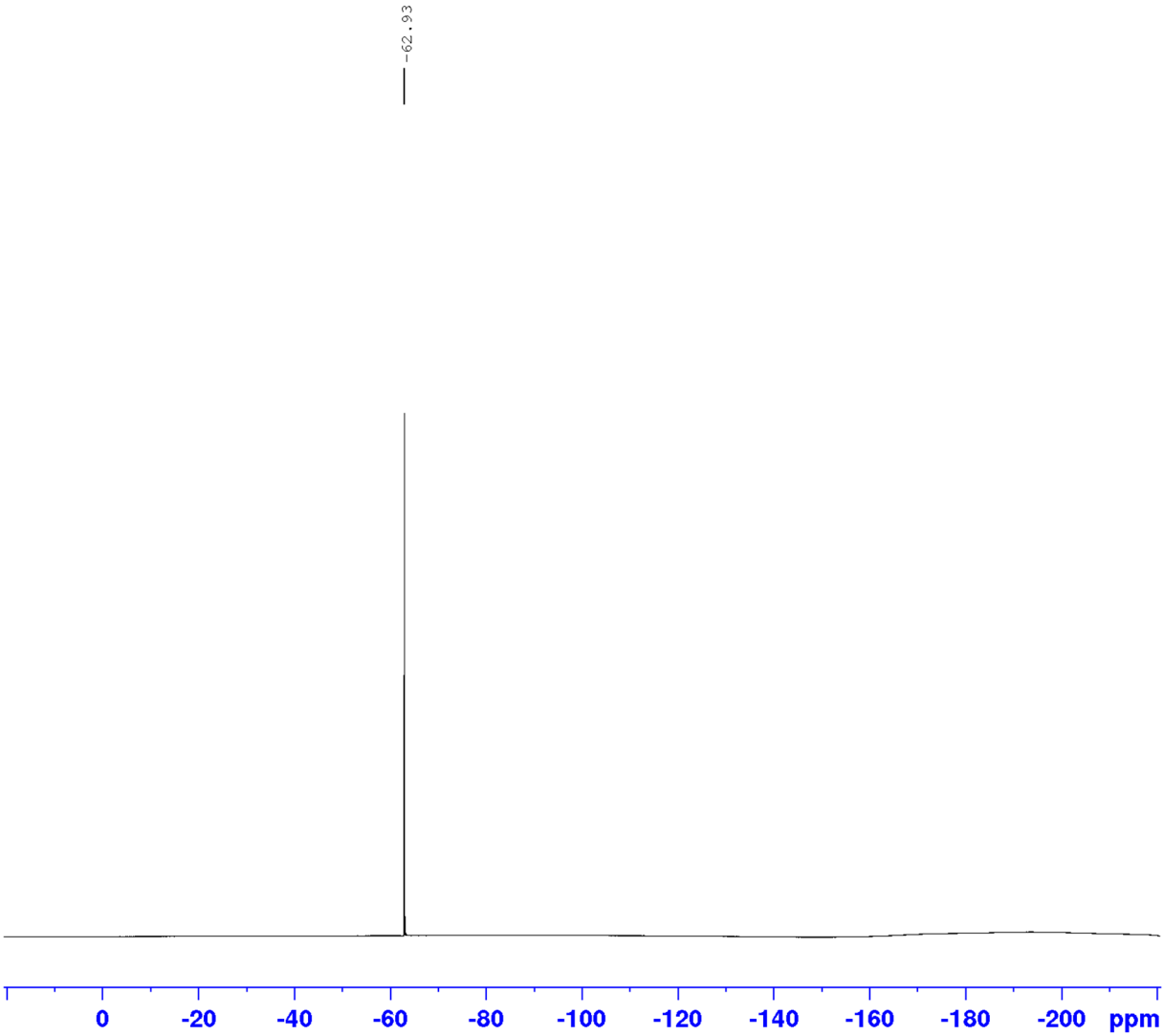


**Figure S3:** $^{19}F$ NMR (470 MHz, $CDCl_3$, 25 °C) of $N^1$,$N^2$-bis(3,5-bis(trifluoromethyl)phenyl) acenaphthylene-1,2-diimine **L1**.

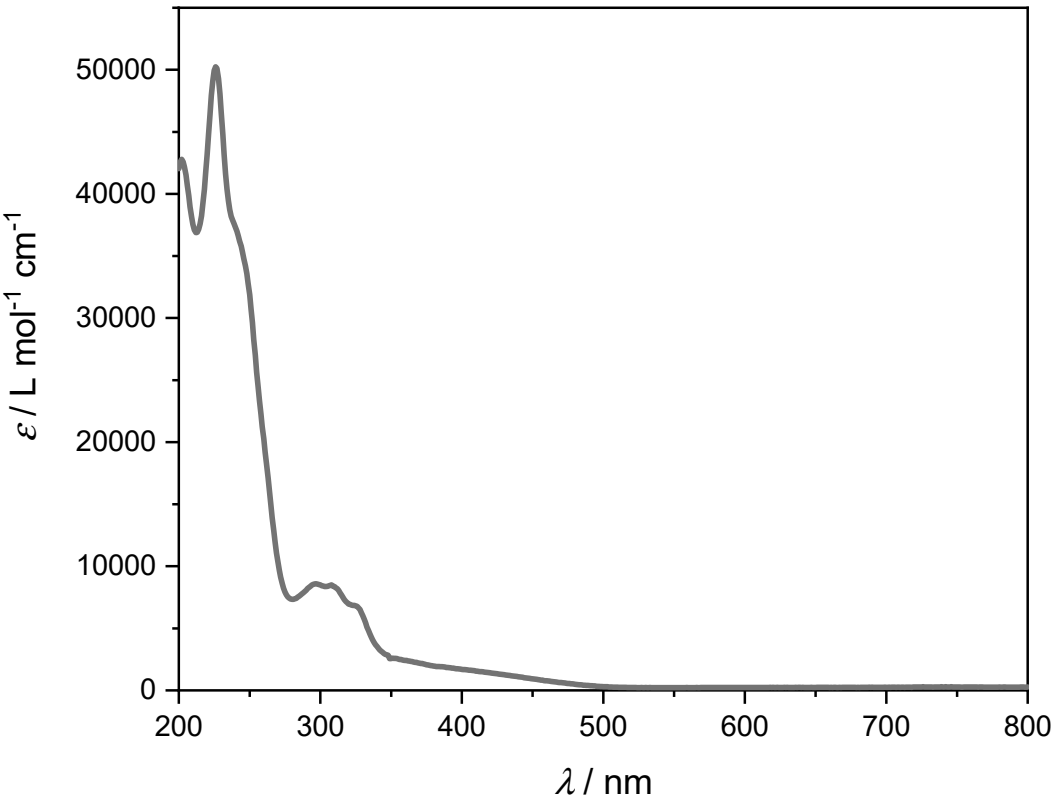


**Figure S4:** UV-vis absorption spectrum of $N^1$,$N^2$-bis(3,5-bis(trifluoromethyl)phenyl)acenaphthylene-1,2-diimine **L1** in ACN.

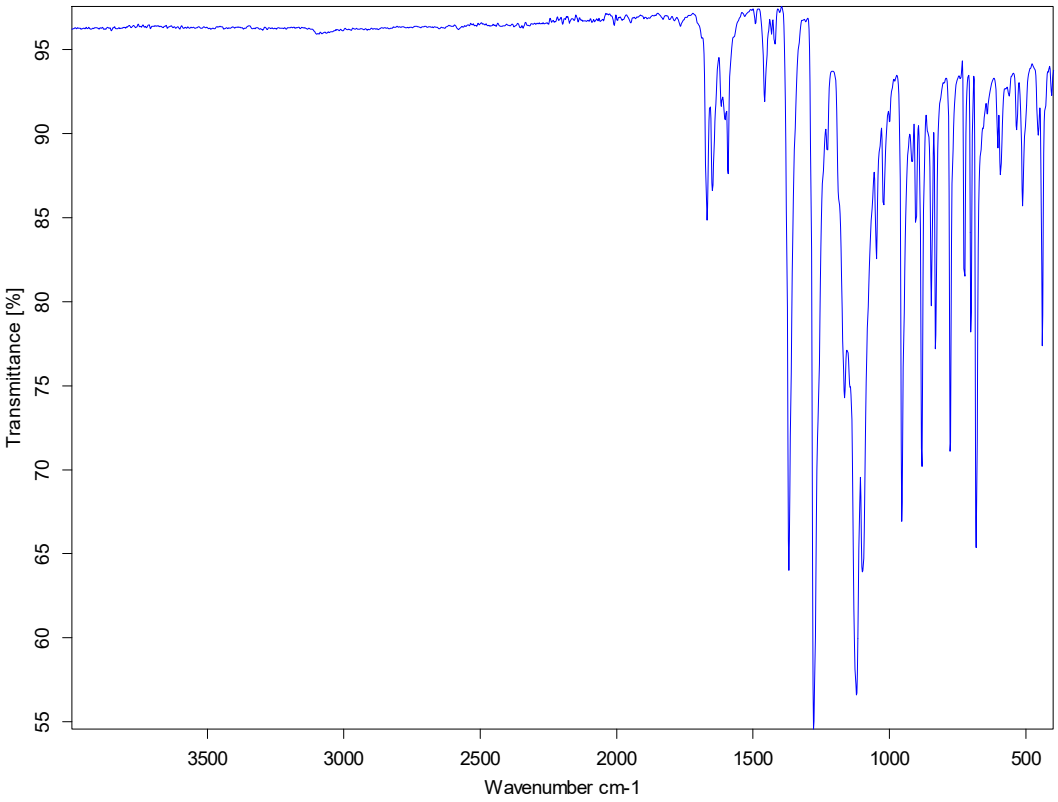


**Figure S5:** IR absorption spectrum of $N^1$,$N^2$-bis(3,5-bis(trifluoromethyl)phenyl)acenaphthylene-1,2-diimine **L1**.

## 2,6-diisopropyl-BIAN (L2)

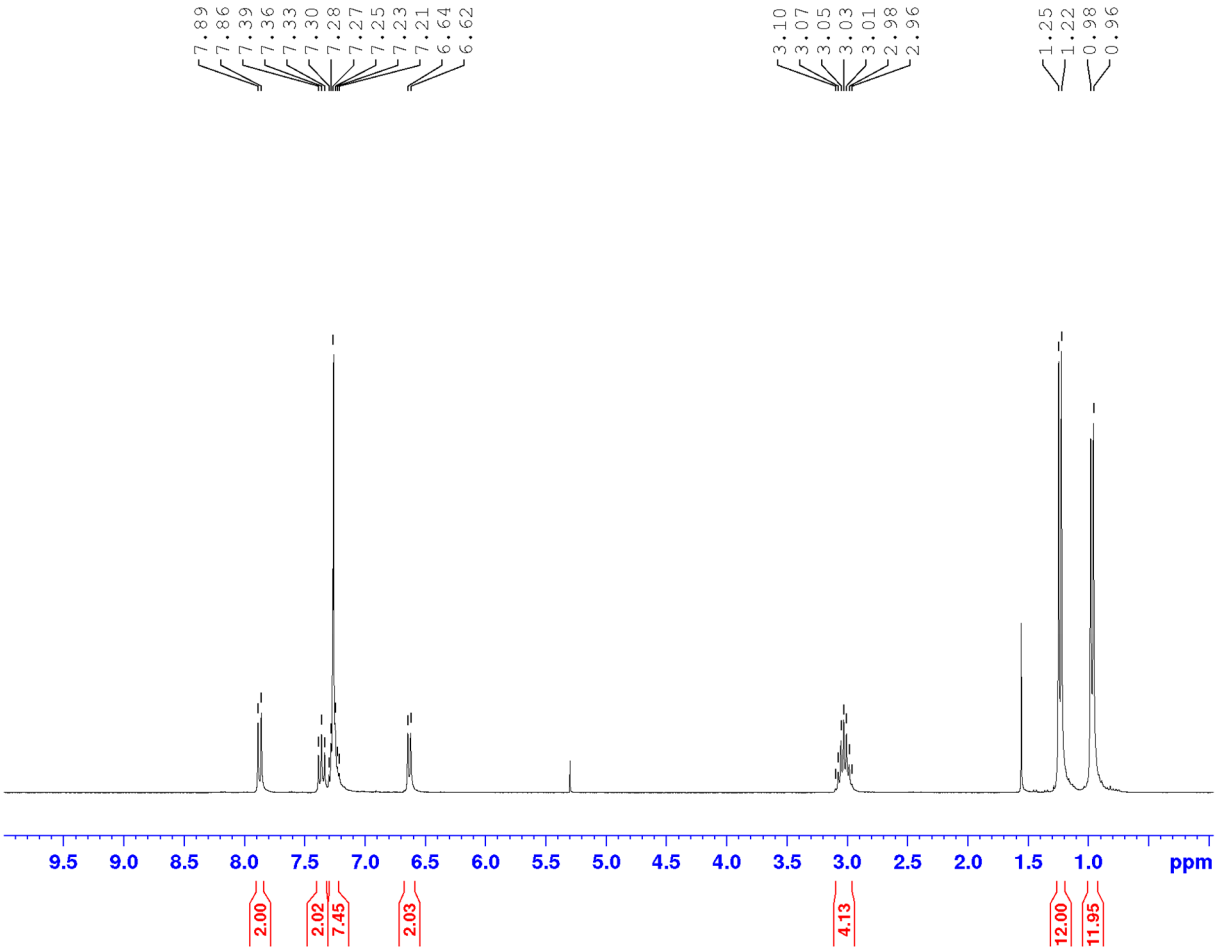


**Figure S6:** $^{1}$H NMR (300 MHz, $CDCl_3$, 25 °C) of $N^1$,$N^2$-bis(2,6-diisopropylphenyl)acenaphthylene-1,2-diimine **L2**.

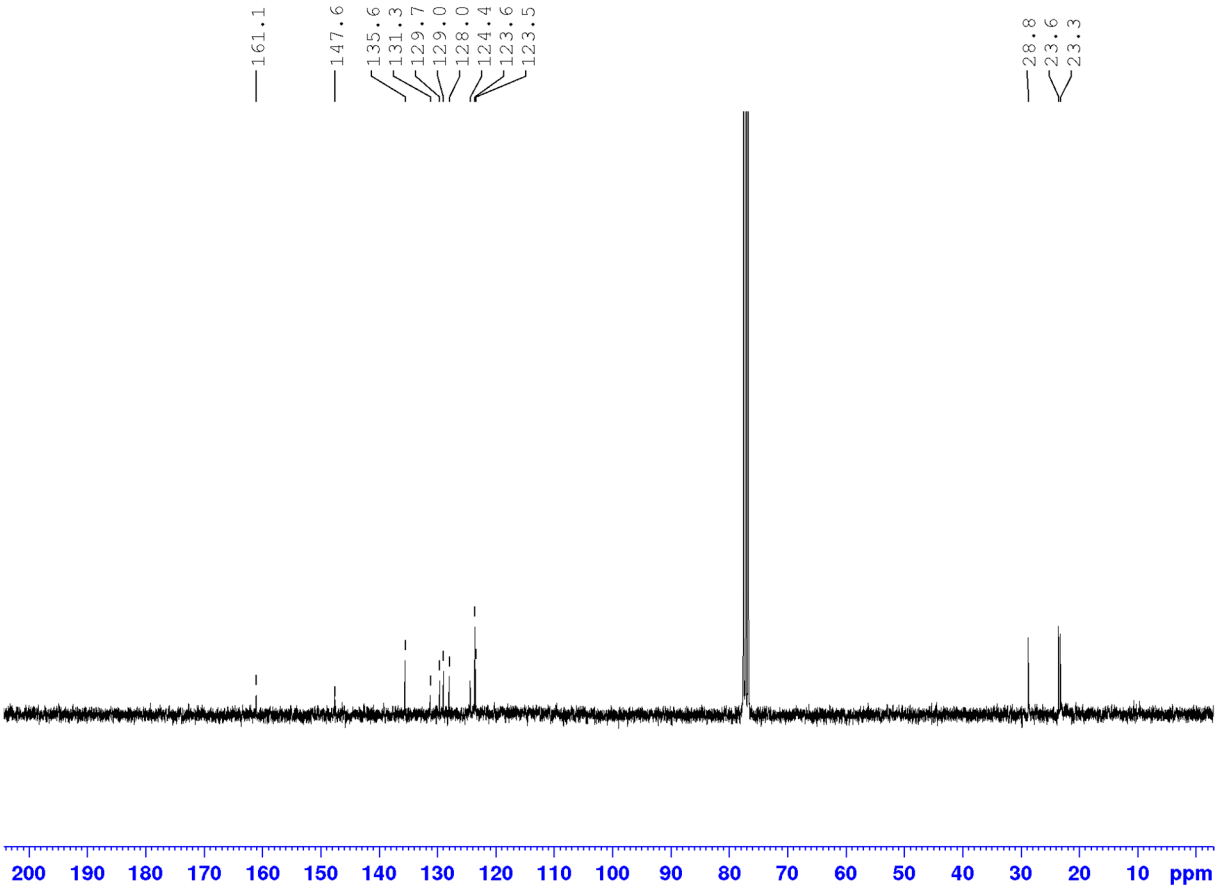


**Figure S7:** $^{13}C$ NMR (75 MHz, $CDCl_3$, 25 °C) of $N^1$,$N^2$-bis(2,6-diisopropylphenyl)acenaphthylene-1,2-diimine **L2**.

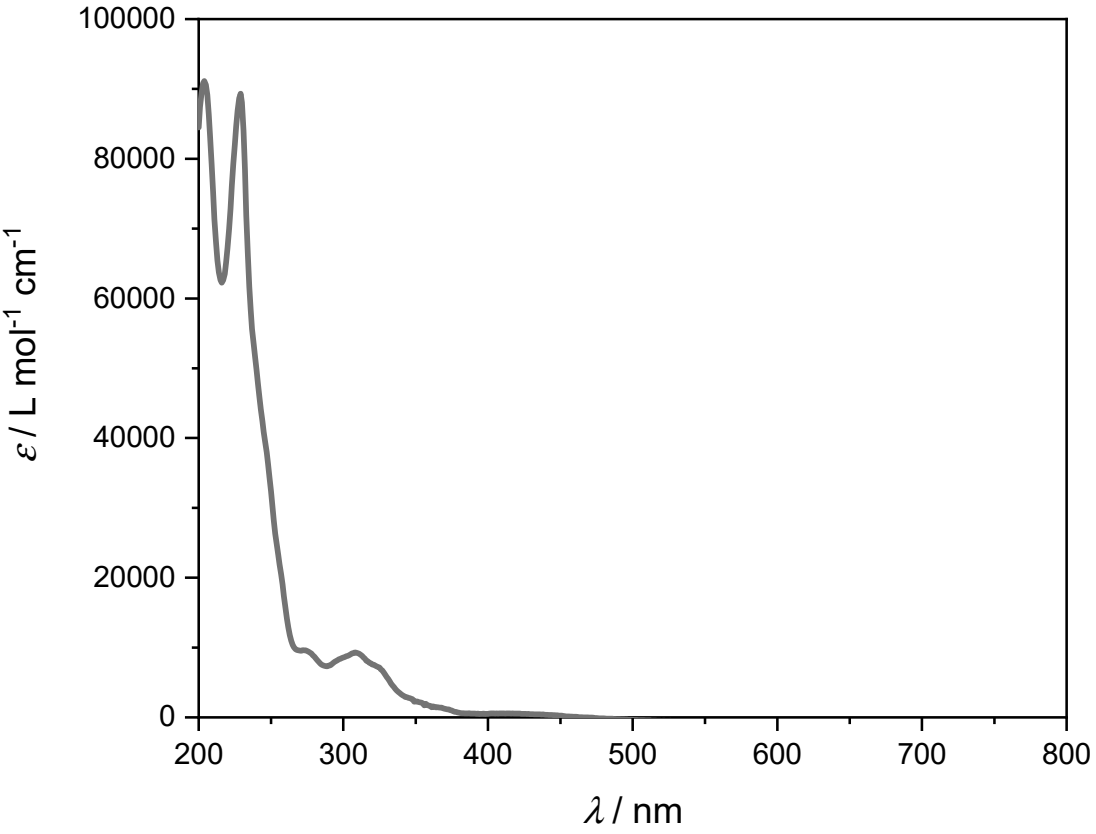


**Figure S8:** UV-vis absorption spectrum of $N^1$,$N^2$-bis(2,6-diisopropylphenyl)acenaphthylene-1,2-diimine **L2** in ACN.

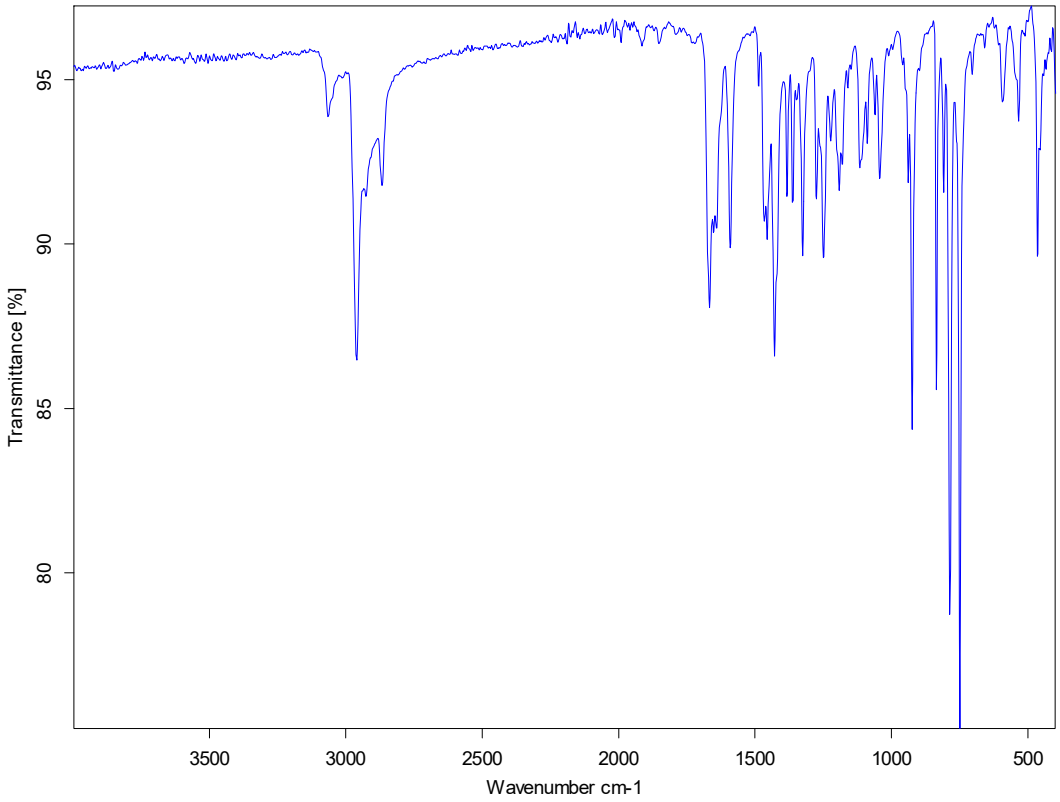


**Figure S9:** IR absorption spectrum of $N^1$,$N^2$-bis(2,6-diisopropylphenyl)acenaphthylene-1,2-diimine **L2**.

## 1-Pyrene-BIAN (L3)

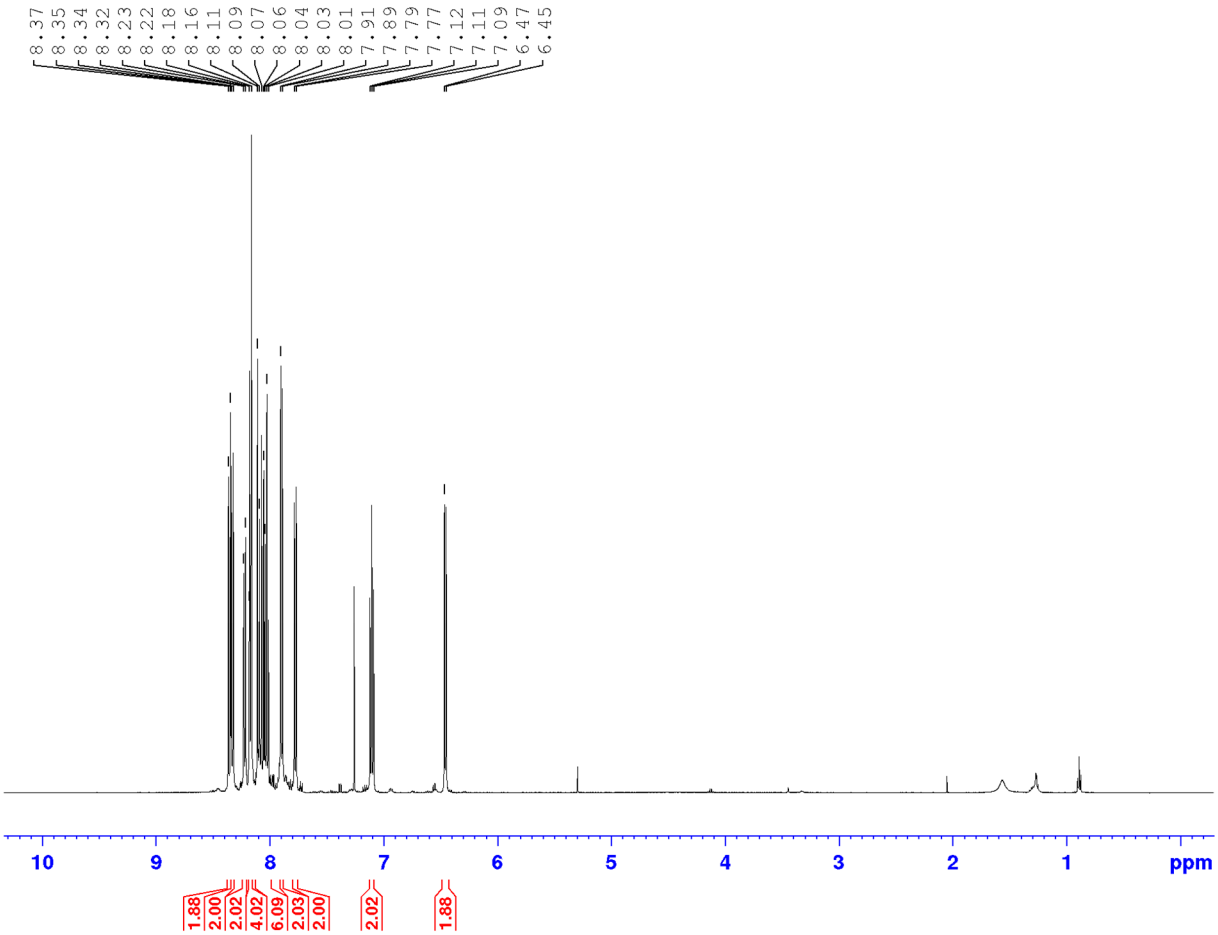


**Figure S10:** $^{1}$H NMR (500 MHz, $CDCl_3$, 25 °C) of *N*$^{1}$,*N*$^{2}$-di(pyren-1-yl)acenaphthylene-1,2-diimine **L3**.

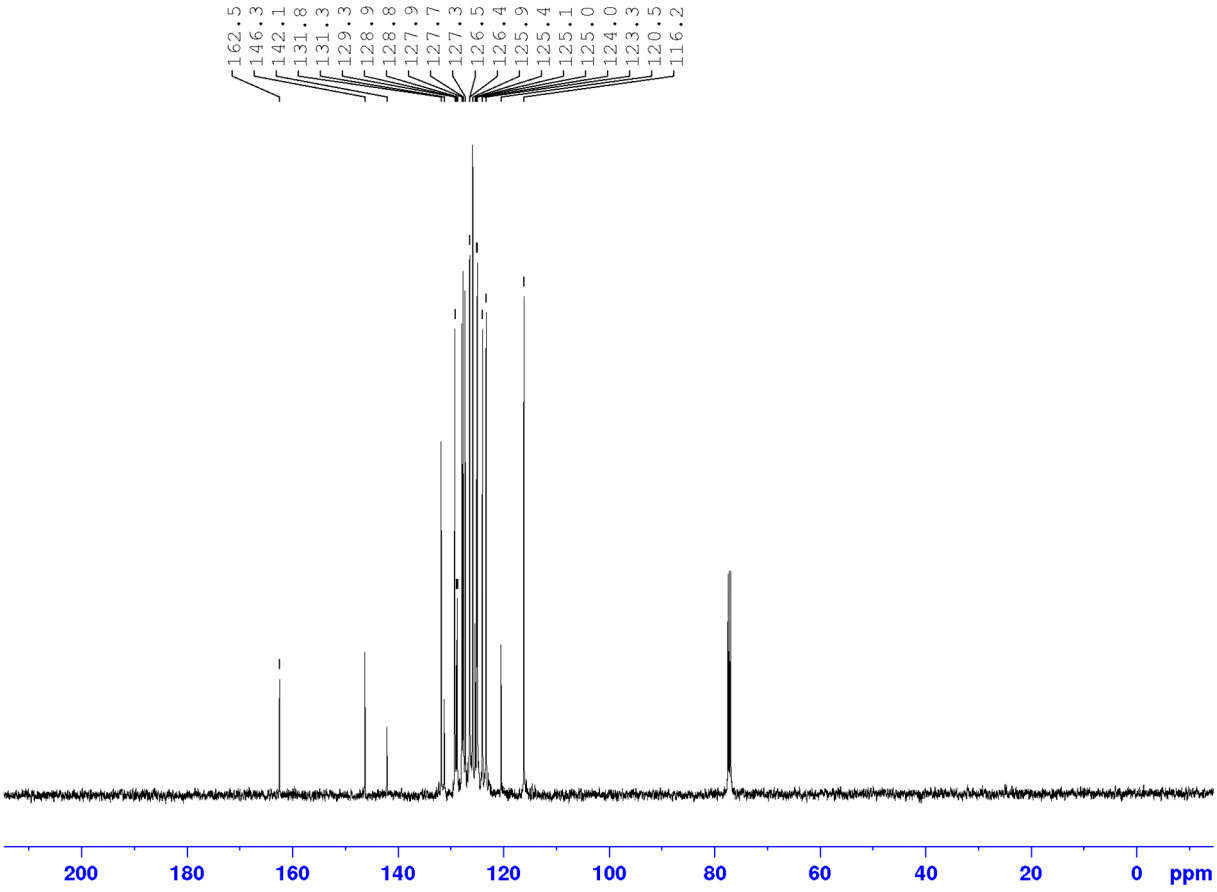


**Figure S11:** $^{13}C$ NMR (126 MHz, $CDCl_3$, 25 °C) of *N*$^{1}$,*N*$^{2}$-di(pyren-1-yl)acenaphthylene-1,2-diimine **L3**.

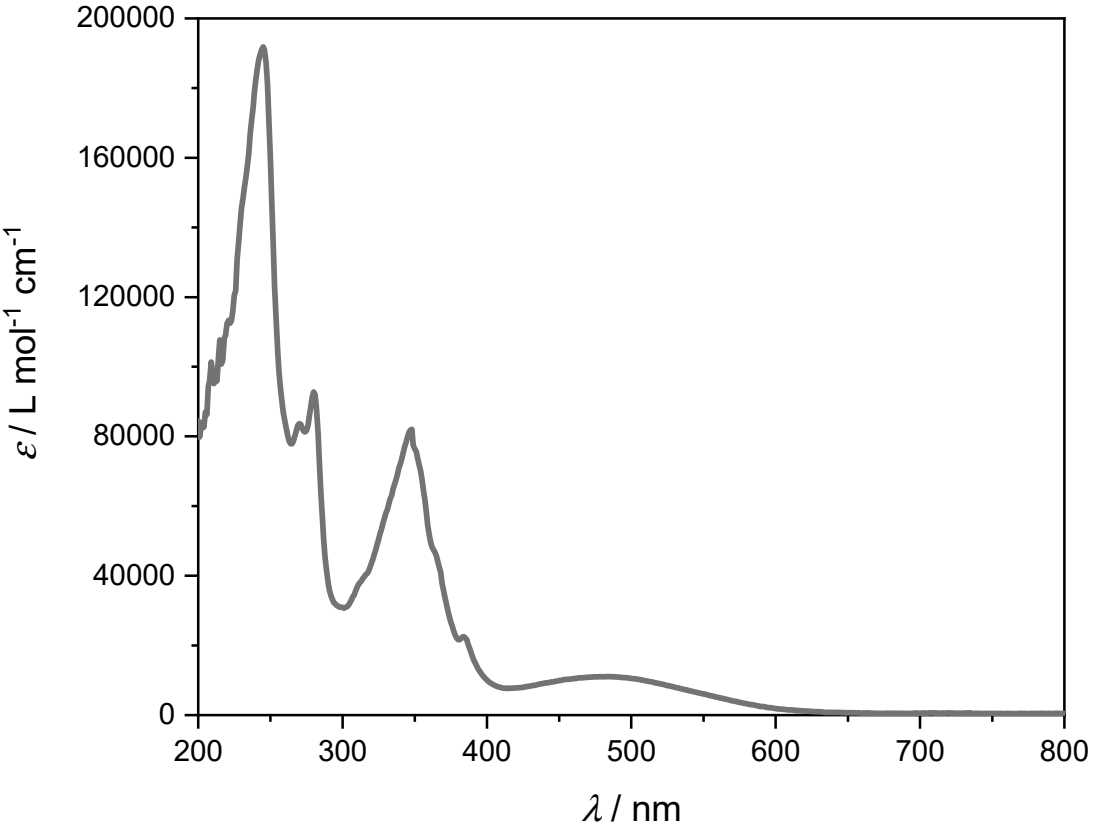


**Figure S12:** UV-vis absorption spectrum of $N^1$,$N^2$-di(pyren-1-yl)acenaphthylene-1,2-diimine **L3** in DCM.

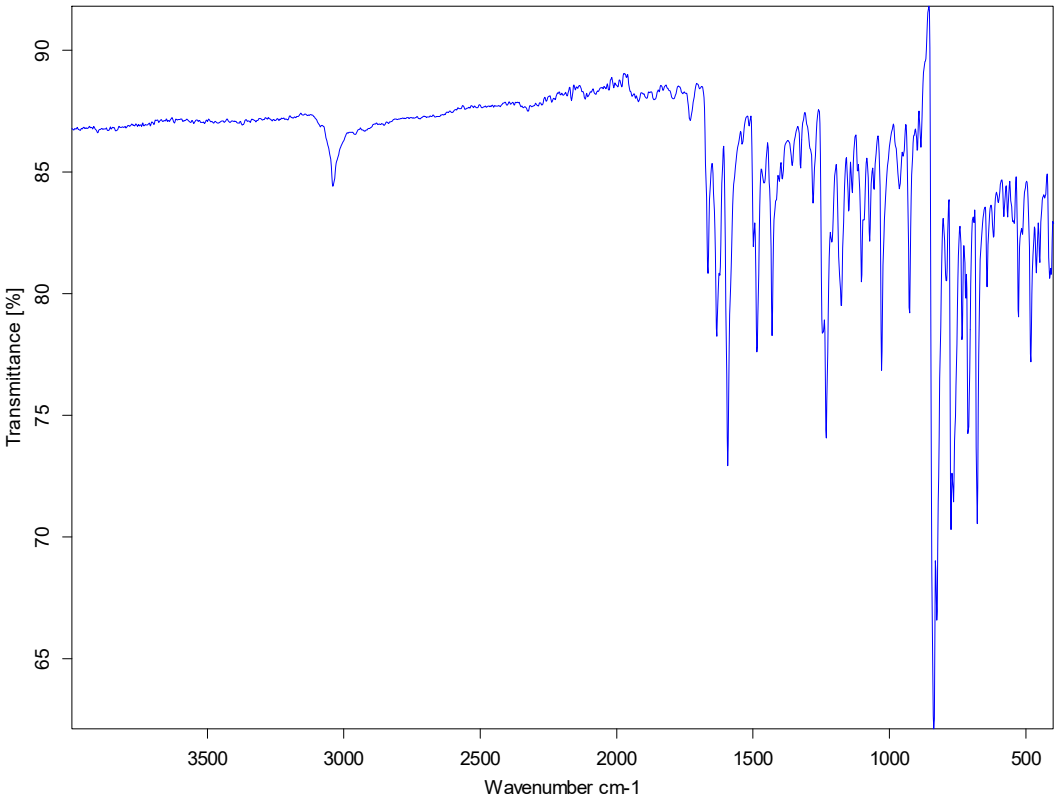


**Figure S13:** IR absorption spectrum of $N^1$,$N^2$-di(pyren-1-yl)acenaphthylene-1,2-diimine **L3**.

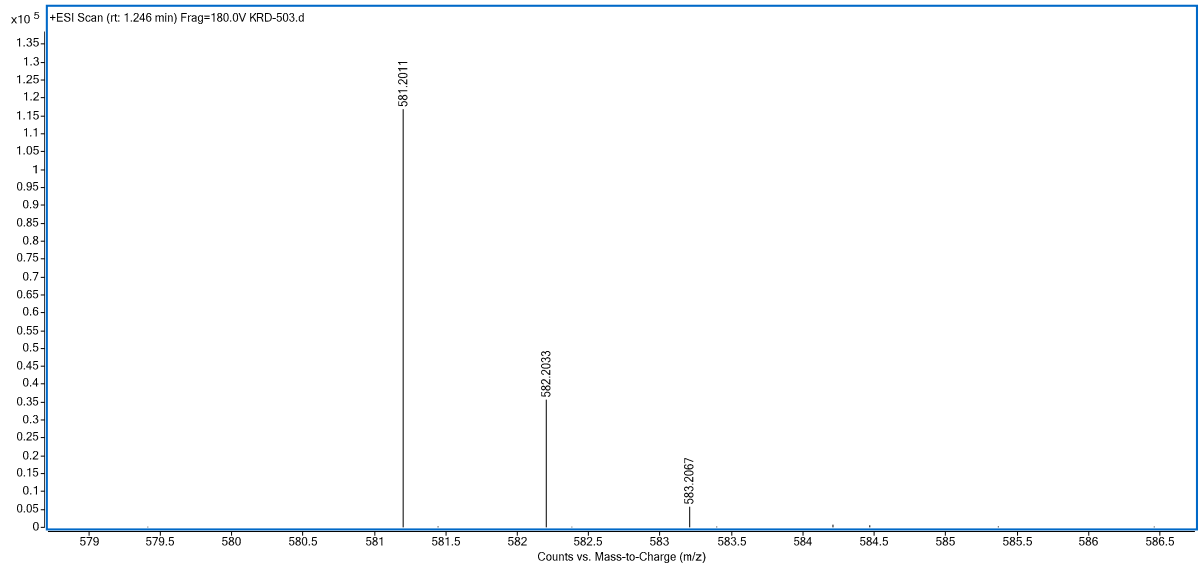


**Figure S14:** HRMS spectrum of $N^1$,$N^2$-di(pyren-1-yl)acenaphthylene-1,2-diimine **L3**.

## 4-Methoxy-BIAN (L4)

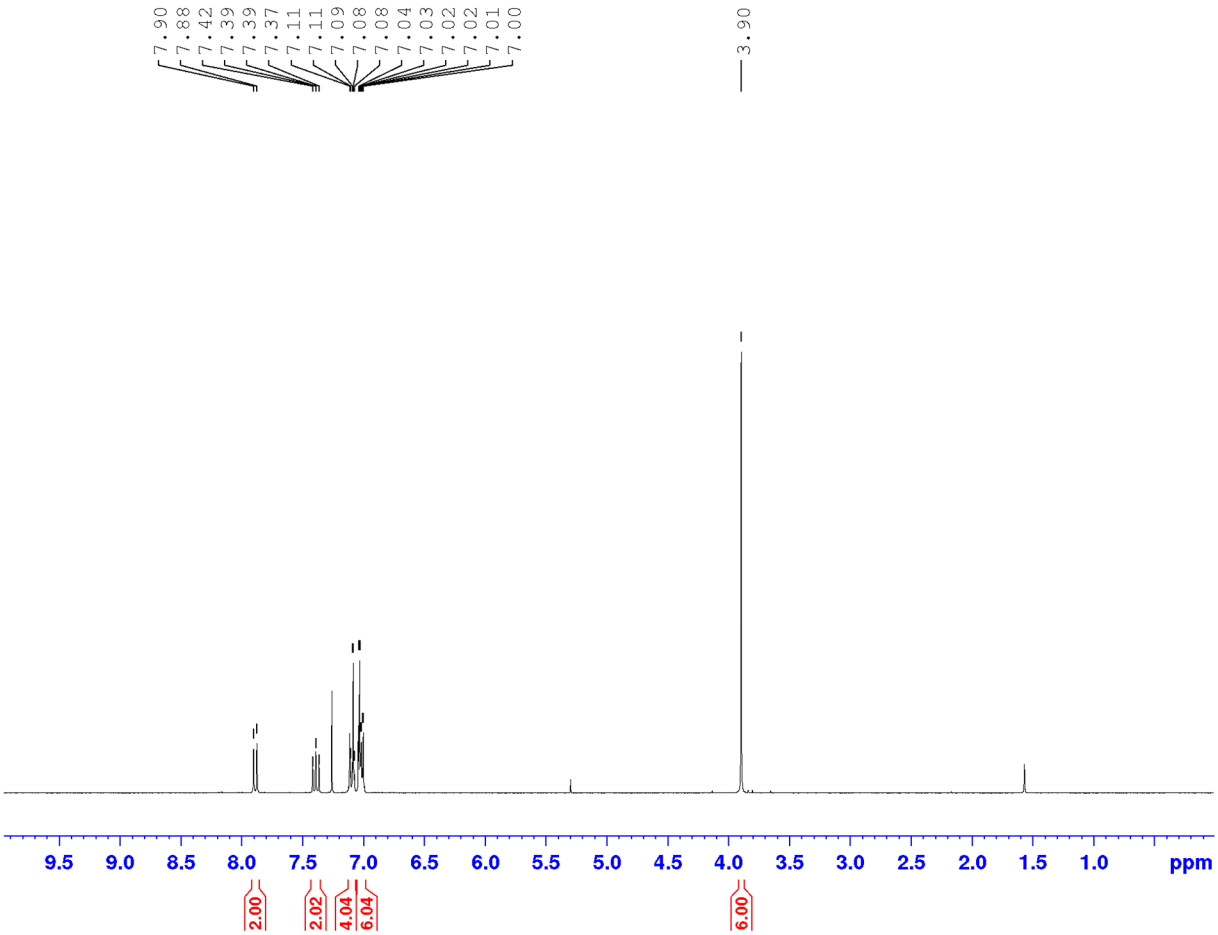


**Figure S15:** $^{1}$H NMR (300 MHz, $CDCl_3$, 25 °C) of $N^1$,$N^2$-bis(4-methoxyphenyl)acenaphthylene-1,2-diimine **L4**.

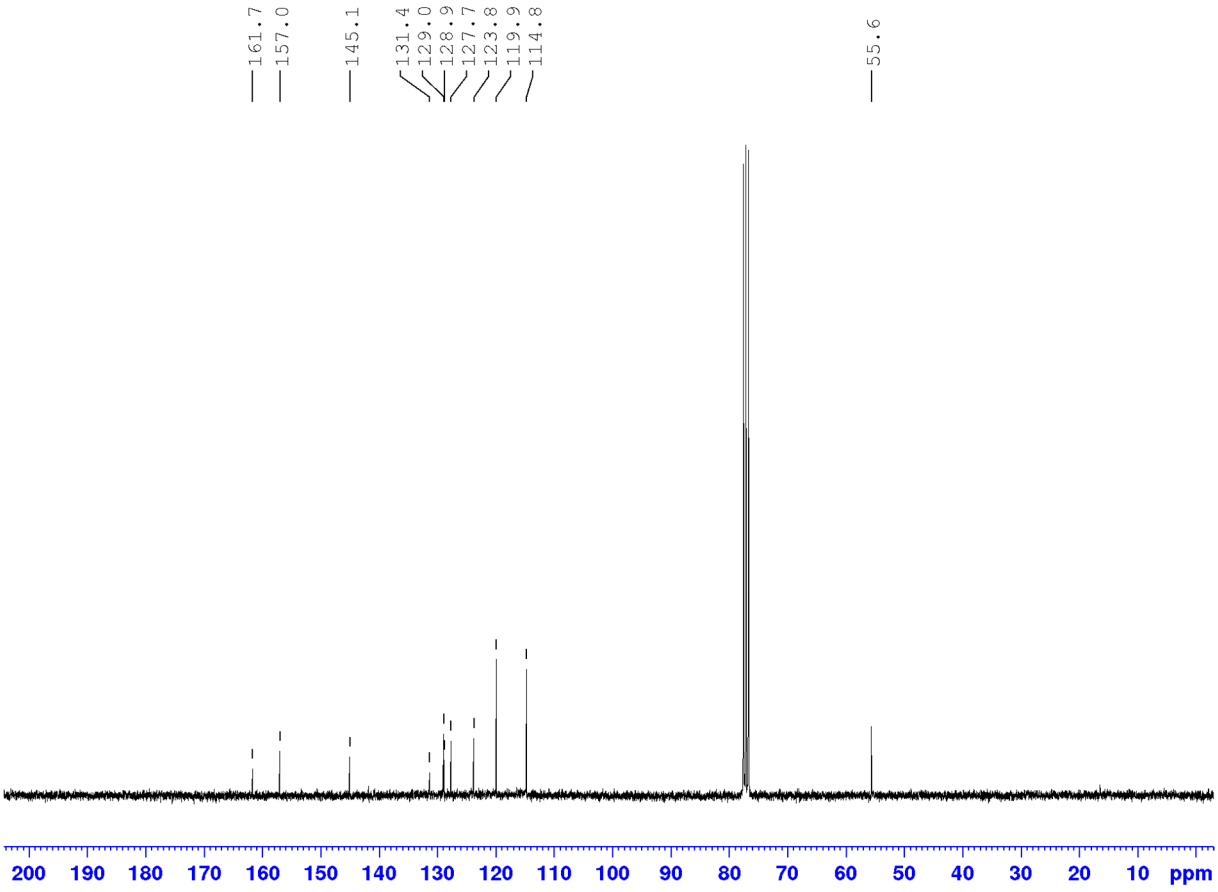


**Figure S16:** $^{13}C$ NMR (75 MHz, $CDCl_3$, 25 °C) of $N^1$,$N^2$-bis(4-methoxyphenyl)acenaphthylene-1,2-diimine **L4**.

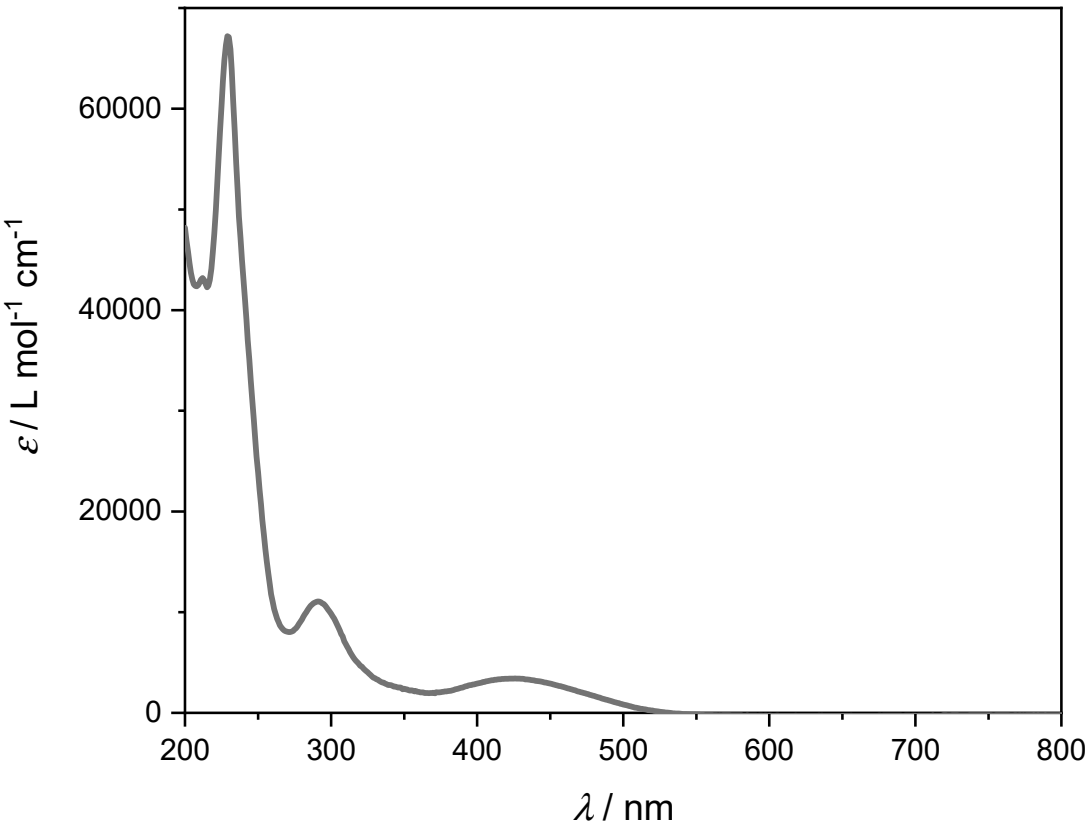


**Figure S17:** UV-vis absorption spectrum of $N^1$,$N^2$-bis(4-methoxyphenyl)acenaphthylene-1,2-diimine **L4** in ACN.

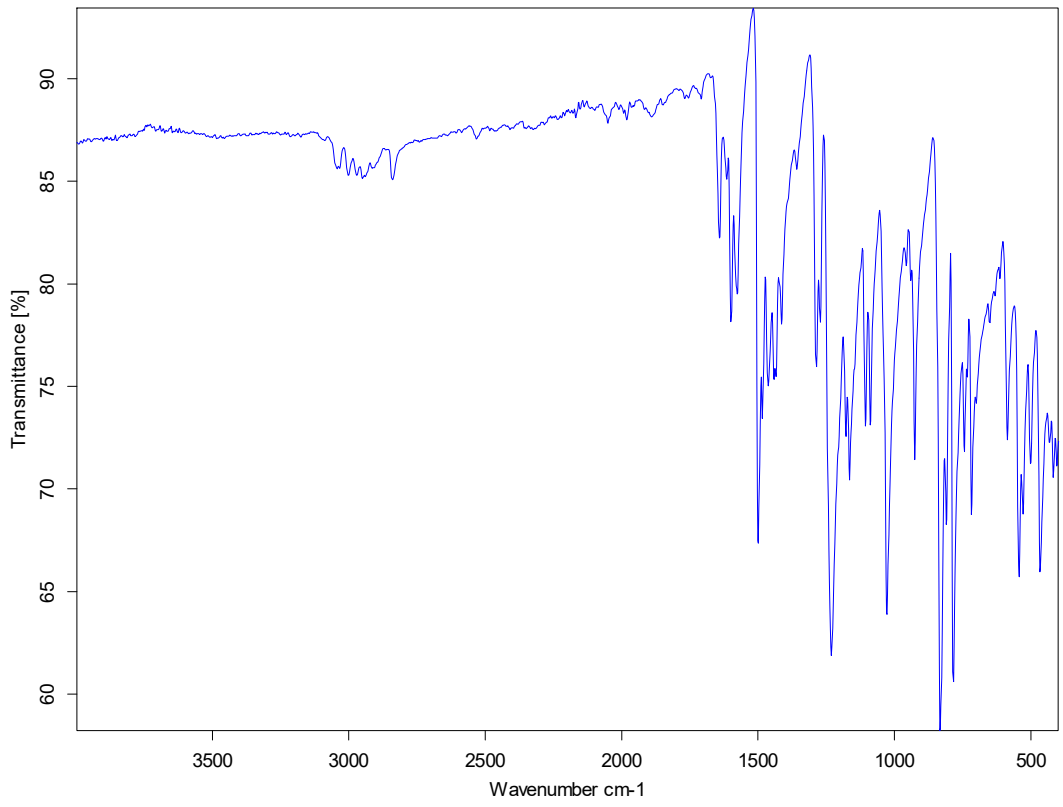


**Figure S18:** IR absorption spectrum of $N^1$,$N^2$-bis(4-methoxyphenyl)acenaphthylene-1,2-diimine **L4**.

## 3,4,5-Trimethoxy-BIAN (L5)

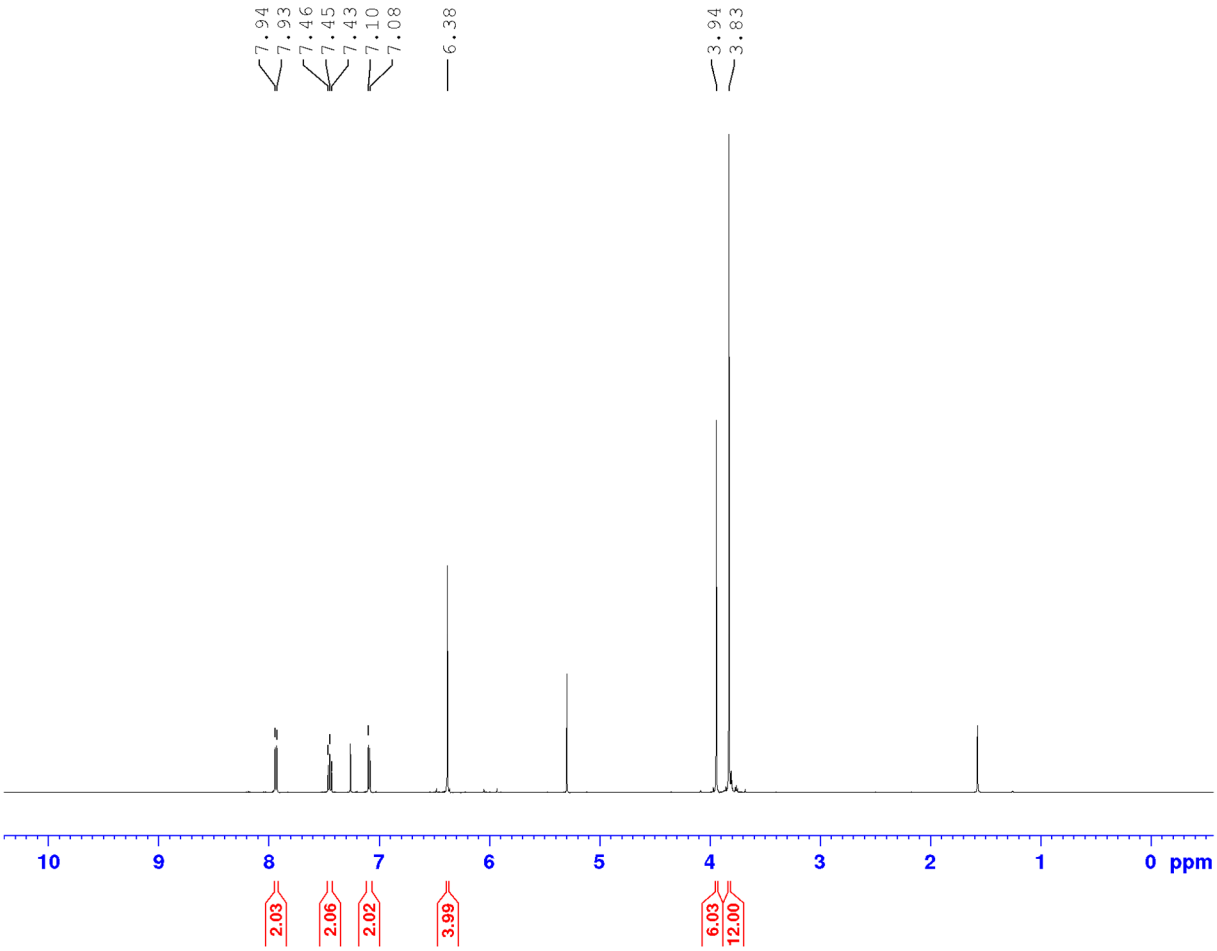


**Figure S19:** $^{1}$H NMR (500 MHz, $CDCl_3$, 25 °C) of *N*$^{1}$,*N*$^{2}$-bis(3,4,5-trimethoxyphenyl)acenaphthylene-1,2-diimine **L5**.

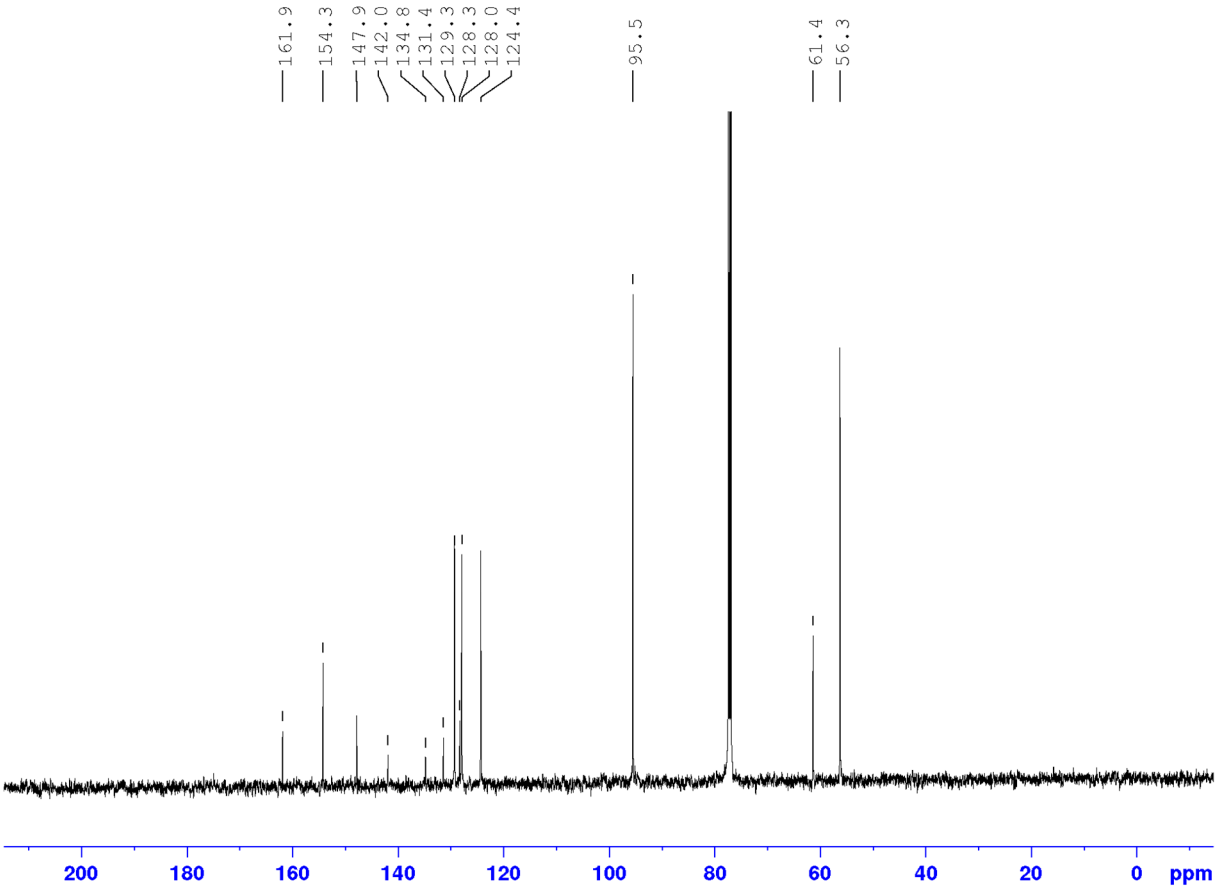


**Figure S20:** $^{13}C$ NMR (126 MHz, $CDCl_3$, 25 °C) of $N^1$,$N^2$-bis(3,4,5-trimethoxyphenyl)acenaphthylene-1,2-diimine **L5**.

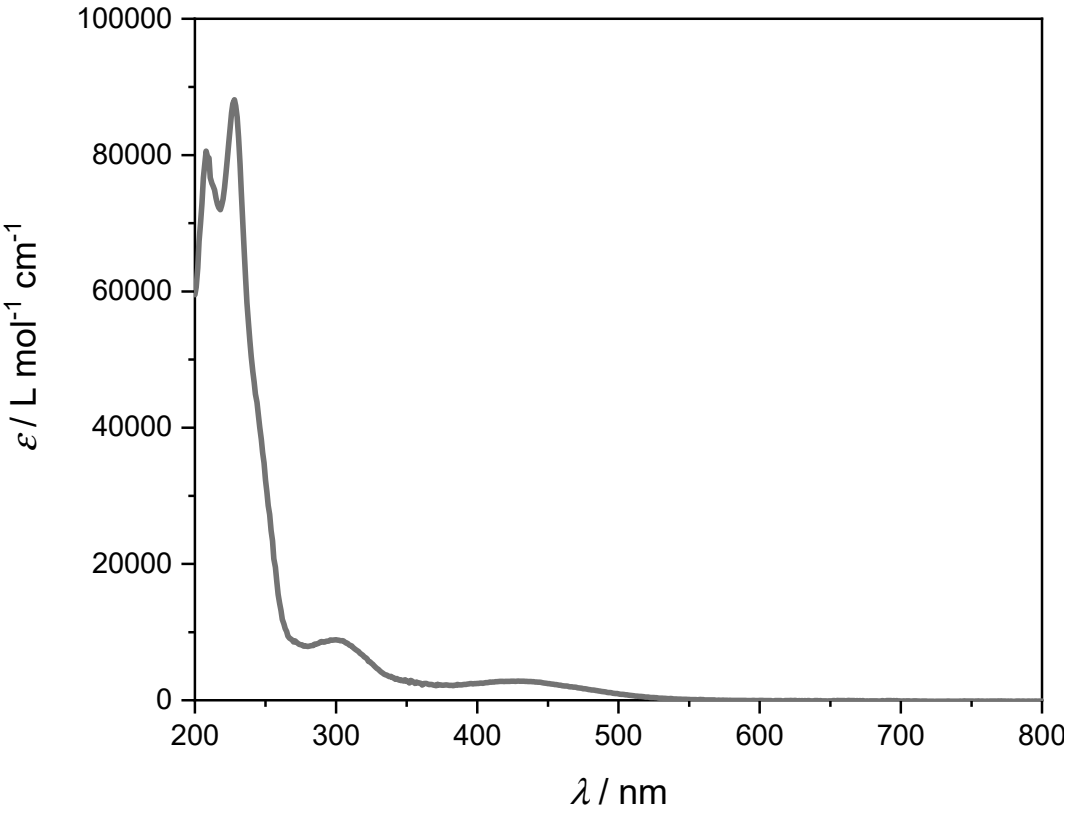


**Figure S21:** UV-vis absorption spectrum of $N^1$,$N^2$-bis(3,4,5-trimethoxyphenyl)acenaphthylene-1,2-diimine **L5** in ACN.

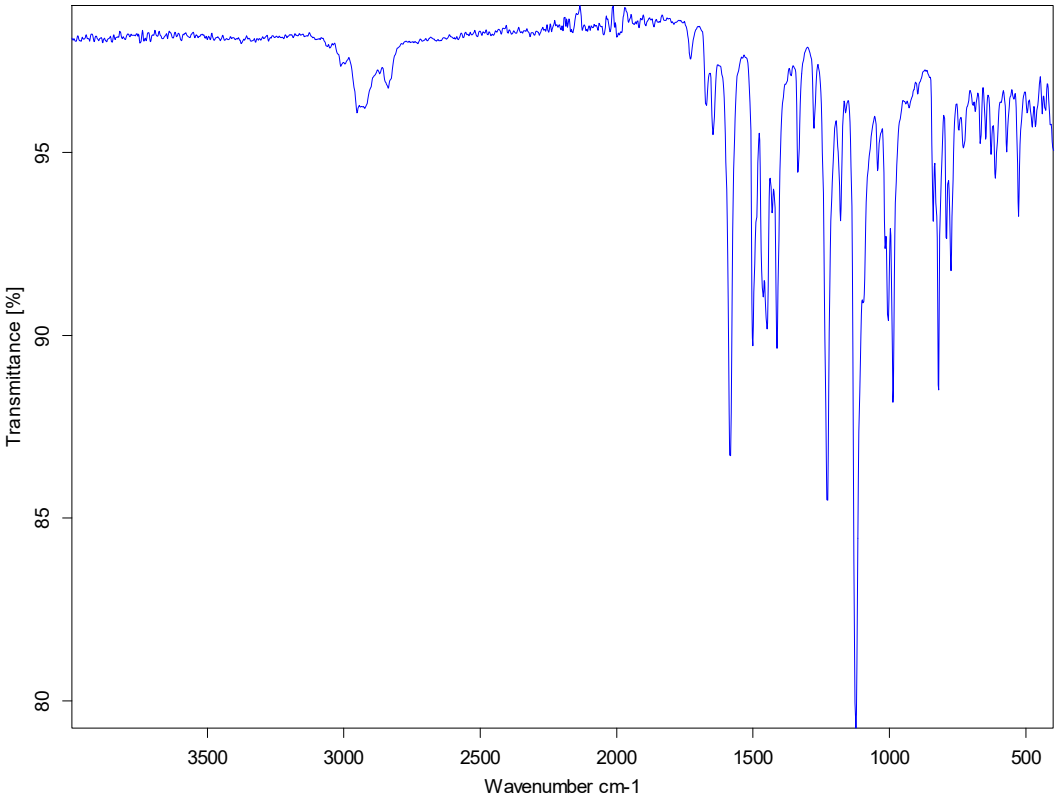


**Figure S22:** IR absorption spectrum of $N^1$,$N^2$-bis(3,4,5-trimethoxyphenyl)acenaphthylene-1,2-diimine **L5**.

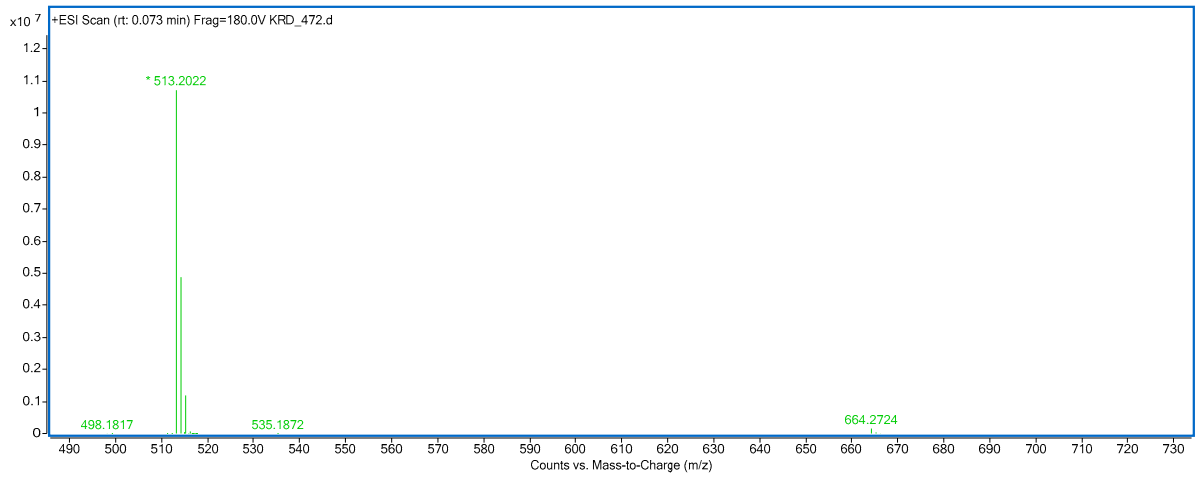


**Figure S23:** HRMS spectrum of $N^1$,$N^2$-bis(3,4,5-trimethoxyphenyl)acenaphthylene-1,2-diimine **L5**.

## 4-Diethylamino-BIAN (L6)

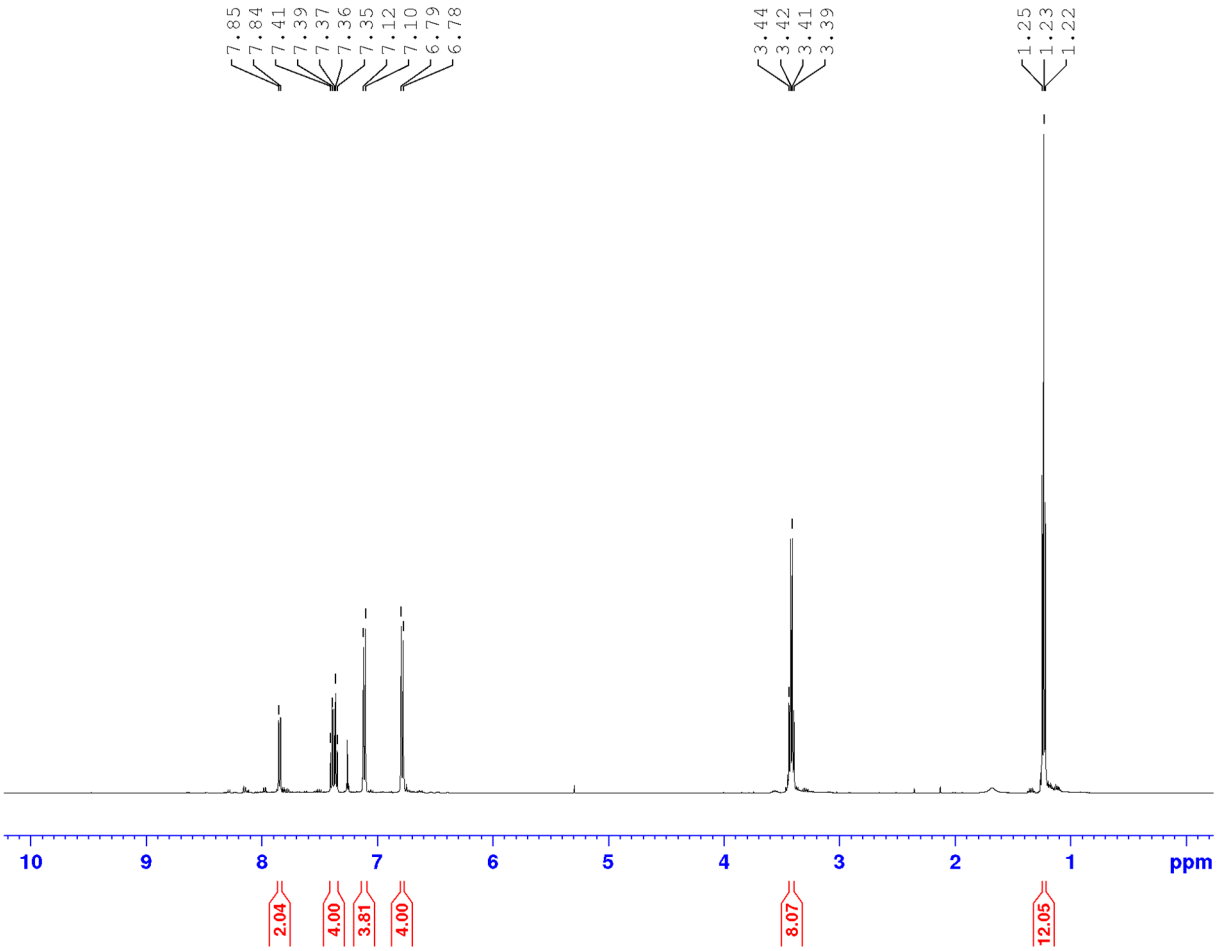


**Figure S24:** $^{1}$H NMR (500 MHz, $CDCl_3$, 25 °C) of *N*$^{1}$,*N*$^{2}$-bis(4-(*N*,*N*-diethylamino)phenyl) acenaphthylene-1,2-diimine **L6**.

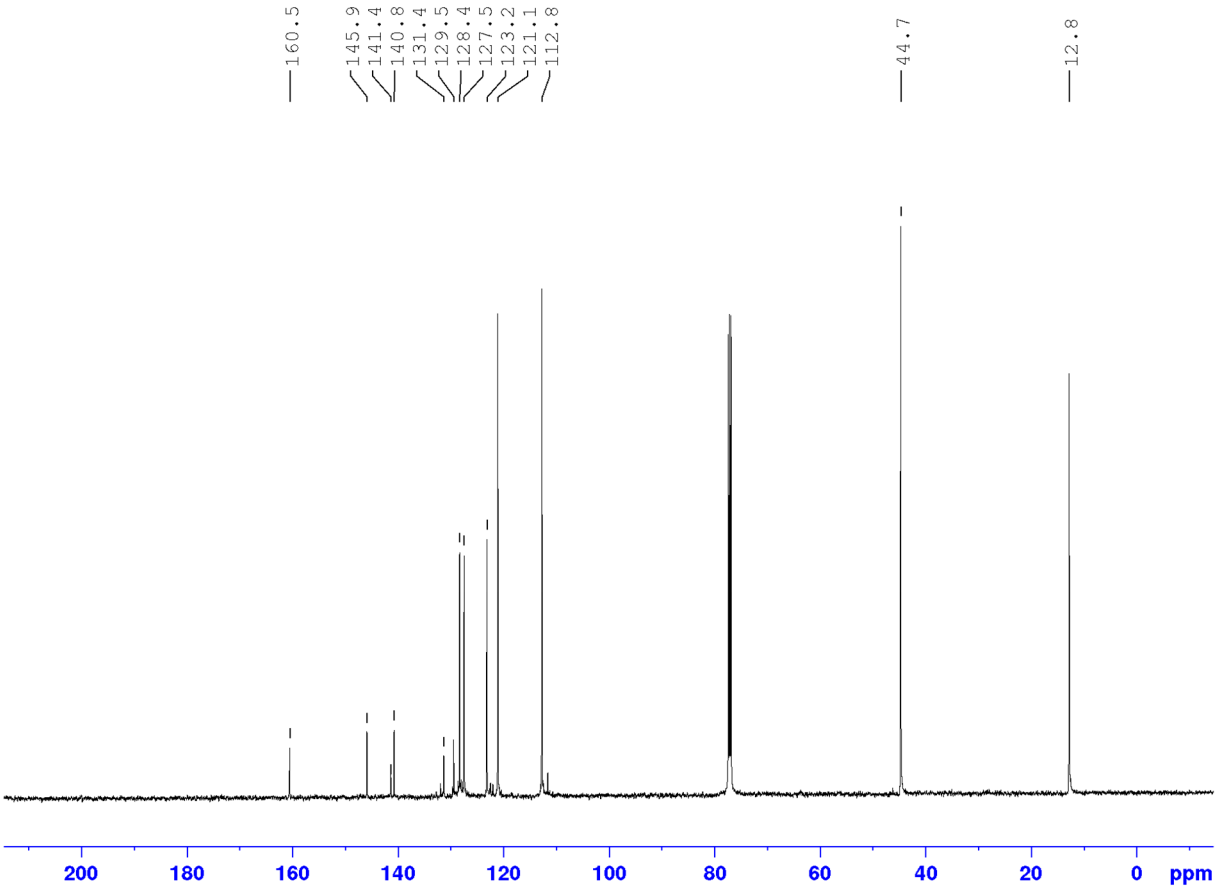


**Figure S25:** $^{13}C$ NMR (126 MHz, $CDCl_3$, 25 °C) of $N^1$,$N^2$-bis(4-(*N*,*N*-diethylamino)phenyl) acenaphthylene-1,2-diimine **L6**.

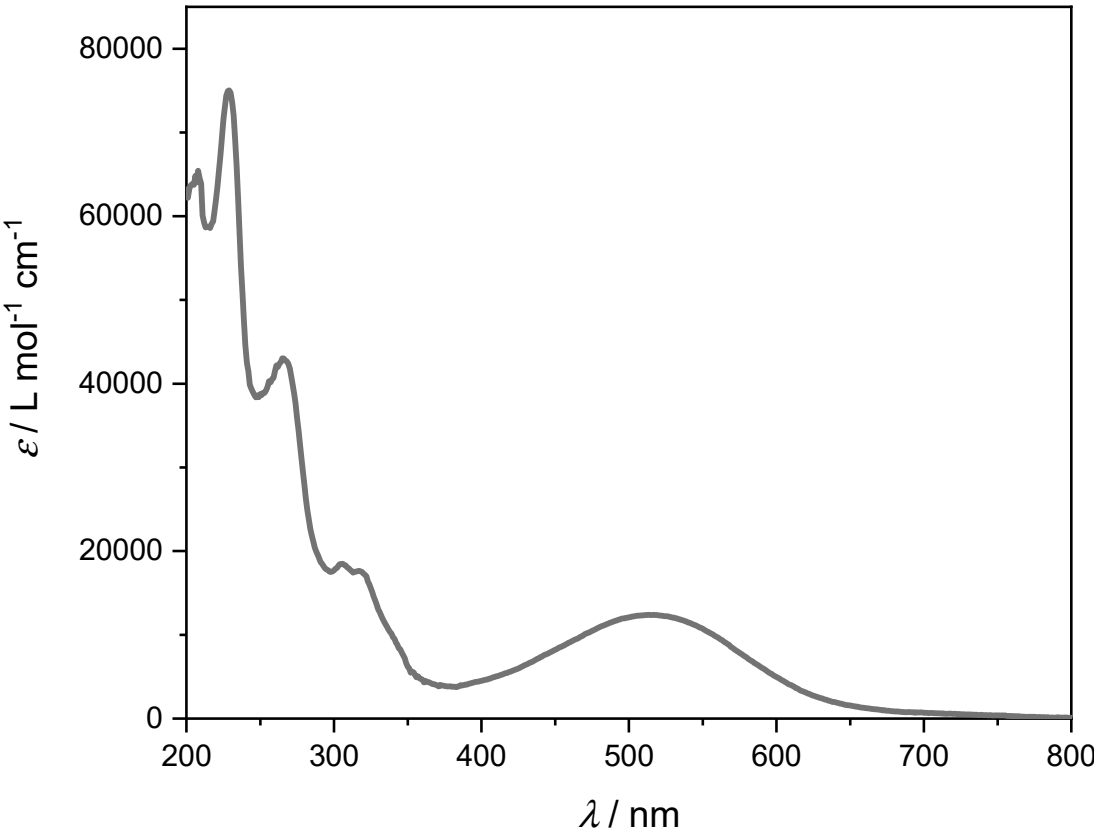


**Figure S26:** UV-vis absorption spectrum of $N^1$,$N^2$-bis(4-(*N*,*N*-diethylamino)phenyl)acenaphthylene-1,2-diimine **L6** in ACN.

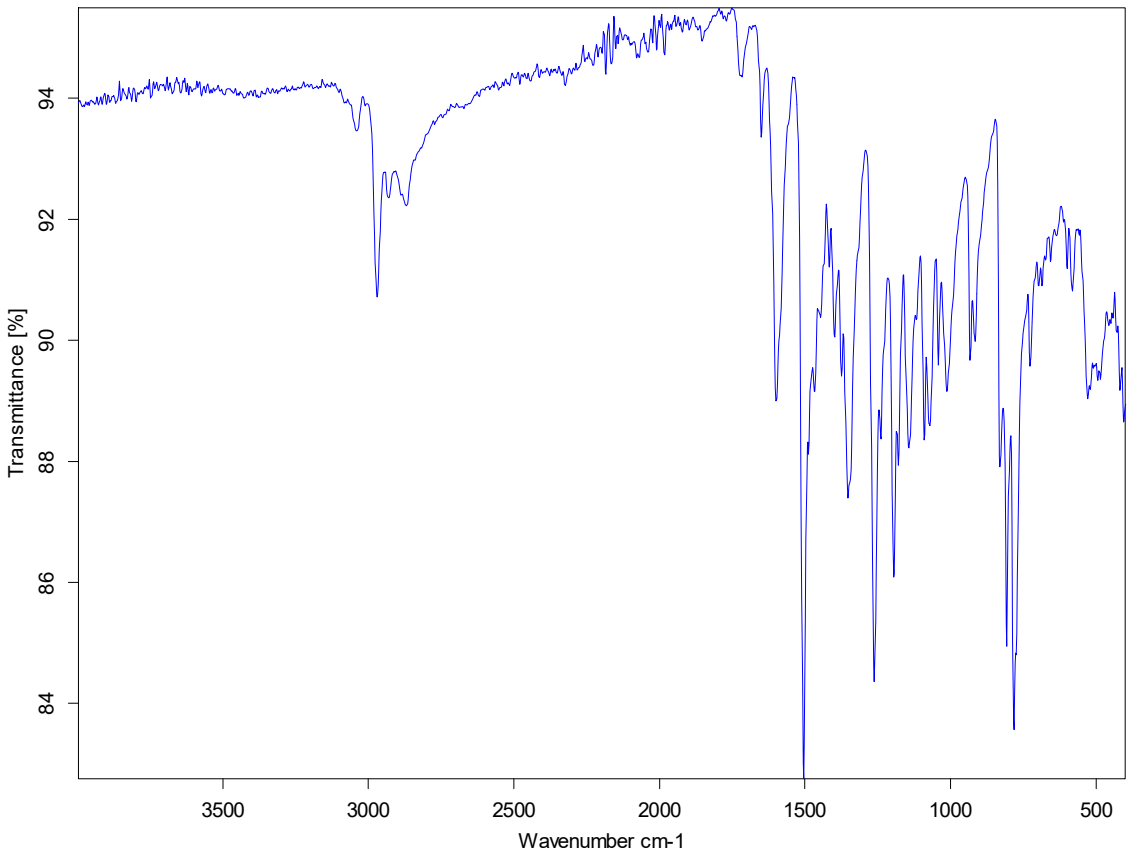


**Figure S27:** IR absorption spectrum of *N*[1],*N*[2]-bis(4-(*N*,*N*-diethylamino)phenyl)acenaphthylene-1,2-diimine **L6**.

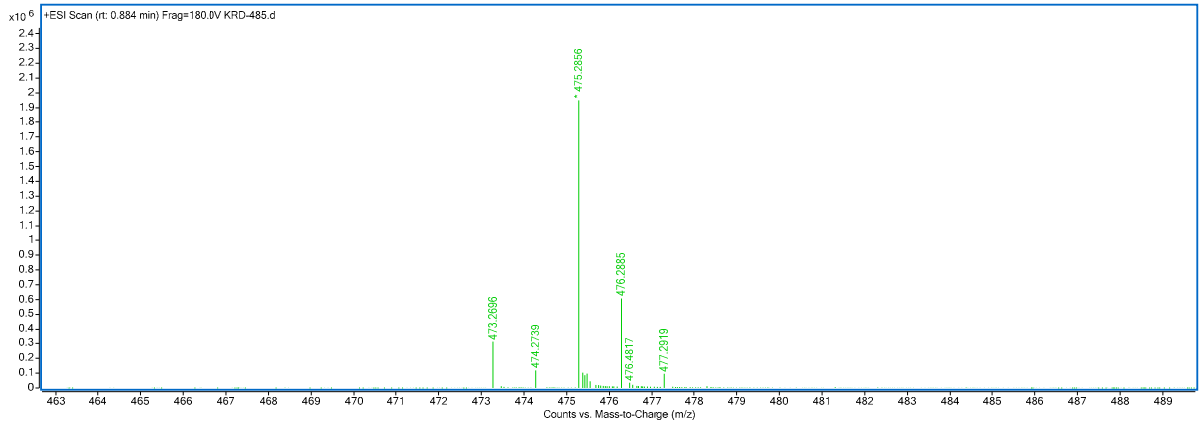


**Figure S28:** HRMS spectrum of *N*[1],*N*[2]-bis(4-(*N*,*N*-diethylamino)phenyl)acenaphthylene-1,2-diimine **L6**.

## Spectral data Ag-BIAN complexes

### [Ag(3,5-bis-$CF_3$-BIAN)$_2$]$BF_4$ (Ag1)

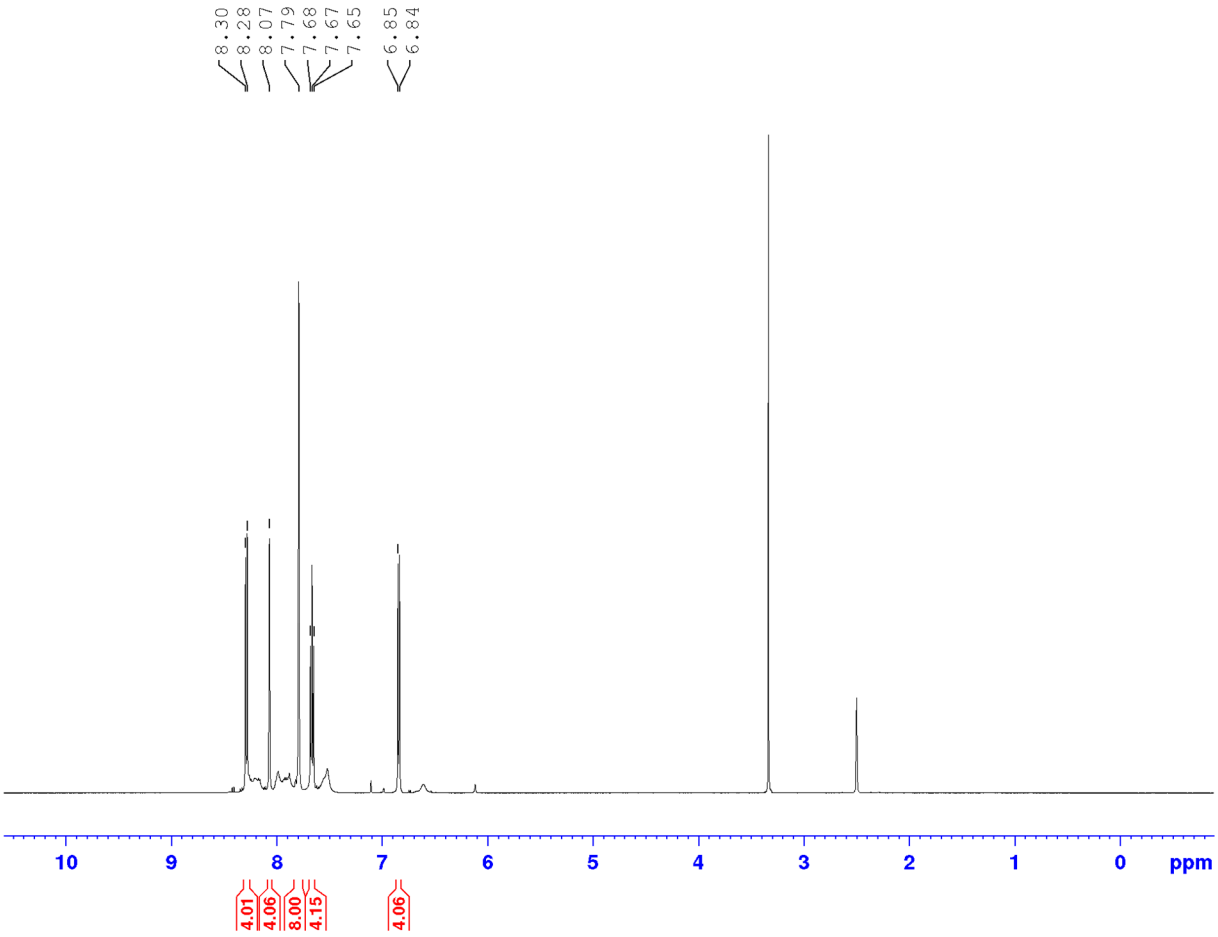


**Figure S29:** $^1$H NMR (500 MHz, DMSO-d6, 25 °C) of [Ag(3,5-bis-$CF_3$-BIAN)$_2$]$BF_4$ **Ag1**.

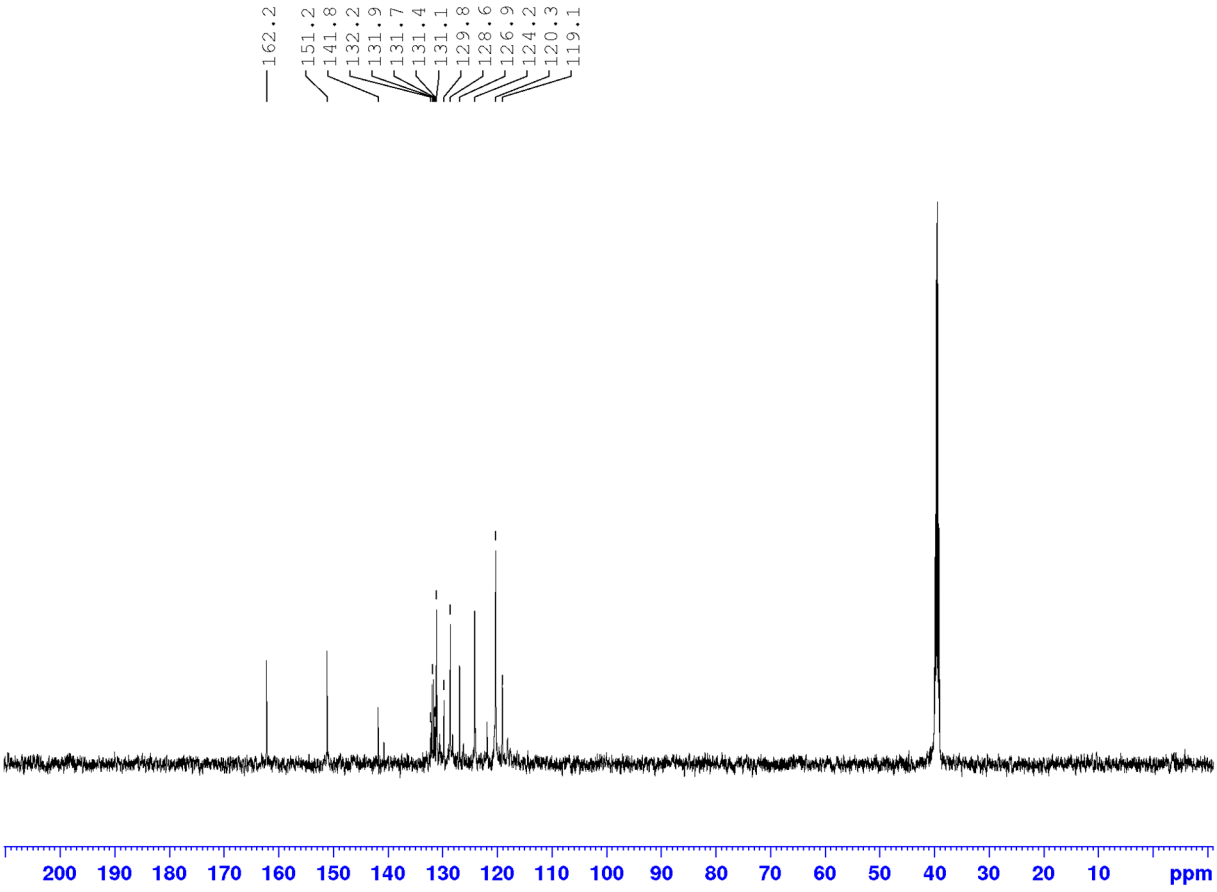


**Figure S30:** $^{13}C$ NMR (126 MHz, DMSO-d6, 25 °C) of $[Ag(3,5\text{-bis-}CF_3\text{-BIAN})_2]BF_4$ **Ag1**.

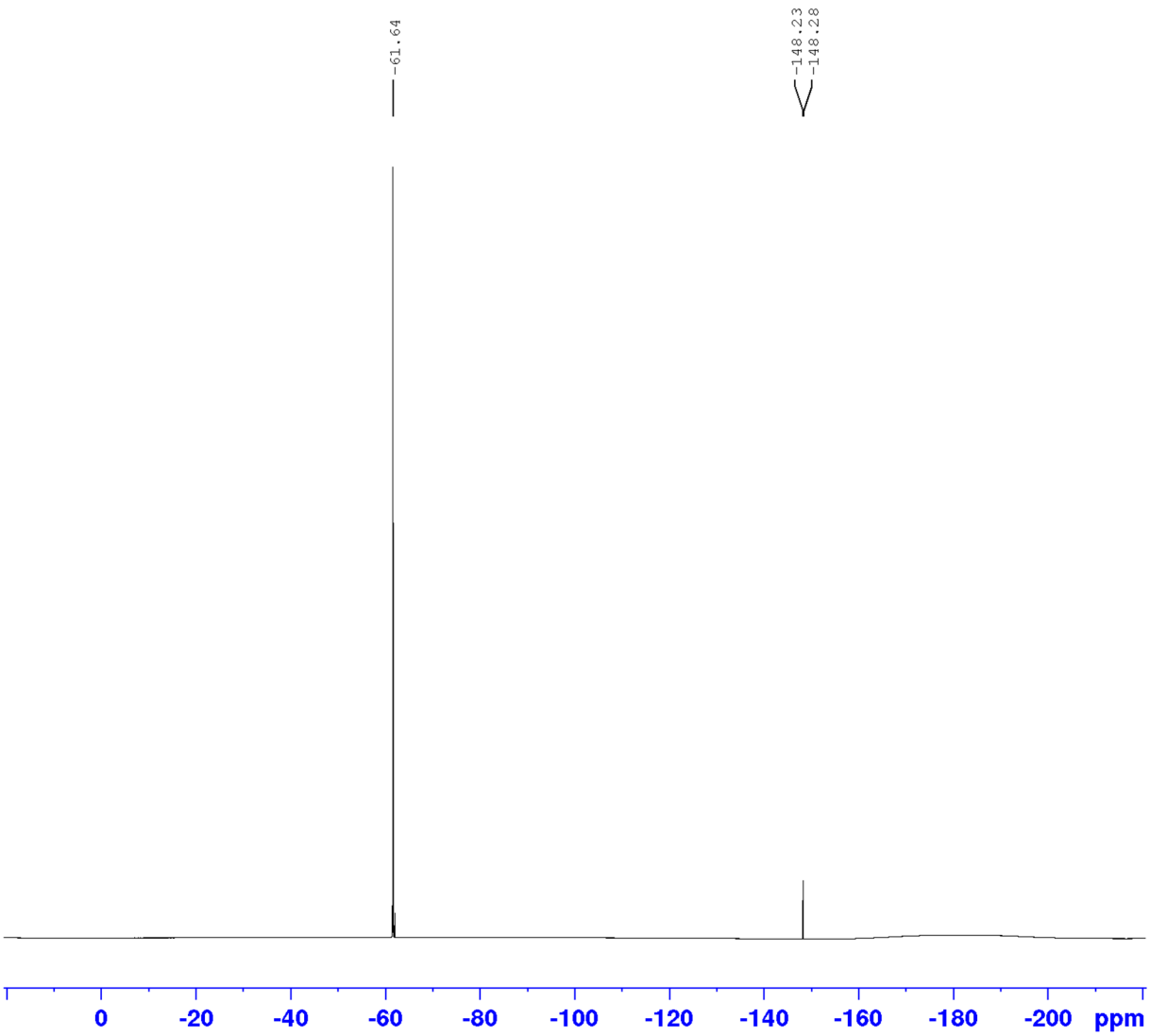


**Figure S31:** $^{19}F$ NMR (470 MHz, DMSO-d6, 25 °C) of [Ag(3,5-bis-$CF_3$-BIAN)$_2$]$BF_4$ **Ag1**.

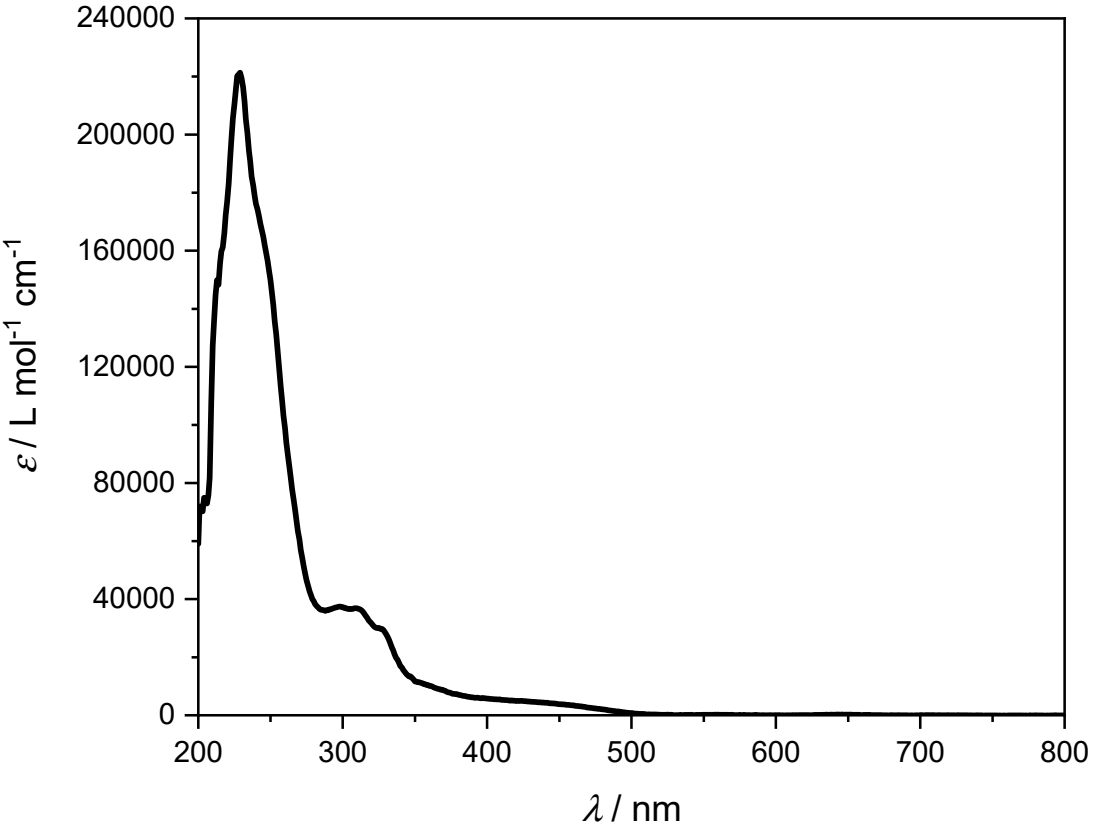


**Figure S32:** UV-vis absorption spectrum of [Ag(3,5-bis-$CF_3$-BIAN)$_2$]$BF_4$ **Ag1** in THF.

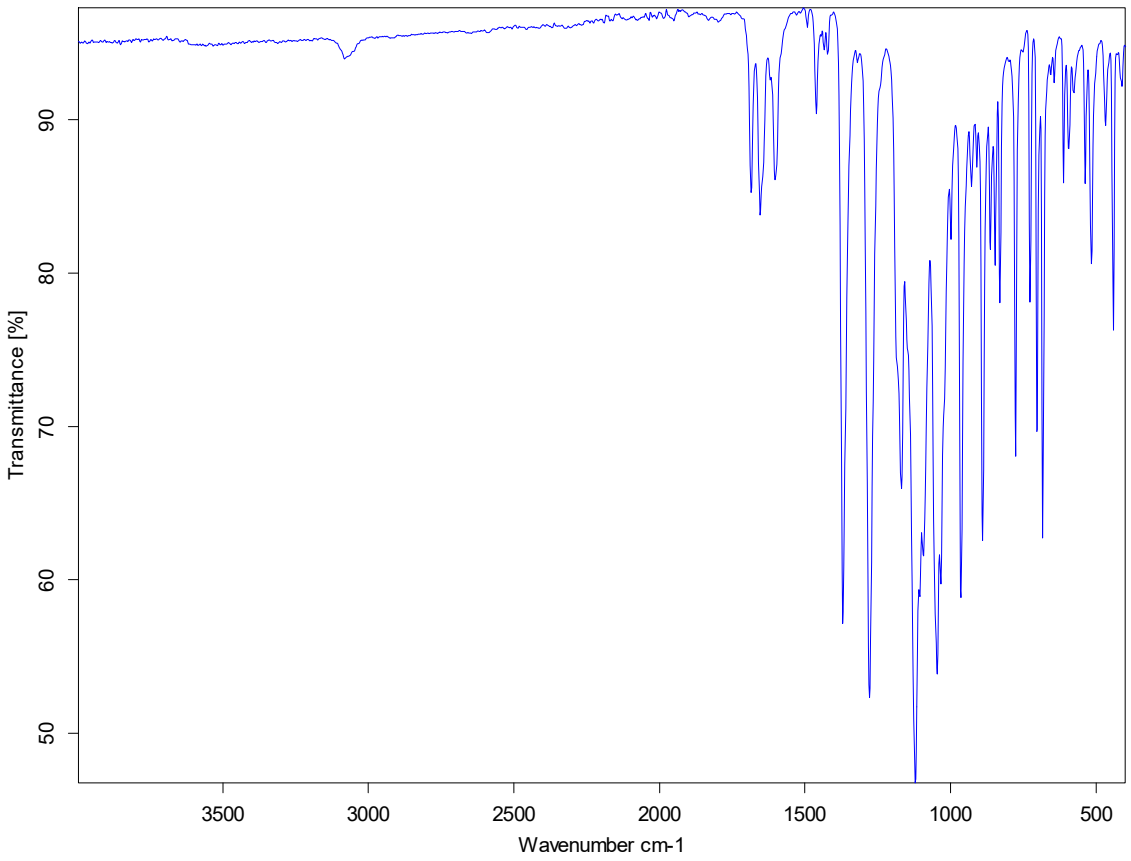


**Figure S33:** IR absorption spectrum of [Ag(3,5-bis-$CF_3$-BIAN)$_2$]$BF_4$ **Ag1**.

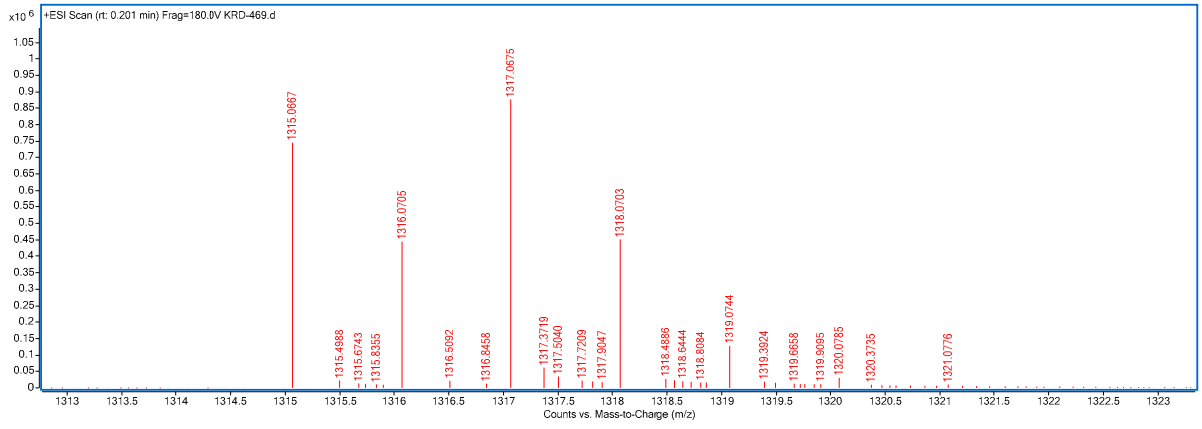


**Figure S34:** HRMS spectrum of [Ag(3,5-bis-$CF_3$-BIAN)$_2$]$BF_4$ **Ag1**.

## [Ag(2,6-dipp-BIAN)$_2$]BF$_4$ (Ag2)

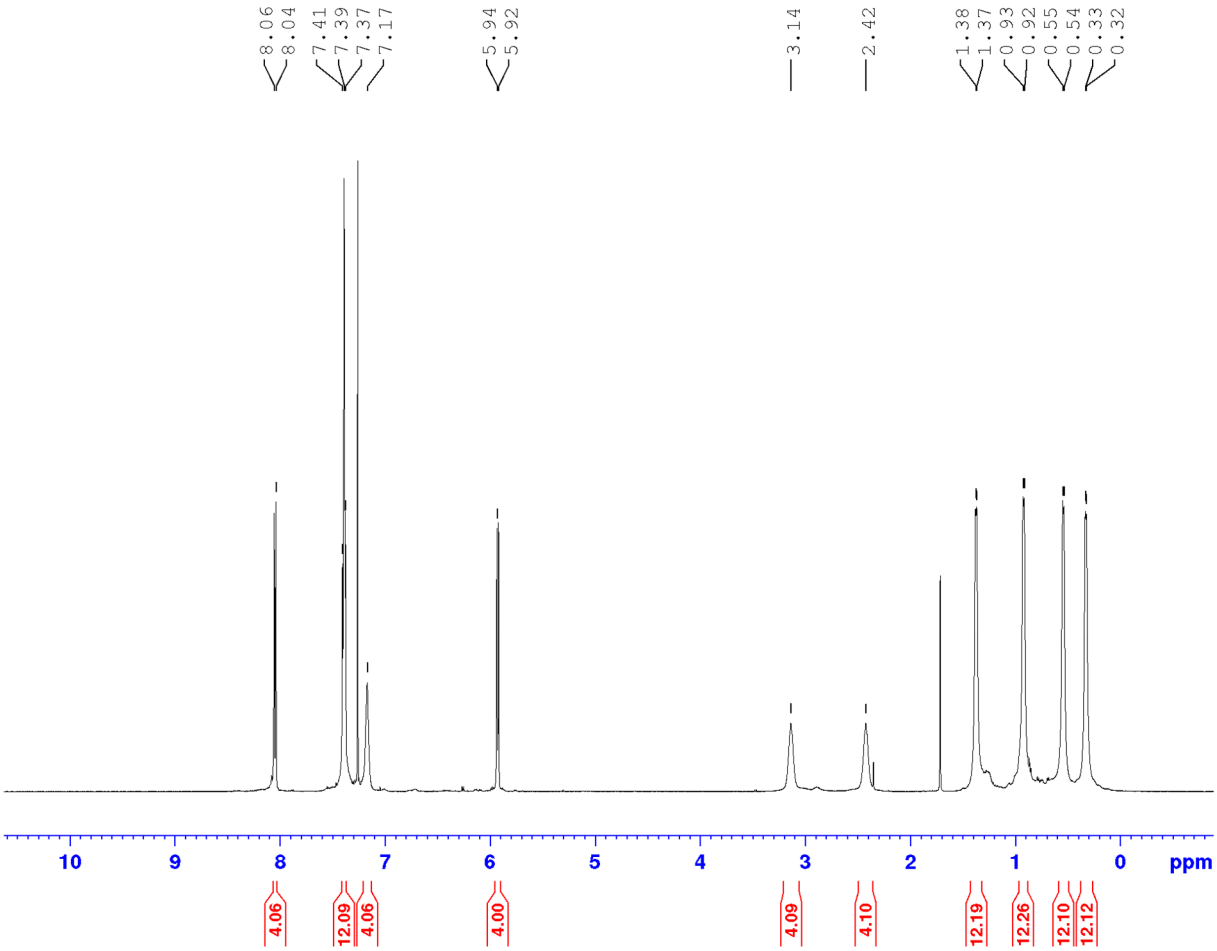


**Figure S35:** $^1$H NMR (500 MHz, $CDCl_3$, 0 °C) of [Ag(2,6-dipp-BIAN)$_2$]BF$_4$ **Ag2**.

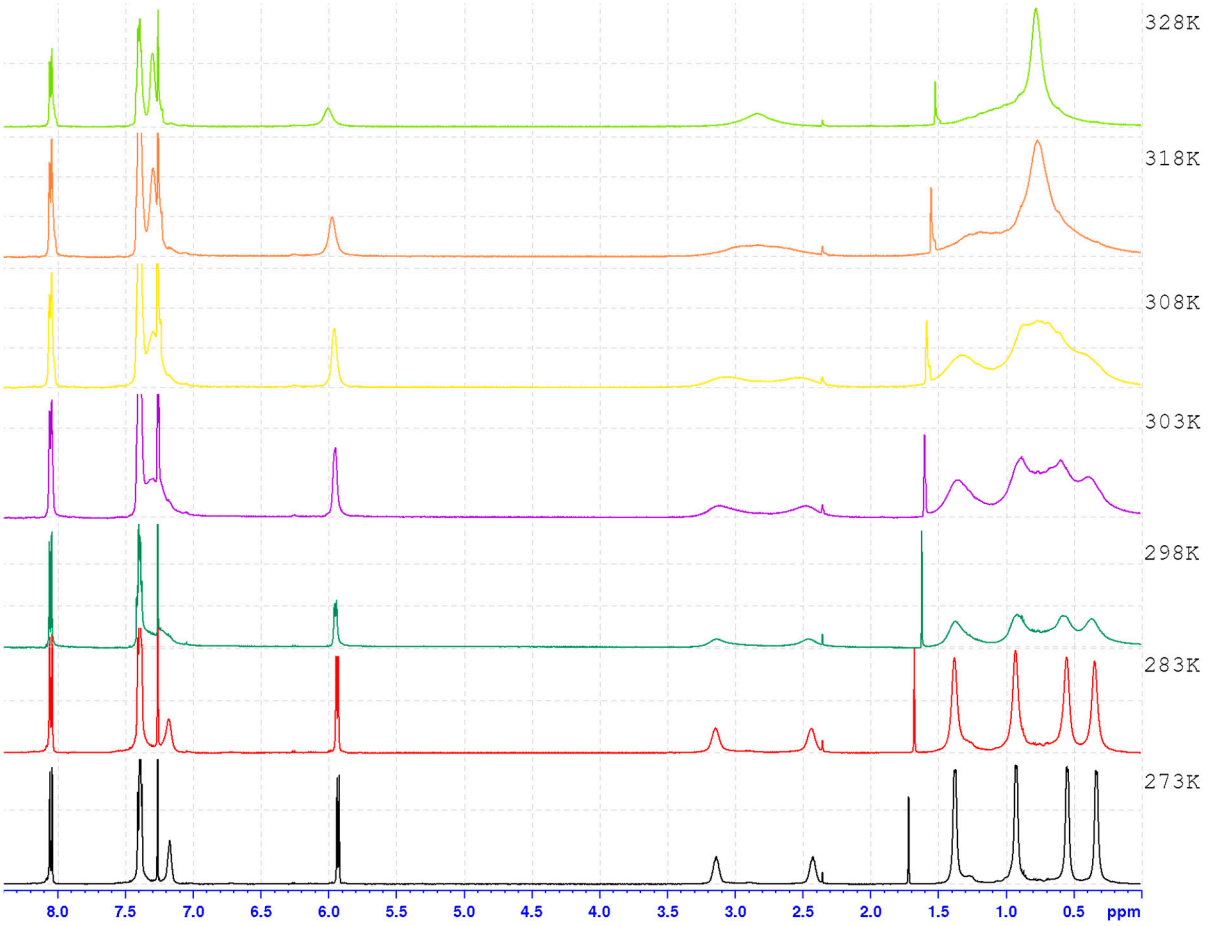


**Figure S36:** Stacked $^{1}$H NMR spectra (500 MHz, $CDCl_3$) of $[Ag(2,6\text{-dipp-BIAN})_2]BF_4$ **Ag2** at various temperatures from 0 °C (bottom) to 55 °C (top).

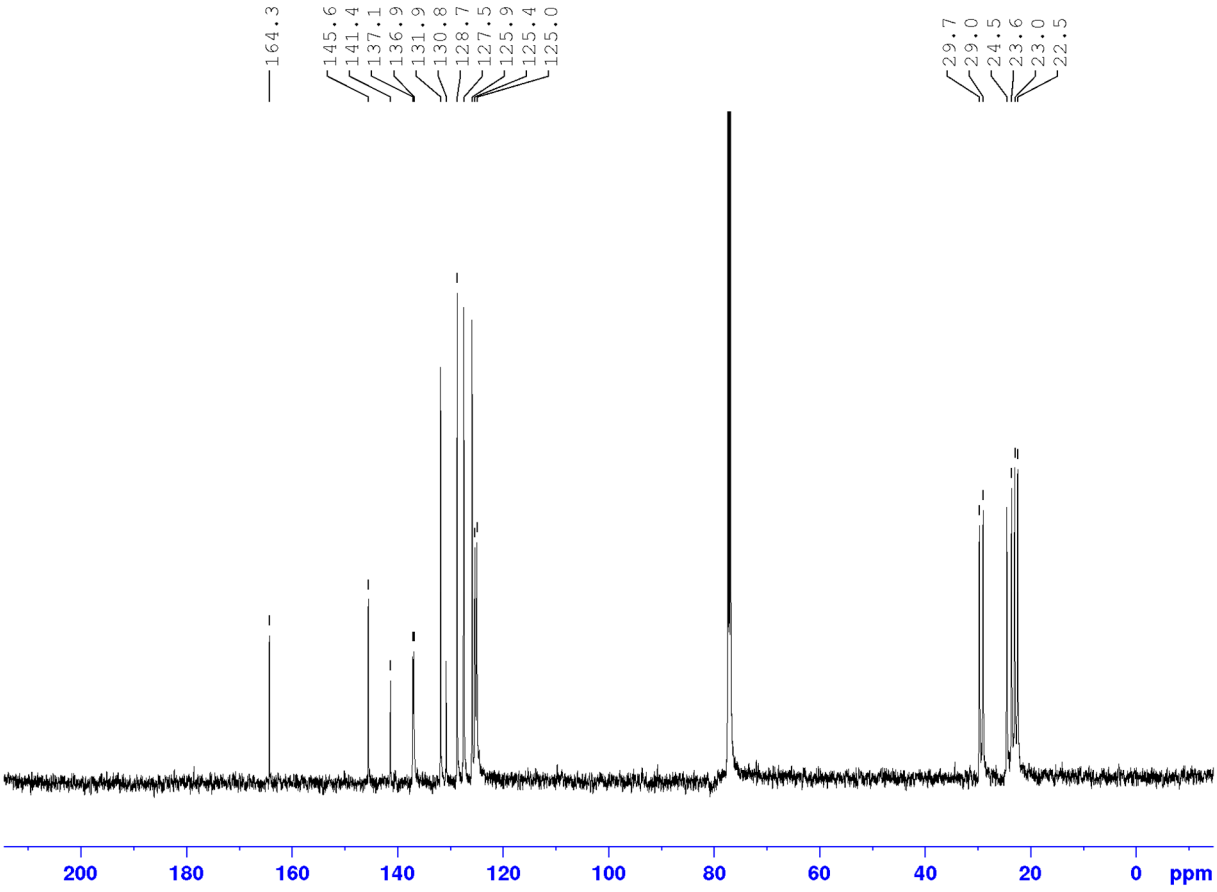


**Figure S37:** $^{13}C$ NMR (126 MHz, $CDCl_3$, 0 °C) of $[Ag(2,6\text{-dipp-BIAN})_2]BF_4$ **Ag2**.

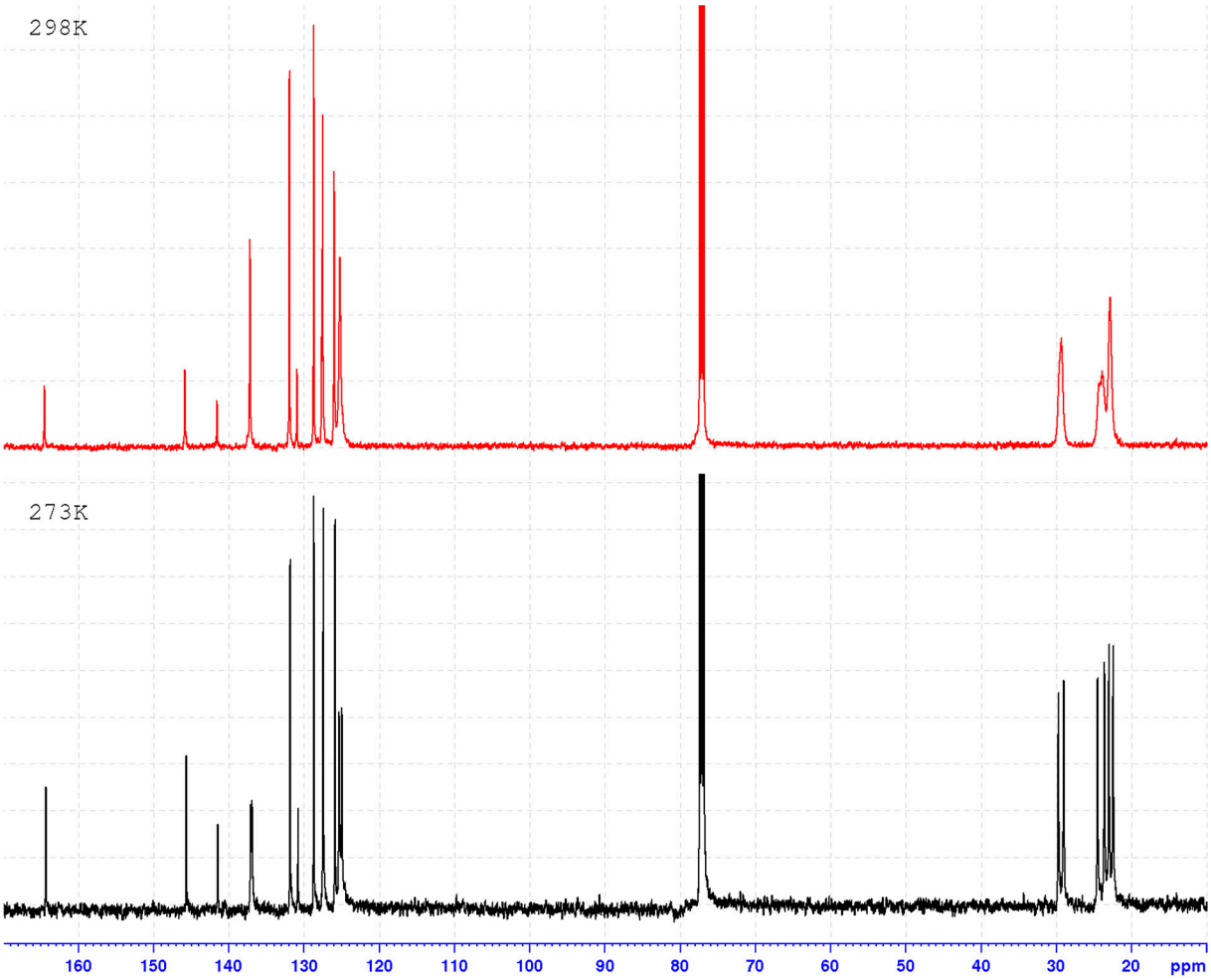


**Figure S38:** Stacked $^{13}C$ NMR spectra (126 MHz, $CDCl_3$) of $[Ag(2,6\text{-dipp-BIAN})_2]BF_4$ **Ag2** at 0 °C (bottom) and 25 °C (top).

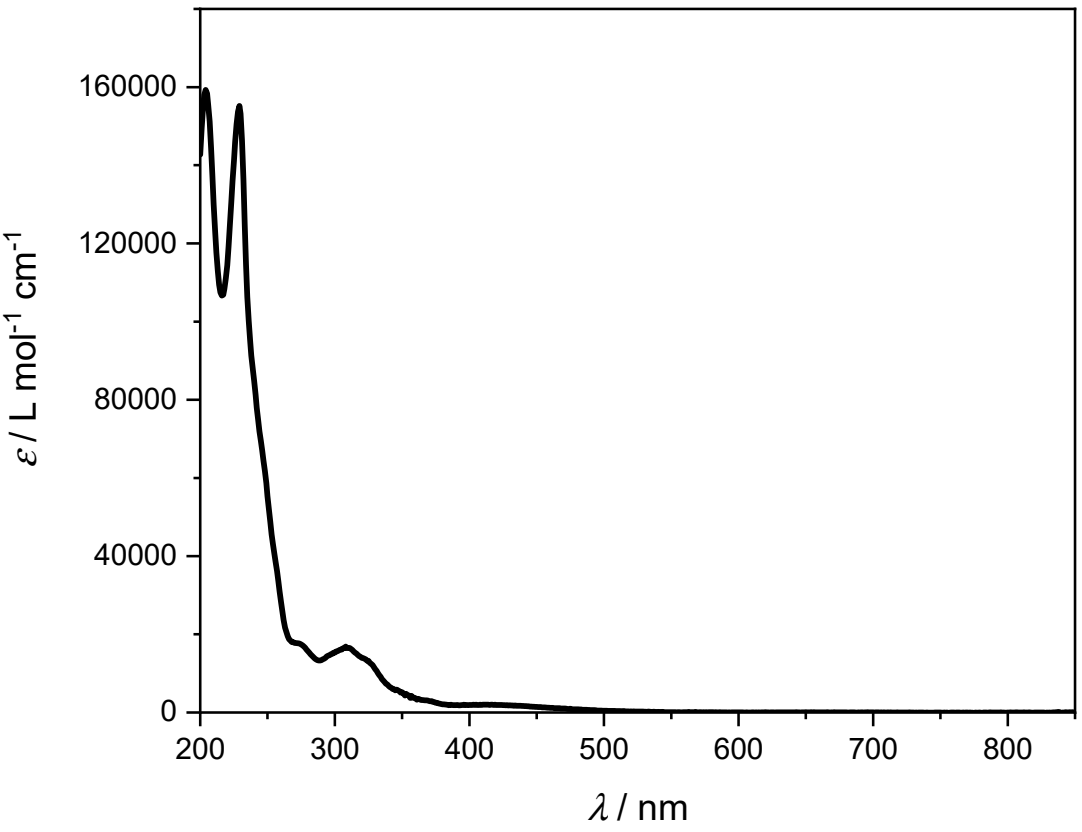


**Figure S39:** UV-vis absorption spectrum of $[Ag(2,6\text{-dipp-BIAN})_2]BF_4$ **Ag2** in ACN.

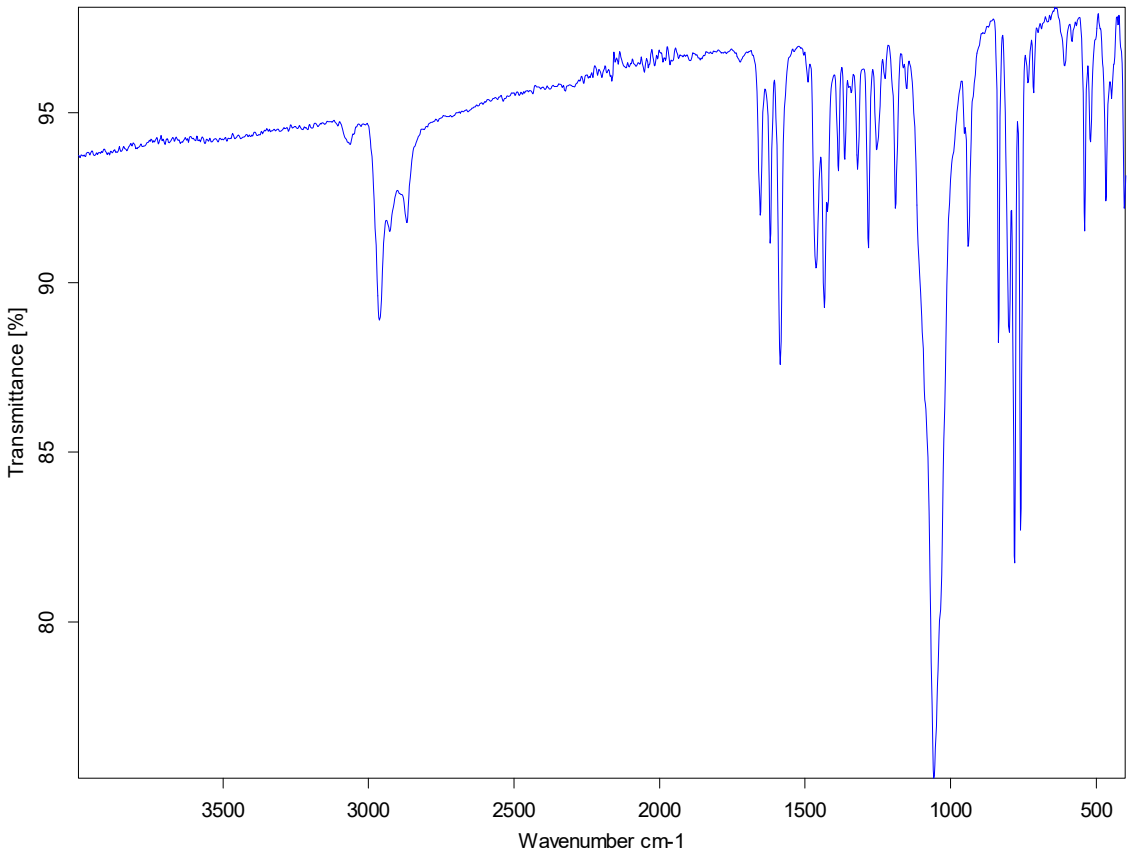


**Figure S40:** IR absorption spectrum of $[Ag(2,6\text{-dipp-BIAN})_2]BF_4$ **Ag2**.

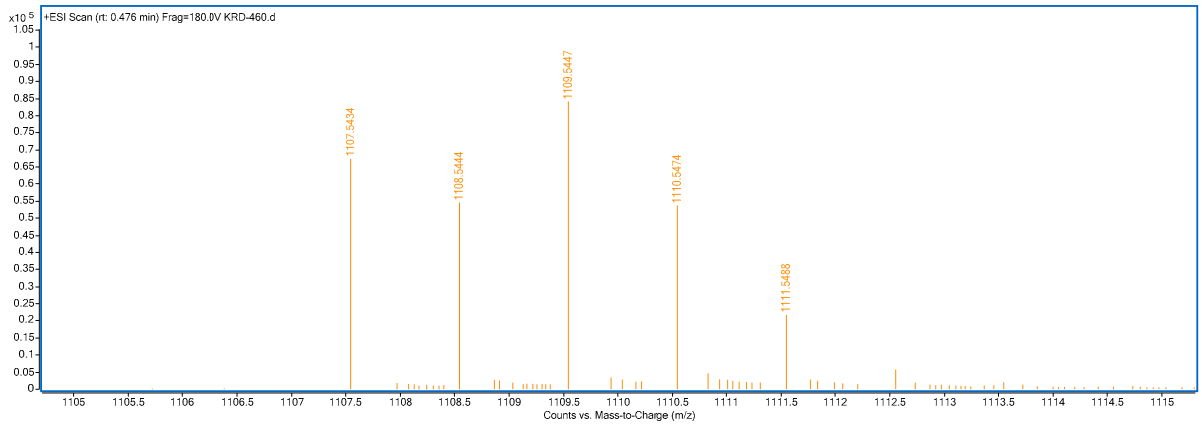


**Figure S41:** HRMS spectrum of $[Ag(2,6\text{-dipp-BIAN})_2]BF_4$ **Ag2**.

## [Ag(1-pyrene-BIAN)$_2$]BF$_4$ (Ag3)

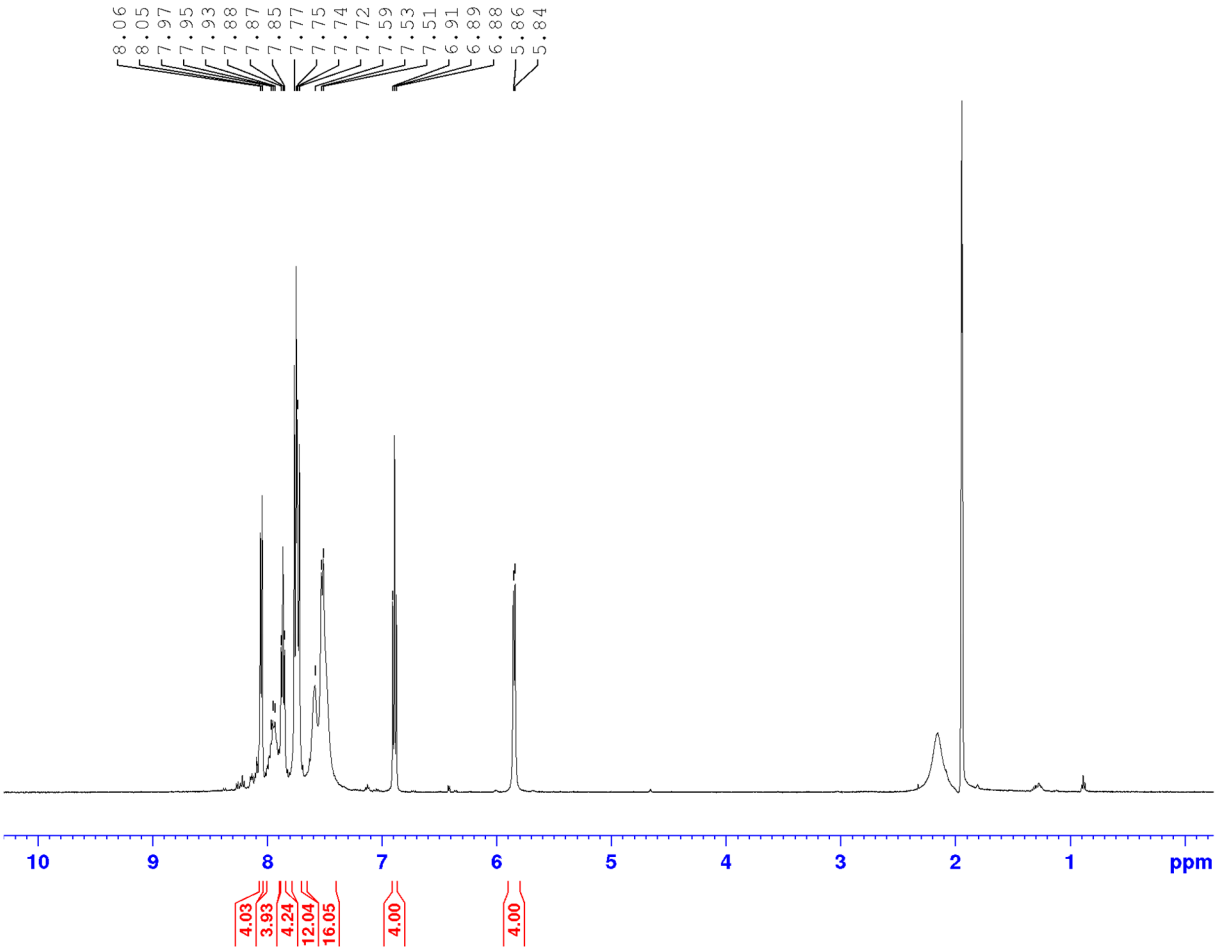


**Figure S42:** $^1$H NMR (500 MHz, $CD_3CN$, 25 °C) of [Ag(1-pyrene-BIAN)$_2$]BF$_4$ **Ag3**.

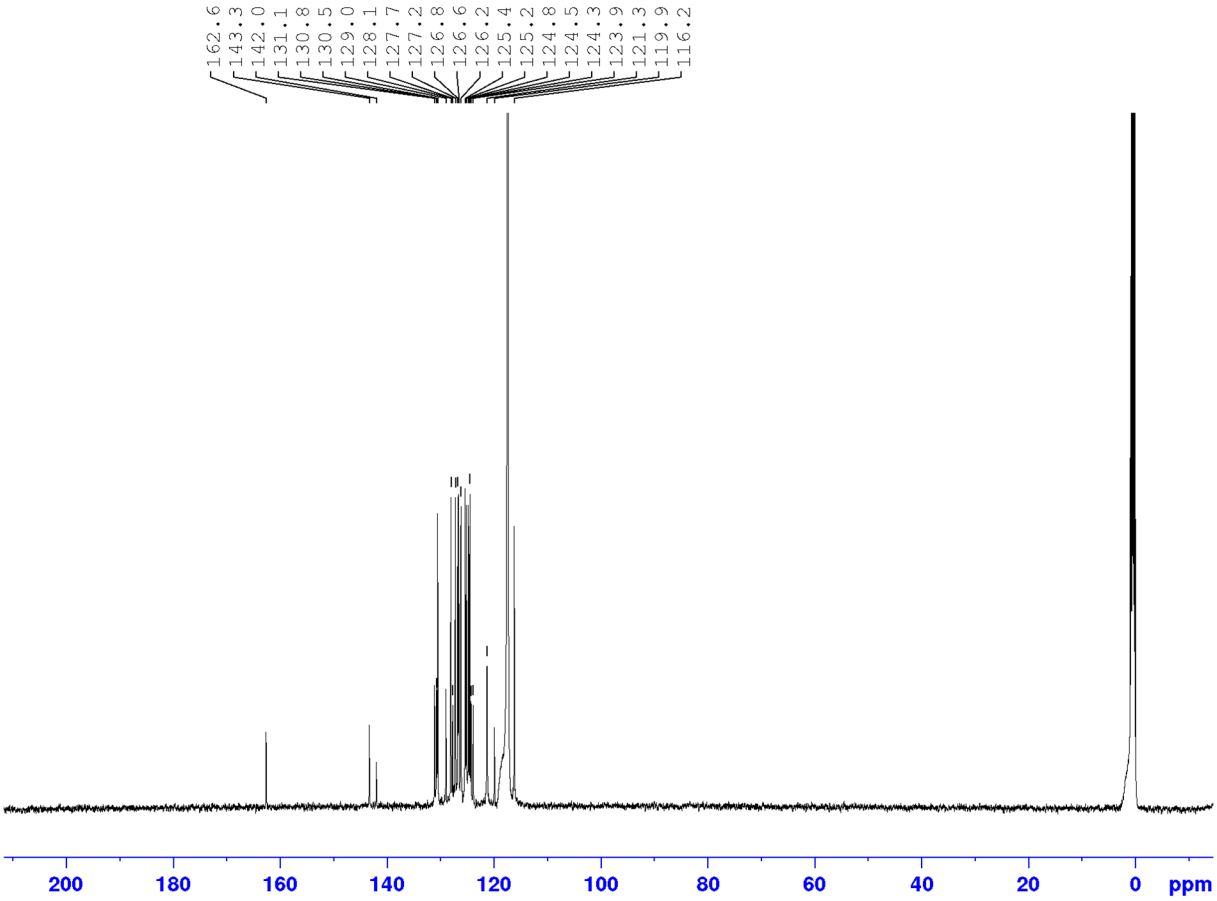


**Figure S43:** $^{13}C$ NMR (126 MHz, $CD_3CN$, 25 °C) of $[Ag(1\text{-pyrene-BIAN})_2]BF_4$ **Ag3**.

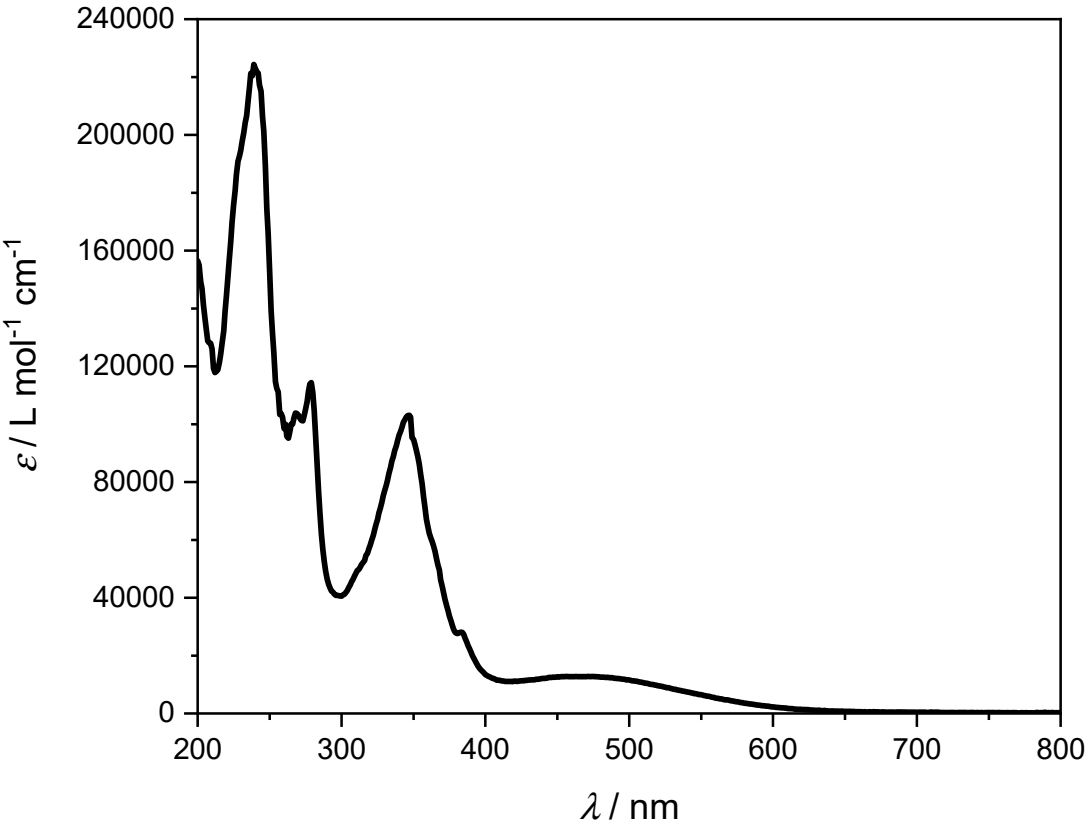


**Figure S44:** UV-vis absorption spectrum of $[Ag(1\text{-pyrene-BIAN})_2]BF_4$ **Ag3** in ACN.

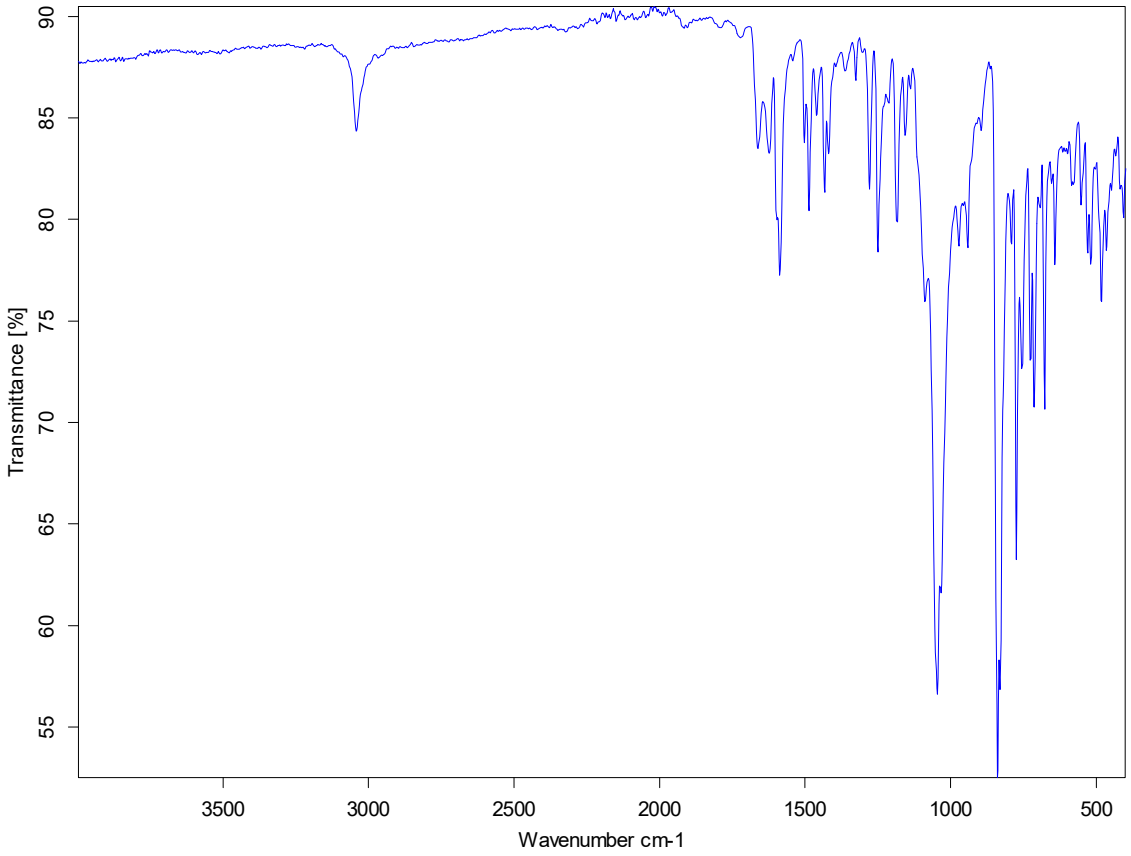


**Figure S45:** IR absorption spectrum of [Ag(1-pyrene-BIAN)$_2$]BF$_4$ **Ag3**.

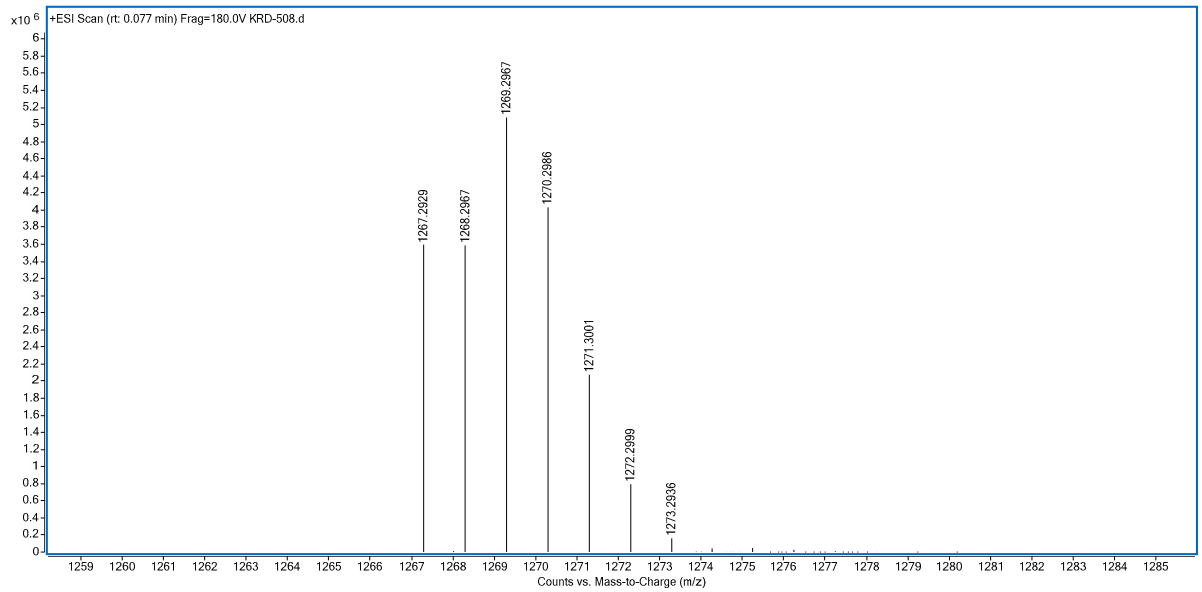


**Figure S46:** HRMS spectrum of [Ag(1-pyrene-BIAN)$_2$]BF$_4$ **Ag3**.

## [Ag(4-OMe-BIAN)$_2$]BF$_4$ (Ag4)

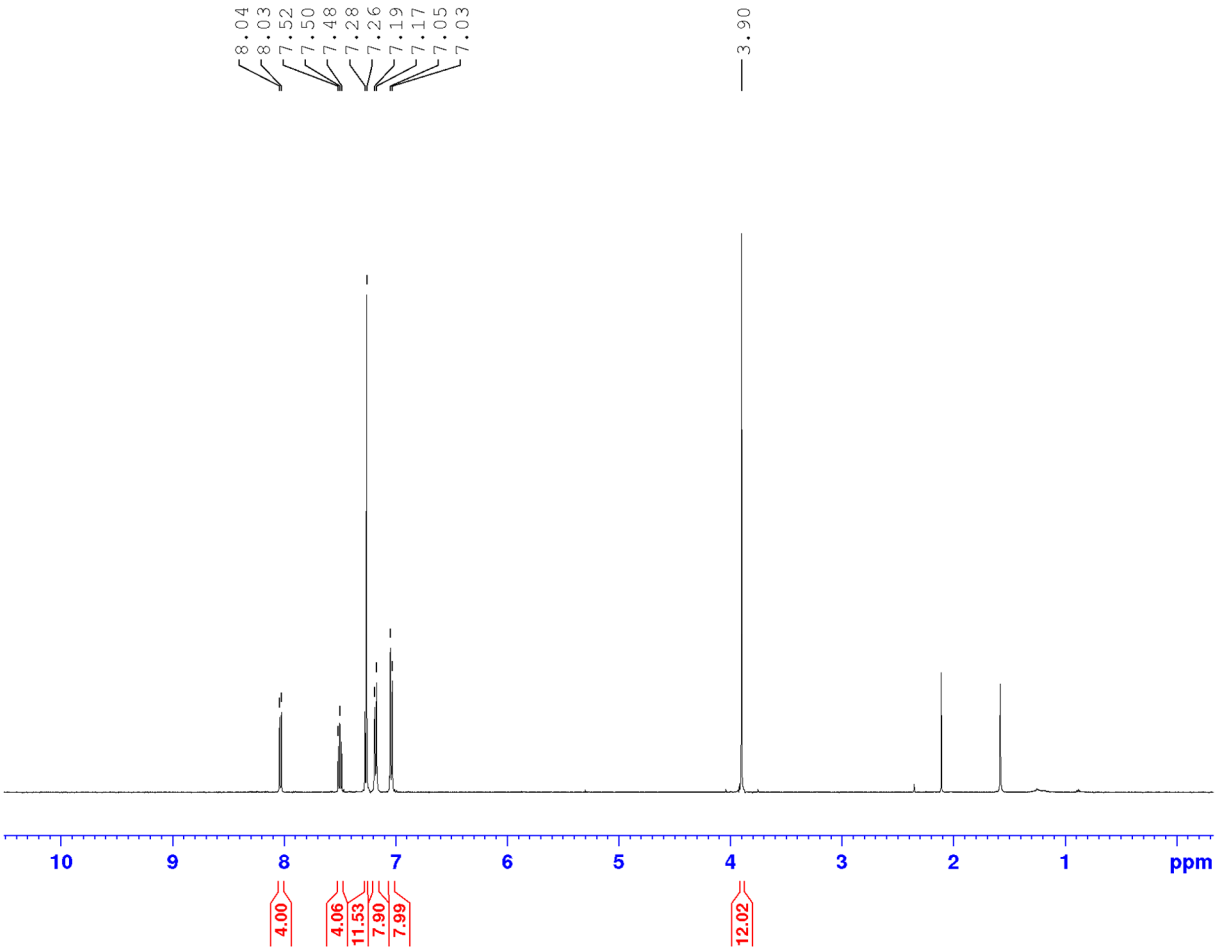


**Figure S47:** $^1$H NMR (500 MHz, $CDCl_3$, 25 °C) of [Ag(4-OMe-BIAN)$_2$]BF$_4$ **Ag4**.

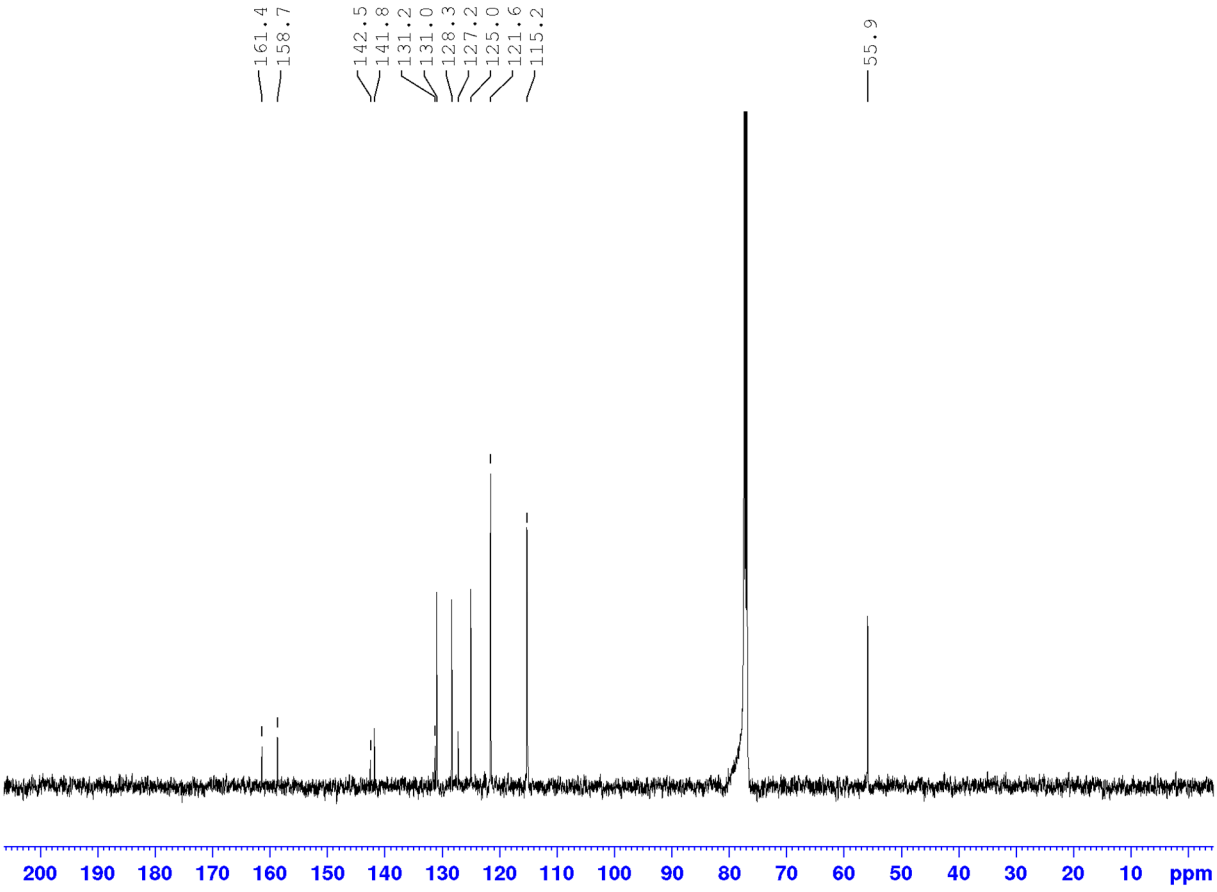


**Figure S48:** $^{13}C$ NMR (126 MHz, $CDCl_3$, 25 °C) of $[Ag(4\text{-OMe-BIAN})_2]BF_4$ **Ag4**.

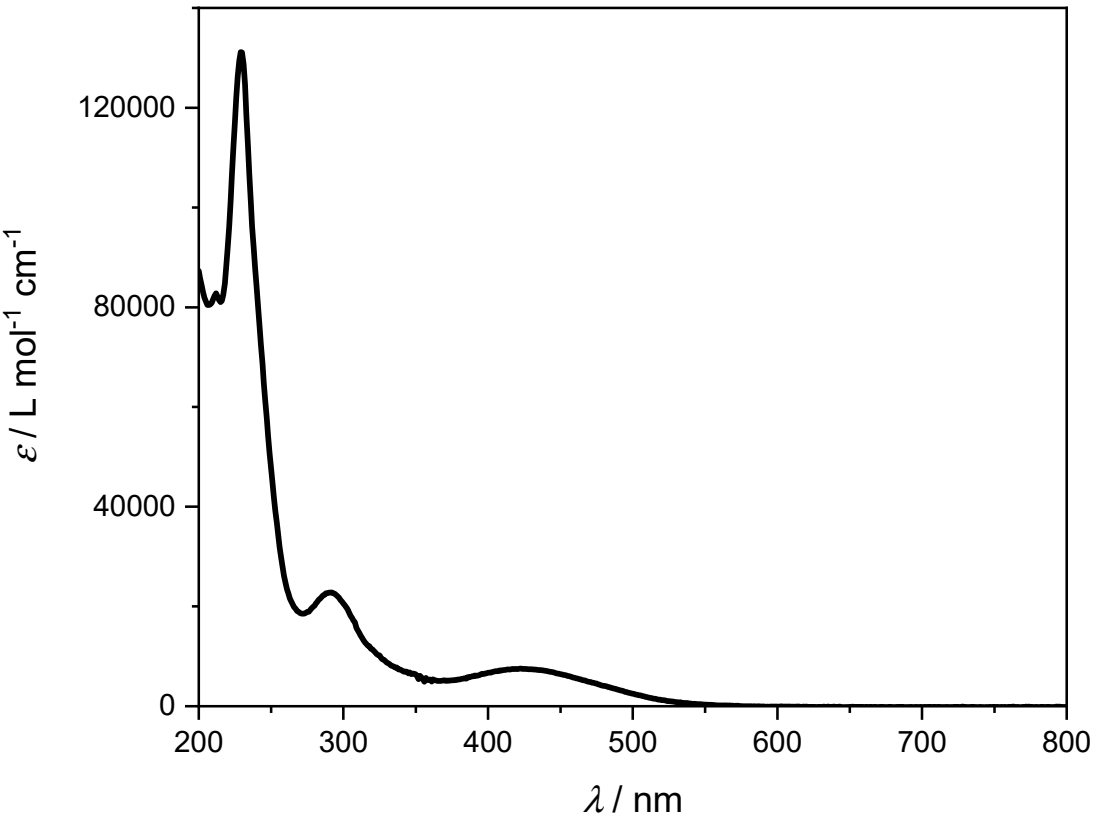


**Figure S49:** UV-vis absorption spectrum of $[Ag(4\text{-OMe-BIAN})_2]BF_4$ **Ag4** in ACN.

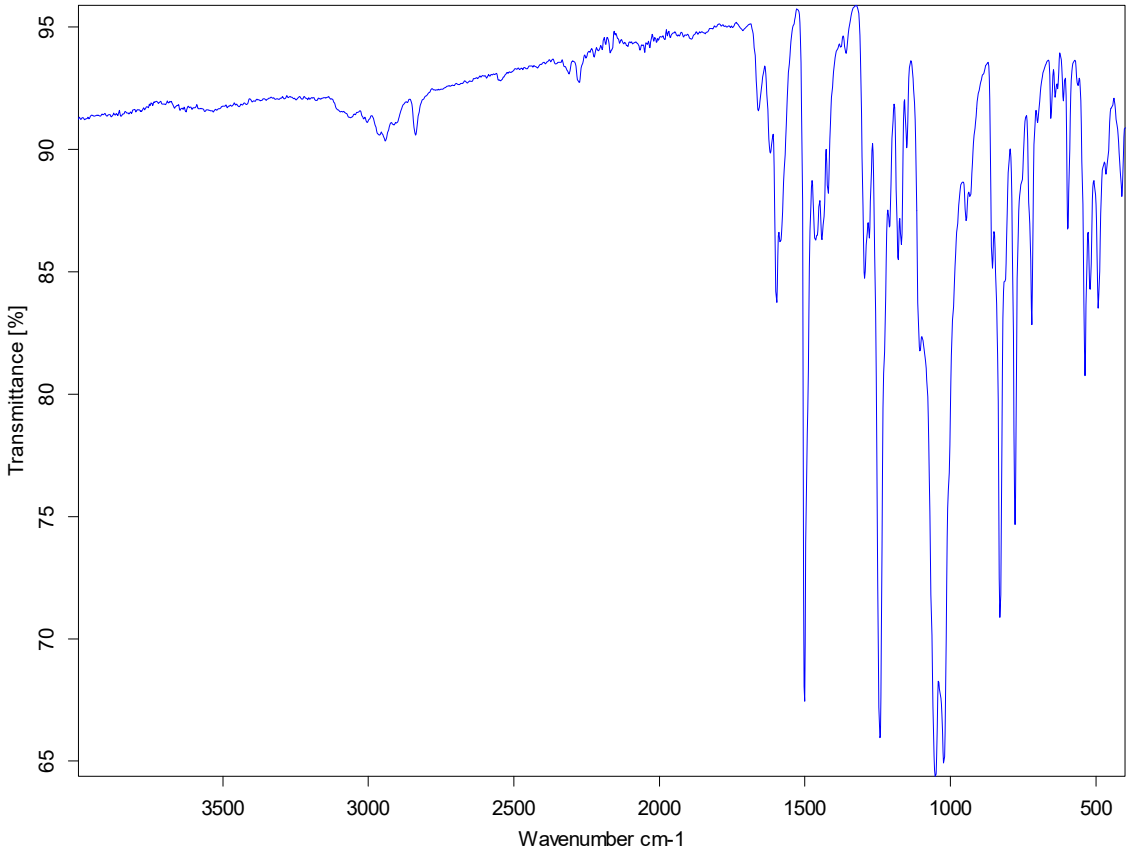


**Figure S50:** IR absorption spectrum of $[Ag(4\text{-OMe-BIAN})_2]BF_4$ **Ag4**.

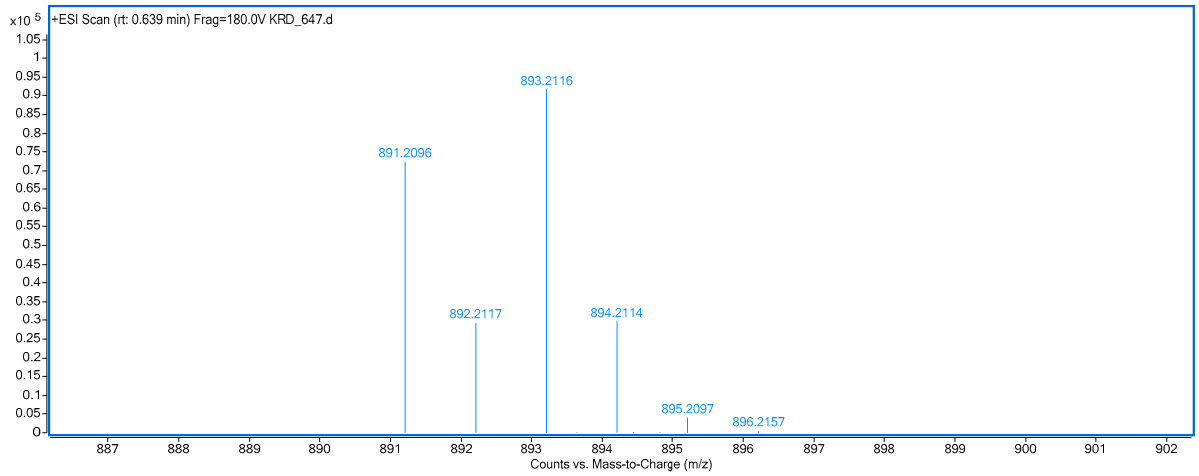


**Figure S51:** HRMS spectrum of $[Ag(4\text{-OMe-BIAN})_2]BF_4$ **Ag4**.

## [Ag(3,4,5-trimethoxy-BIAN)$_2$]BF$_4$ (Ag5)

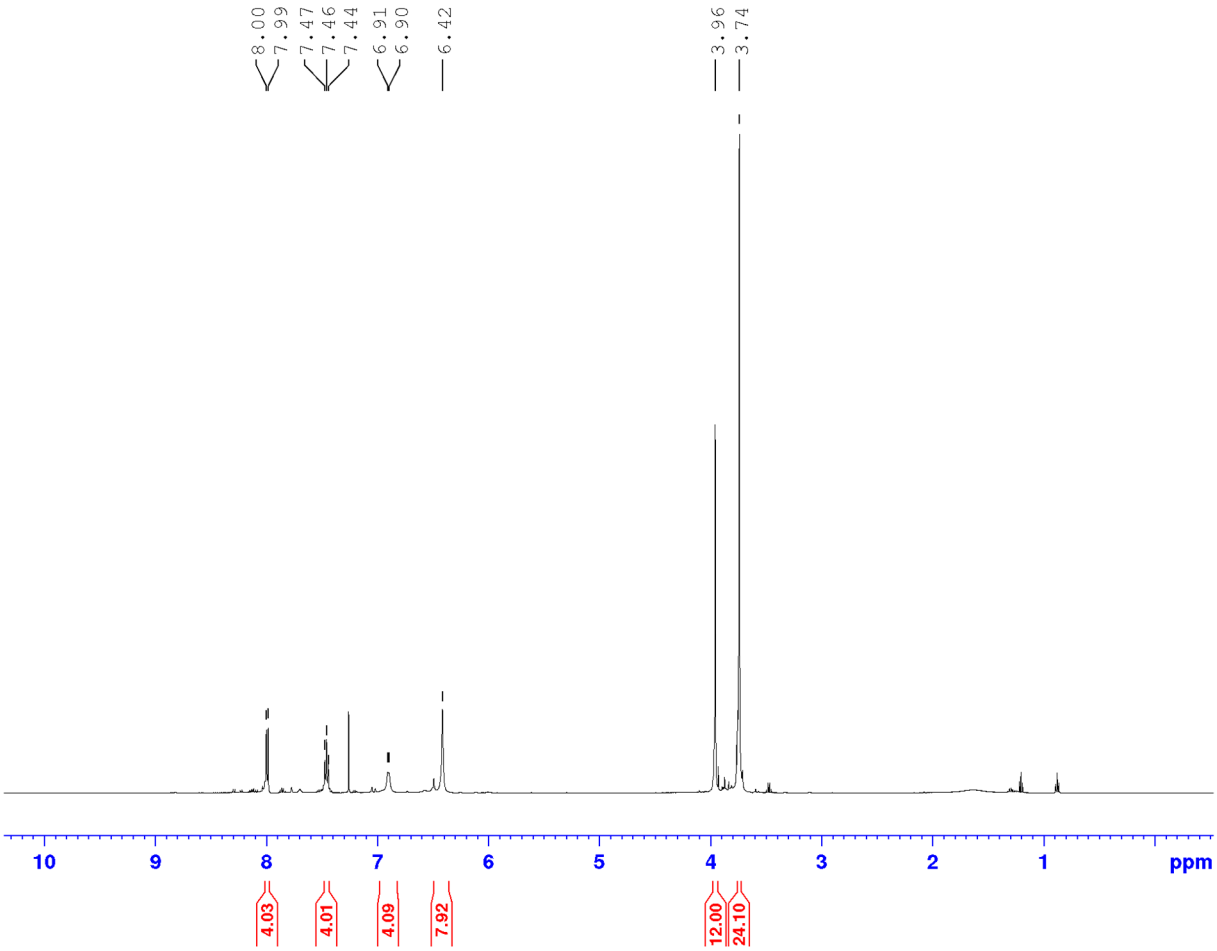


**Figure S52:** $^1$H NMR (500 MHz, $CDCl_3$, 25 °C) of [Ag(3,4,5-tri-OMe-BIAN)$_2$]BF$_4$ **Ag5**.

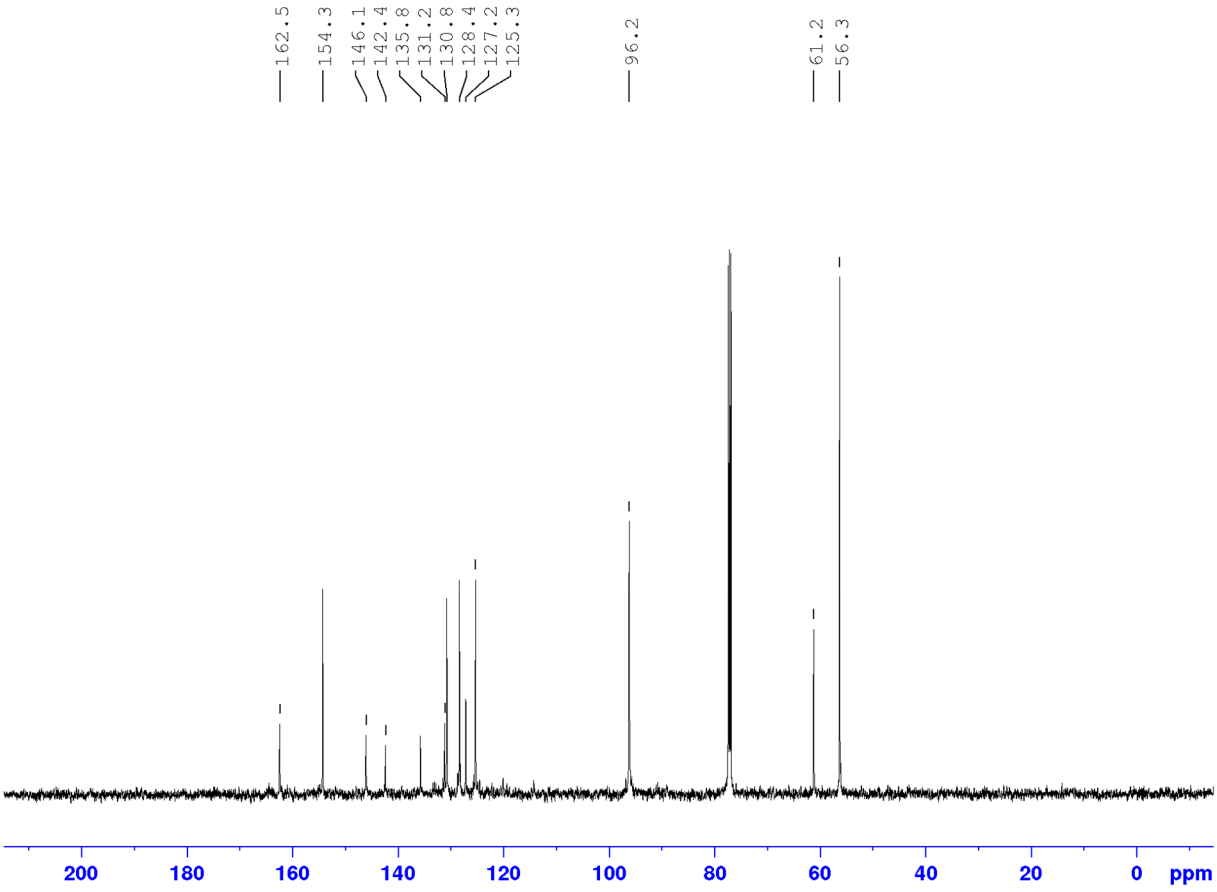


**Figure S53:** $^{13}C$ NMR (126 MHz, $CDCl_3$, 25 °C) of $[Ag(3,4,5\text{-tri-OMe-BIAN})_2]BF_4$ **Ag5**.

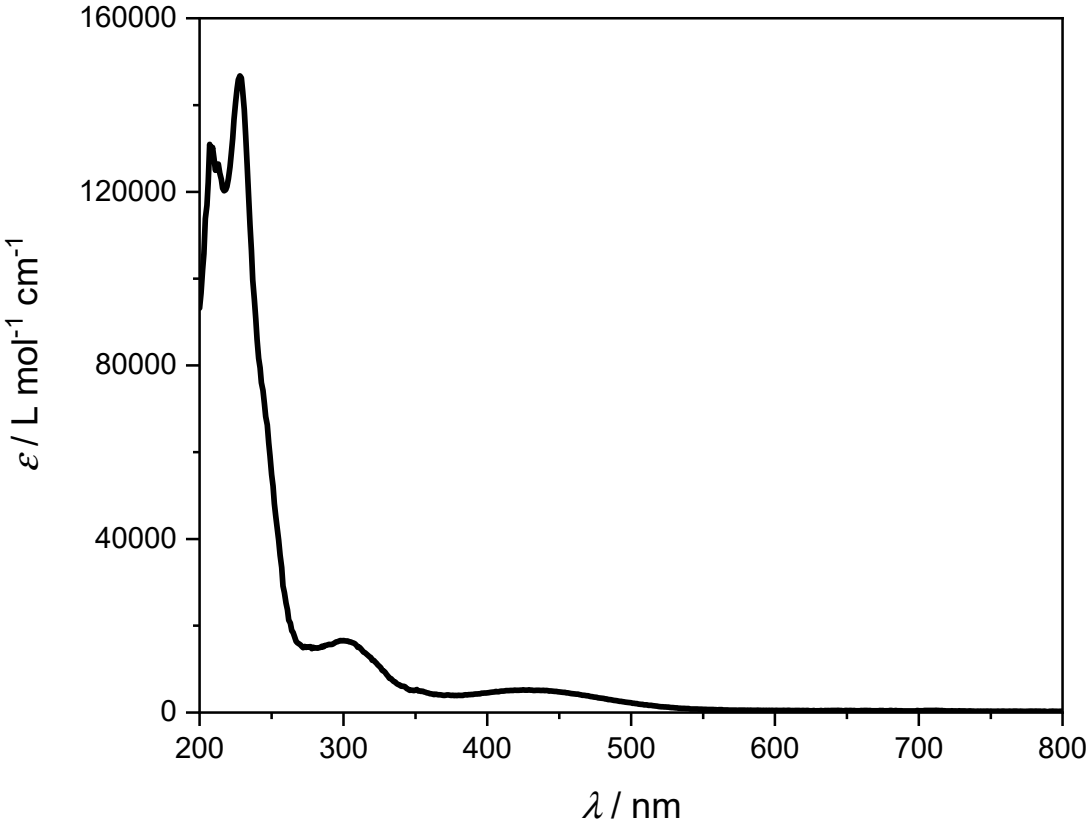


**Figure S54:** UV-vis absorption spectrum of $[Ag(3,4,5\text{-tri-OMe-BIAN})_2]BF_4$ **Ag5** in ACN.

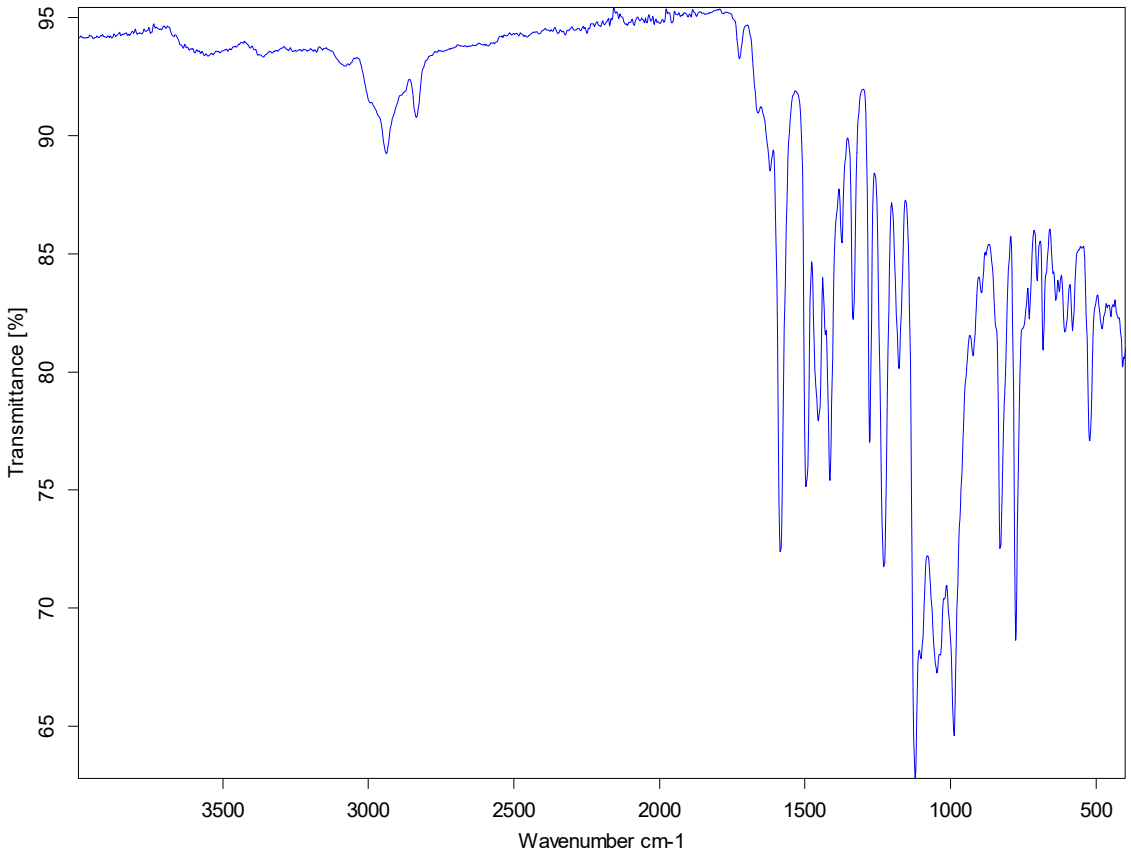


**Figure S55:** IR absorption spectrum of $[Ag(3,4,5\text{-tri-OMe-BIAN})_2]BF_4$ **Ag5**.

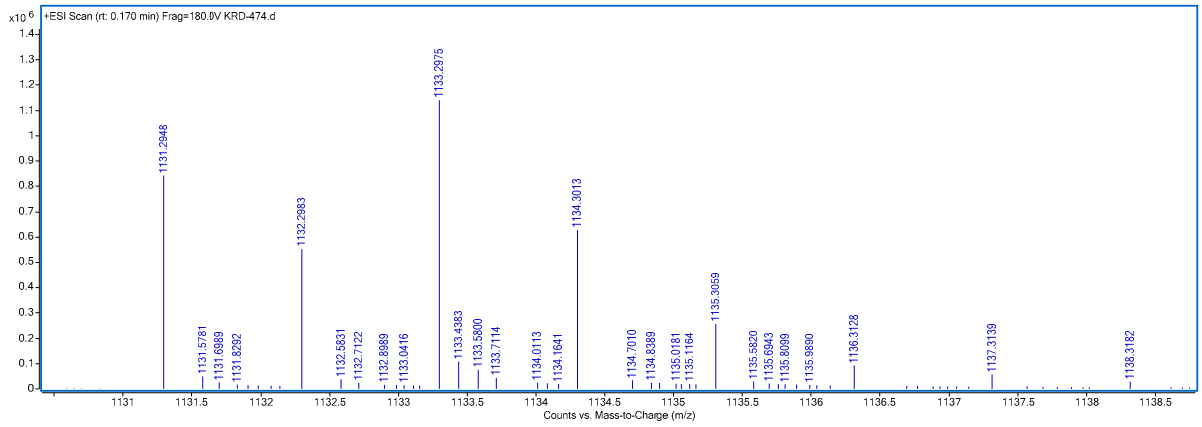


**Figure S56:** HRMS spectrum of $[Ag(3,4,5\text{-tri-OMe-BIAN})_2]BF_4$ **Ag5**.

## [Ag(4-diethylamino-BIAN)$_2$]BF$_4$ (Ag6)

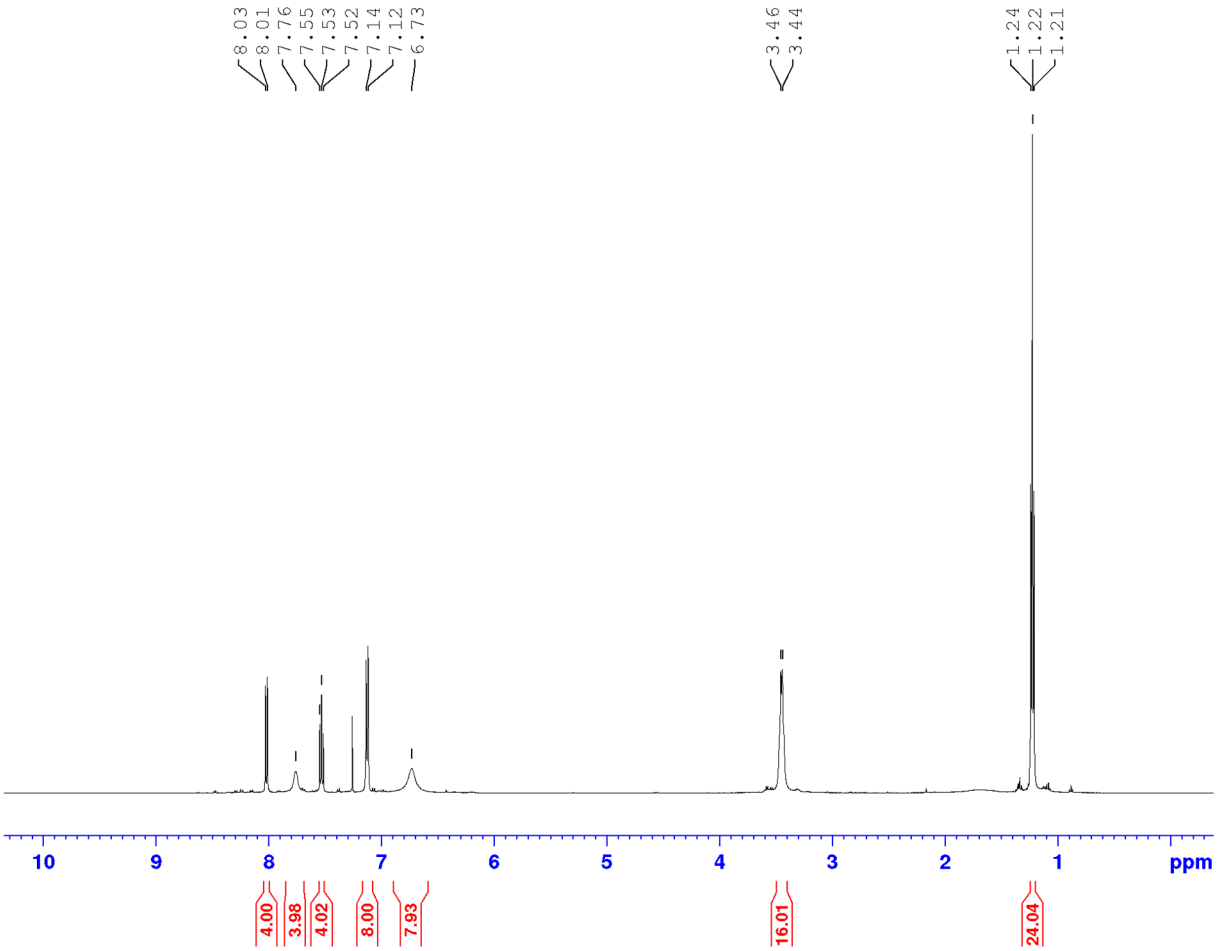


**Figure S57:** $^1$H NMR (500 MHz, $CDCl_3$, 25 °C) of [Ag(4-diethylamino-BIAN)$_2$]BF$_4$ **Ag6**.

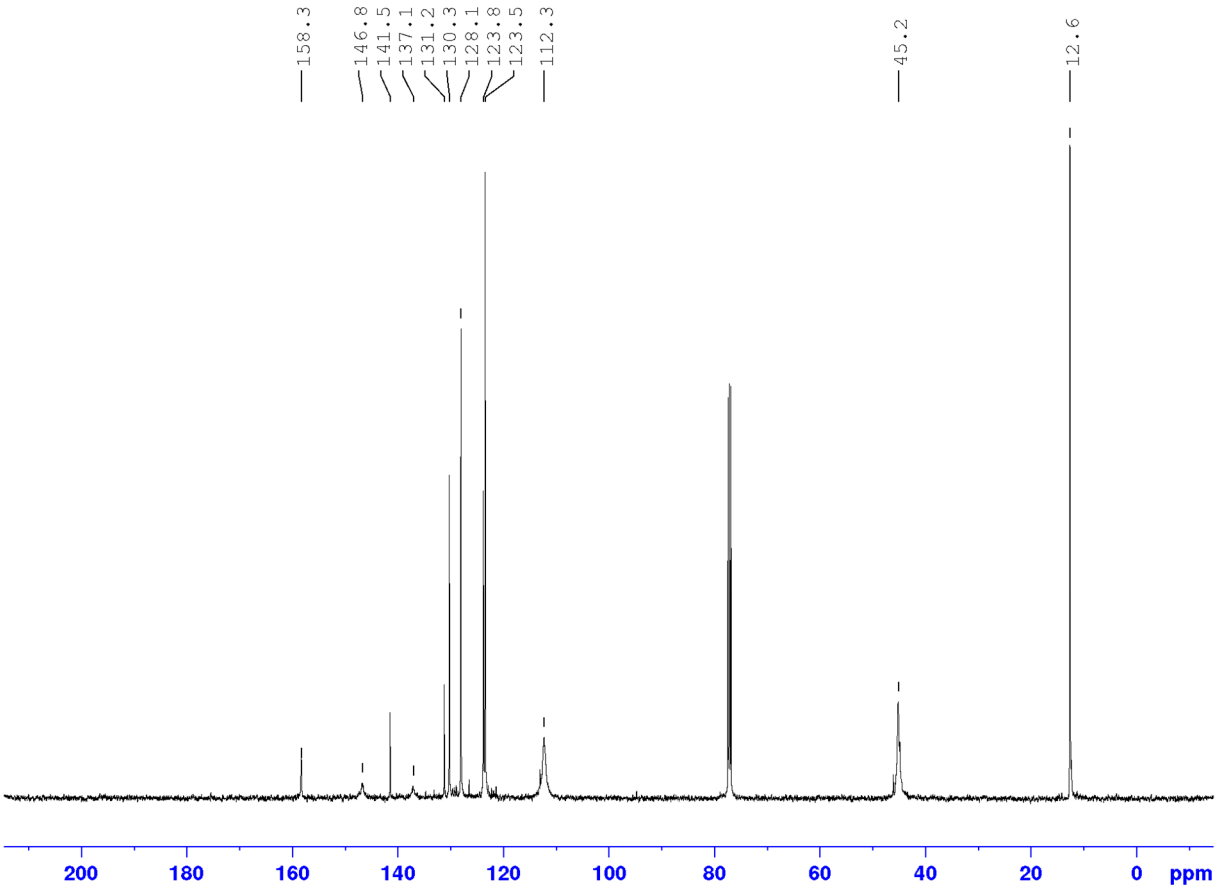


**Figure S58:** $^{13}C$ NMR (126 MHz, $CDCl_3$, 25 °C) of [Ag(4-diethylamino-BIAN)$_2$]$BF_4$ **Ag6**.

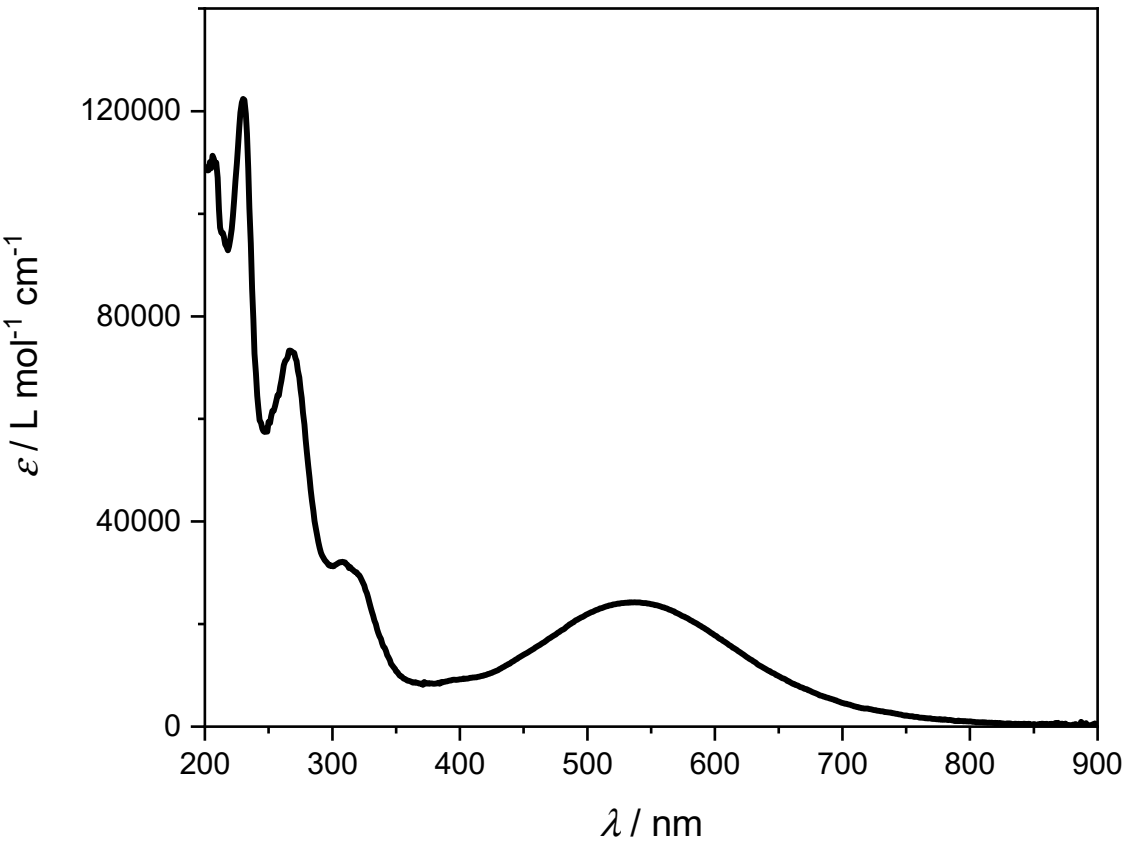


**Figure S59:** UV-vis absorption spectrum of $[Ag(4\text{-diethylamino-BIAN})_2]BF_4$ **Ag6** in ACN.

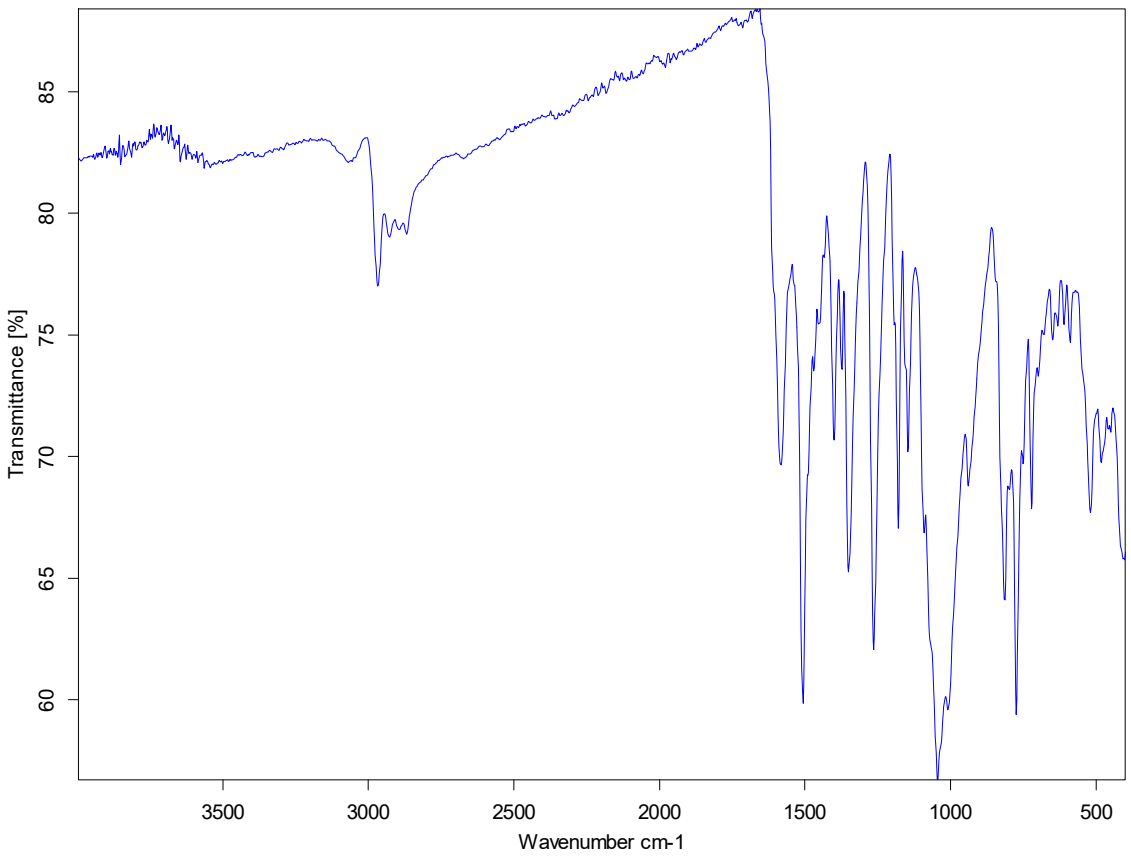


**Figure S60:** IR absorption spectrum of [Ag(4-diethylamino-BIAN)$_2$]BF$_4$ **Ag6**.

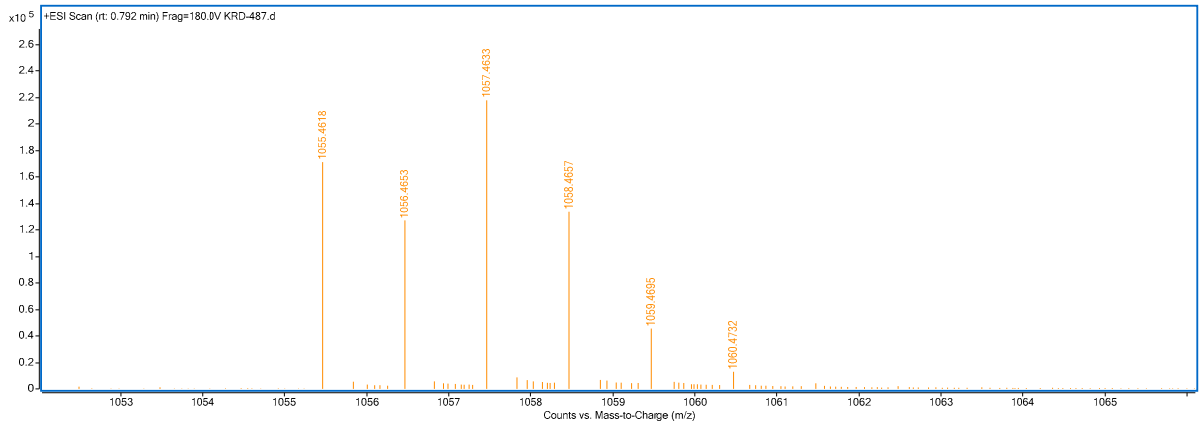


**Figure S61:** HRMS spectrum of [Ag(4-diethylamino-BIAN)$_2$]BF$_4$ **Ag6**.

## XPS data

### General

XPS measurements were performed on a Theta Probe XPS system (Thermofisher, GBR), which features a monochromated Al-$K_\alpha$ X-ray source with an energy of 1486.6 eV. The spot size on the sample surface was 400 µm in diameter. The hemispherical analyzer was set to a pass energy of 20 eV for the recorded high resolution (HR) scans at an energy step size of 0.05 eV. For charge neutralization on the sample surface the system is equipped with a dual flood gun which simultaneously provides electrons and $Ar^+$ ions with low kinetic energy. The data acquisition and evaluation as well as the control of the device is performed via a software package (Avantage) provided by the system manufacturer. Generally, the data evaluation started with the elimination of the peak background by subtracting a function called smart background, provided by the Advantage software. This function is based on the Shirley background with an additional constraint so that the background cannot be of a greater intensity than the actual data at any point in the region. The reference peak for defining the binding energy for all spectra was always the C–C peak at 285 eV.

## Measurements

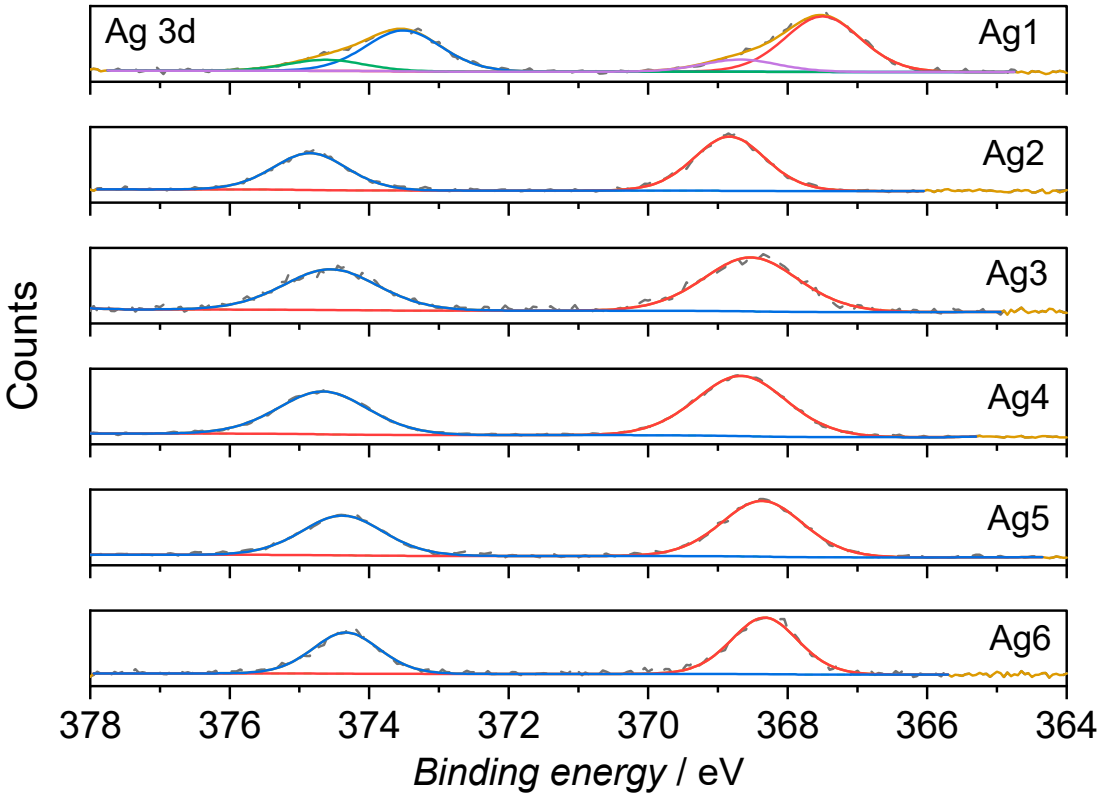


**Figure S62:** XPS spectra of Ag 3d for the explored Ag bis-BIAN complexes **Ag1** (top) to **Ag6** (bottom).

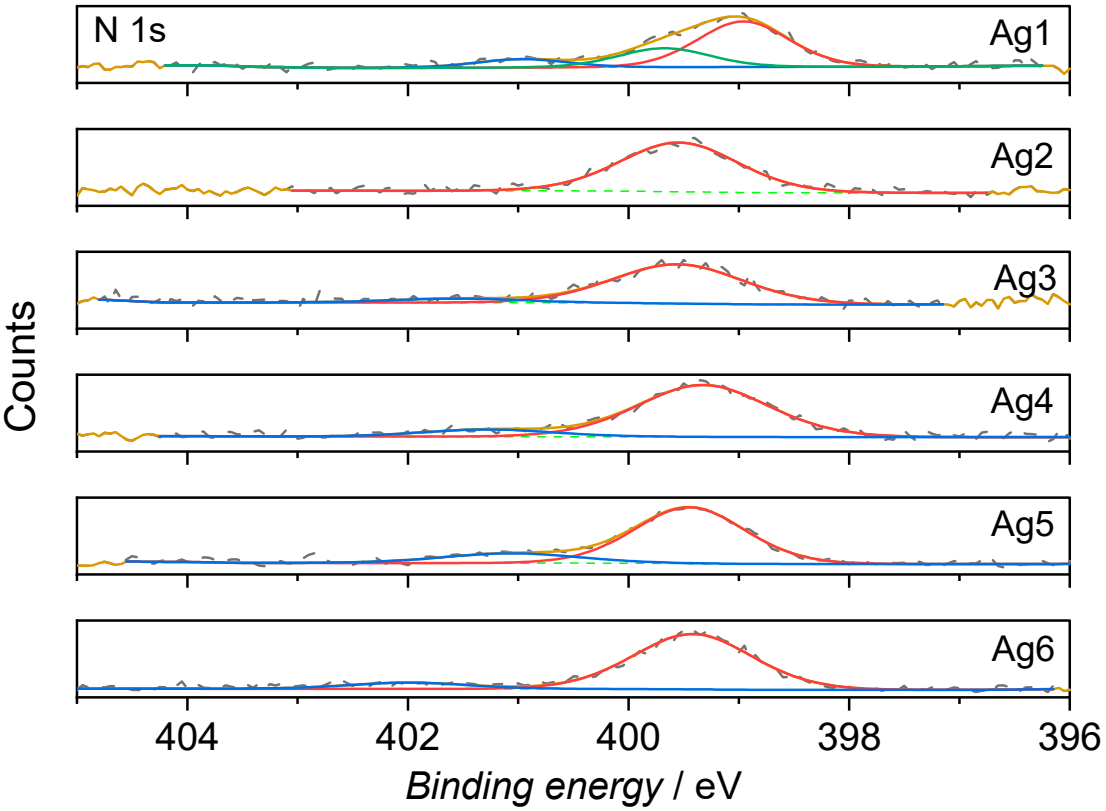


**Figure S63:** XPS spectra of N 1s for the explored Ag bis-BIAN complexes **Ag1** (top) to **Ag6** (bottom).

## Crystallographic data

### General

X-ray quality crystals were obtained *via* slow diffusion of *n*-pentane to a solution of the pertinent complex in DCM at 4 °C and then selected in Fomblin® Y H-VAC 140/13 perfluoropolyether at ambient temperature. The data was collected at 296(2) K on a *Bruker **D8 Quest Eco*** diffractometer using graphite monochromated Mo $K_\alpha$ radiation ($\lambda$ = 0.71073 Å). The data was processed using APEX3 [1], the structures were solved by intrinsic phasing (XT, Version 2018/2) [2] and refined by full matrix least squares procedures on $F^2$ (SHELXL, Version 2018/3) [3] using the graphical interface Shelxle [4] within the SHELXTL suite of programs by Bruker. All non-hydrogen atoms were refined anisotropically. All hydrogen atoms were calculated geometrically, and a riding model was applied in the refinement process. If residual electron density was found in a solvent-accessible void and it was not possible to determine and/or refine the solvent molecule, the electron density was squeezed using PLATON. [5]

### References


[1] Bruker (2019), *APEX3 v2019.11-0*, *SAINT V8.40B*, *SHELXTL-2018*, Bruker Nano, Inc.: Madison (WI), USA, **2019**.

[2] a) G. M. Sheldrick, *SHELXT-2018: Program for the Solution of Crystal Structures*, University of Göttingen, Germany, **2014**. b) G. M Sheldrick, *Acta Crystallogr., Sect. A: Found. Crystallogr.* **2008**, *64*, 112−122. c) G. M. Sheldrick, *Acta Crystallogr., Sect. A: Found. Adv.* **2015**, *71*, 3−8.

[3] a) G. M. Sheldrick, *SHELXL-2018: Program for the Refinement of Crystal Structures*, University of Göttingen, Germany, **2018**. b) G. M. Sheldrick, *Acta Crystallogr., Sect. C: Struct. Chem.* **2015**, *71*, 3−8.

[4] C. B. Hübschle, G. M. Sheldrick, B. Dittrich, *Shelxle: a Qt graphical user interface for SHELXL*, *J. Appl. Crystallogr.* **2011**, *44*, 1281−1284.

[5] a) A. L. Spek, *Acta Crystallogr., Sect. C: Struct. Chem.* **2015**, *71*, 9−18; b) A. L. Spek, *Acta Crystallogr., Sect. D: Biol. Crystallogr.* **2009**, *65*, 148−155; c) A. L. Spek, *J. Appl. Cryst.* **2003**, *36*, 7−13.

### [Ag(4-OMe-BIAN)$_2$]BF$_4$ (Ag4)

For **Ag4**, residual electron density was found in a solvent-accessible void of 892 A³ with an electron count of 208. It was not possible to determine and/or refine the solvent molecule. The electron density was therefore squeezed using PLATON. [5] Disorders in the $BF_4^-$ anion were not refined. Due to measurement at ambient temperature, the ellipsoids are comparably larger.

CCDC 2167847 contains the supplementary crystallographic data for compound **Ag4**. These data can be obtained free of charge from The Cambridge Crystallographic Data Centre at www.ccdc.cam.ac.uk.

**Table S 1:** Crystal data, data collection and structure refinement details for compound **Ag4**.

| Compound | **Ag4** |
|---|---|
| Empirical formula | $C_{52}H_{40}Ag_1N_4O_4B_1F_4$ |
| Formula weight [g/mol] | 979.56 |
| Color | dark red |
| Crystal size [mm] | 0.59 × 0.36 × 0.36 |
| Crystal system | Orthorhombic |
| Space group | *Ccca* |
| *a* [Å] | 12.749(2) |
| *b* [Å] | 22.706(5) |
| *c* [Å] | 17.737(3) |
| *α* [°] | 90 |
| *β* [°] | 90 |
| *γ* [°] | 90 |
| *V* [Å$^3$] | 5134.5(16) |
| *Z* | 4 |
| $D_{calc}$ [g/cm$^3$] | 1.267 |
| *μ* [mm$^{-1}$] | 0.45 |
| *T* [K] | 296 |

| | |
|---|---|
| $\theta$ range [°] | 2.9-24.4 |
| No. of reflections measured | 41788 |
| No. of independent reflections | 2361 |
| Obs. Reflections with $I > 2\sigma(I)$ | 1825 |
| No. of Parameters refined/restraints | 153/0 |
| Absorption correction | multi-scan |
| $T_{min}$, $T_{max}$ | 0.80, 0.86 |
| $\Delta\rho_{min}/\Delta\rho_{max}$ [e Å$^{-3}$] | −0.31/0.40 |
| F(000) | 2000 |
| $R_{int}$ | 0.041 |
| $R_1$ ($R[F^2 \geq 2\sigma(F^{2)})]$) | 0.040 |
| $wR_2$ ($wR(F^2)$) | 0.121 |
| GooF | 1.10 |
| CCDC no. | 2167847 |

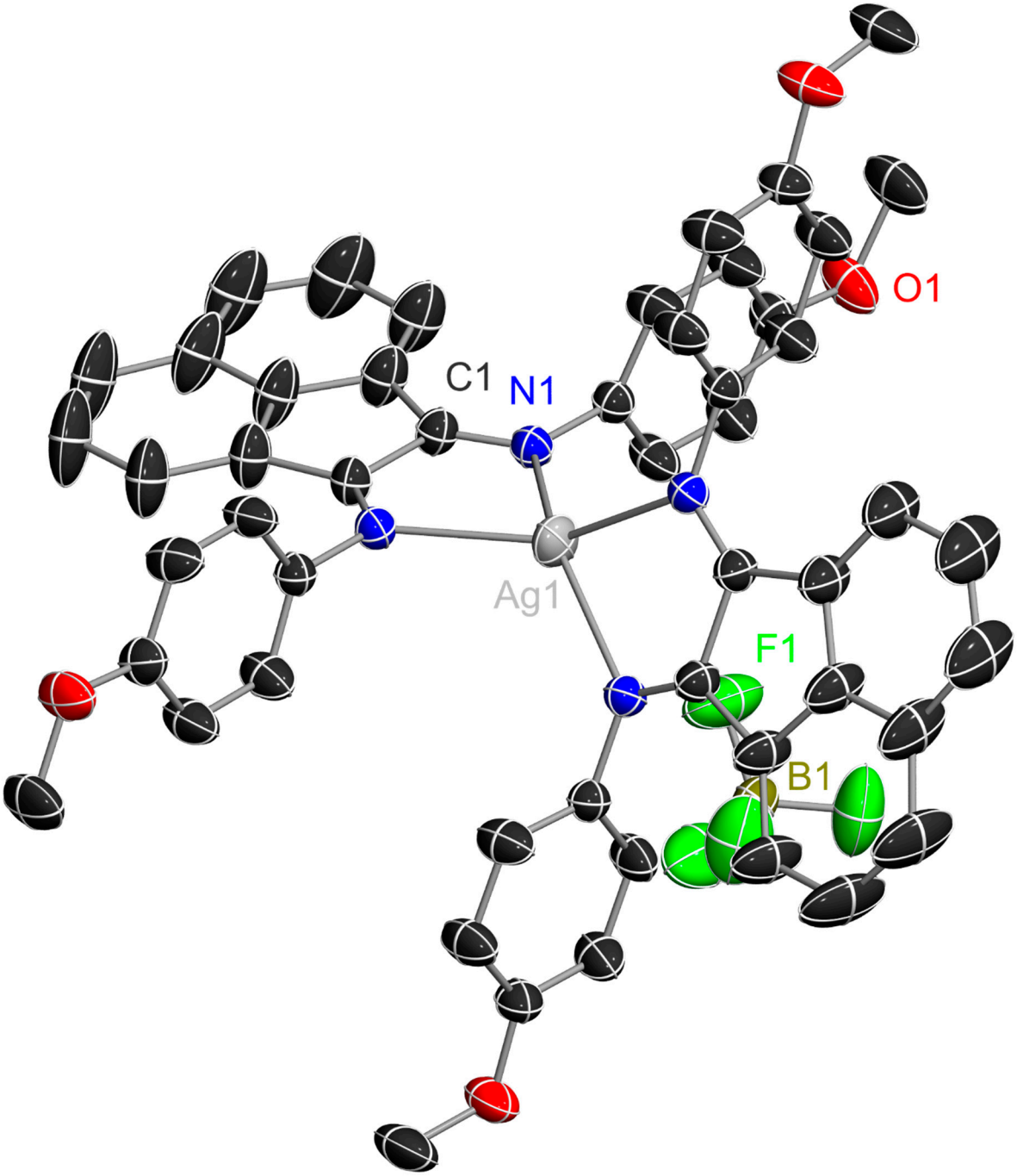


**Figure S64:** Molecular structure of $[Ag(4\text{-OMe-BIAN})_2]BF_4$ **Ag4** (CCDC 2167847) in the crystal (*Ccca*). Thermal ellipsoids drawn at the 30% probability level and 25 °C. Hydrogen atoms are omitted for clarity.

## Homogenous Electrochemistry

### Materials and Methods

Tetrabutylammonium hexafluorophosphate ($TBAPF_6$) for electrochemical measurements was purchased from Sigma-Aldrich and recrystallized twice from absolute ethanol (Acros Organics), dried under high vacuum and stored under argon prior to use. Anhydrous ACN was obtained from a molar sieve MB-SPS-7, M. Braun Inert gas-System GmbH (Garching, Germany) under argon atmosphere. Anhydrous DMF was purchased from Acros Organics. Aqueous solutions for electrochemical experiments were prepared using high purity water (18 MΩ). Homogeneous electrochemical measurements were conducted in a low volume Gamry cell using a three-electrode setup at 25 °C under argon or $CO_2$, respectively, utilizing a Pine WaveDriver 20 DC Bipotentiostat. The investigated solutions were prepared from dry, degassed solvents and contained 0.1M supporting electrolyte ($TBAPF_6$) and 1mM of the respective complexes or ligands, except for $[Ag(2,6\text{-dipp-BIAN})_2]BF_4$ **Ag2** where 0.5mM solutions were examined in ACN due to its limited solubility. Complex **Ag1** was characterized in DMF, since coordinating solvents like ACN caused ligand substitution. For all electrochemical measurements a glassy carbon (Pine, 65 mm long, 6.4 mm OD PCTFE shroud, 3 mm OD disk) as working, platinum wire (Pine, 65 mm long, 7 mm OD epoxy tube shroud, 0.58 $cm^2$ approximate surface area) as counter and non-aqueous pseudo-Ag/AgCl reference electrode were used. Prior to each measurement, the glassy carbon WE was polished with a 0.05 µm alumina suspension (deagglomerated, Allied-high tech products) on a MicroCloth polishing pad (Buehler, PSA). Subsequently, the electrode was cleaned in a ultrasonication bath in pure water for 3 min and finally rinsed with pure water and acetonitrile to remove any excess of alumina particles. Ensuing each experiment, ferrocene was added as internal standard. The obtained half wave potentials for the $Fc/Fc^+$ couple against the respective Ag/AgCl QRE in each solution are listed in Table S 2. The converted potentials against $Fc/Fc^+$ were transformed to V vs NHE with the conversion of +0.630 V vs NHE in ACN and +0.590 V vs NHE in DMF according to literature [49-51]. If not otherwise noted, CVs were recorded at a scan rate of 100 mV/s applying reductive potentials first.

**Table S 2:** Obtained values for the Ferrocene/ferrocenium$^{+}$ half wave potentials vs Ag/AgCl QRE determined for each investigated mixture.

| | $E_{1/2}$ / V vs Ag/AgCl QRE | | |
|---|---|---|---|
| **Compound** | ACN | ACN + 2% $H_2O$ | ACN + 20% $H_2O$ |
| **L4** | 0.403 | - | - |
| **L6** | 0.448 | 0.419 | - |
| **$Ag(ACN)_4BF_4$** | 0.140 | 0.182 | 0.018 |
| **Ag1**[a] | 0.137 | 0.084 | - |
| **Ag2** | 0.204 | 0.192 | - |
| **Ag3** | 0.189 | 0.178 | - |
| **Ag4** | 0.200 | 0.193 | 0.129 |
| **Ag5** | 0.194 | 0.170 | - |
| **Ag6** | 0.239 | 0.239 | 0.163 |

**4-Methoxy-BIAN (L4)**

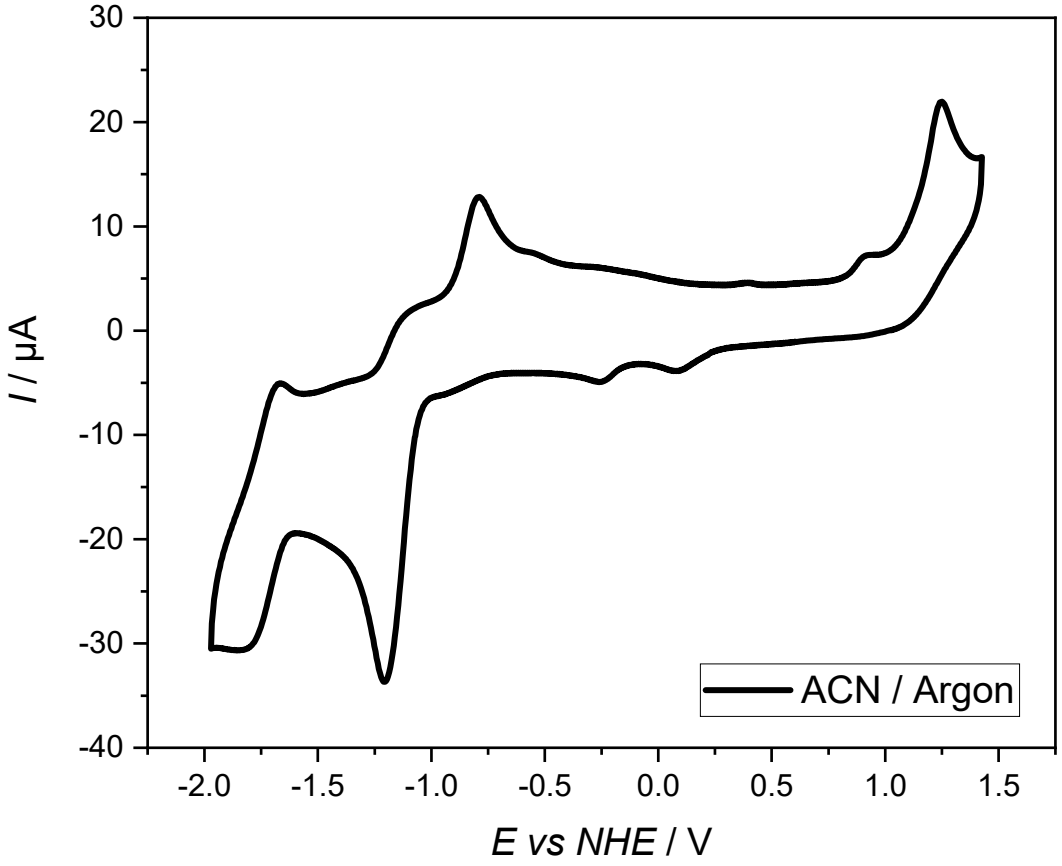


**Figure S65:** Cyclic voltammogram of 4-OMe-BIAN **L4** in acetonitrile under argon.

## 4-Diethylamino-BIAN (L6)

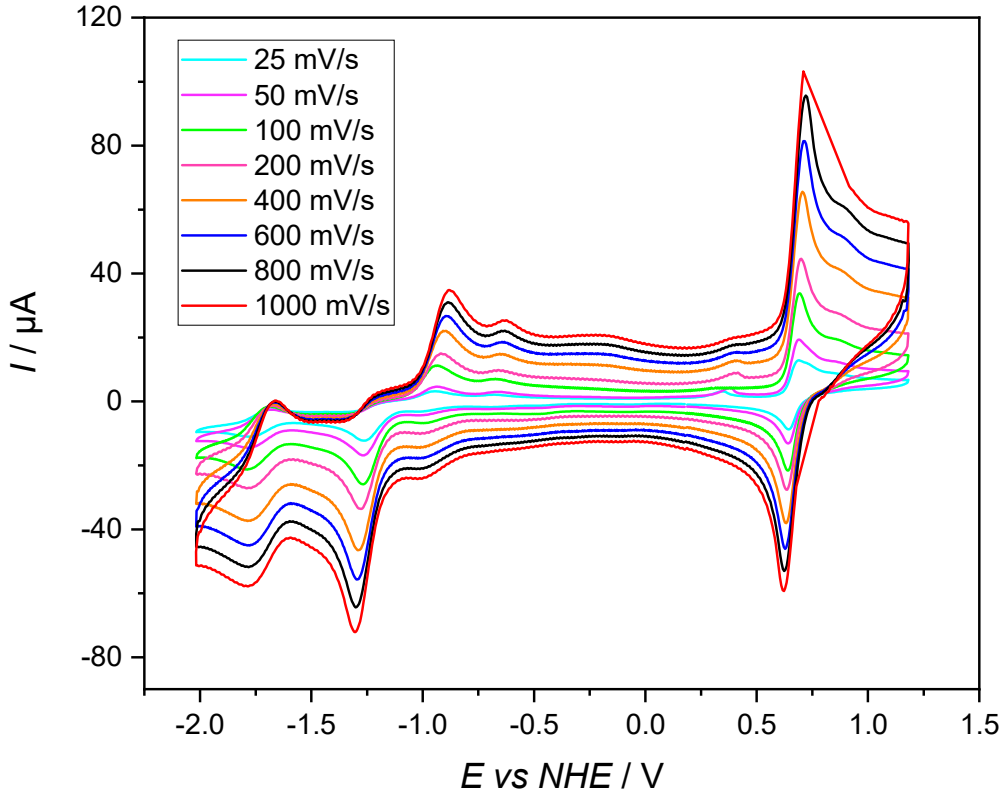


**Figure S66:** Scan rate dependency of 4-diethylamino-BIAN **L6** in acetonitrile under argon.

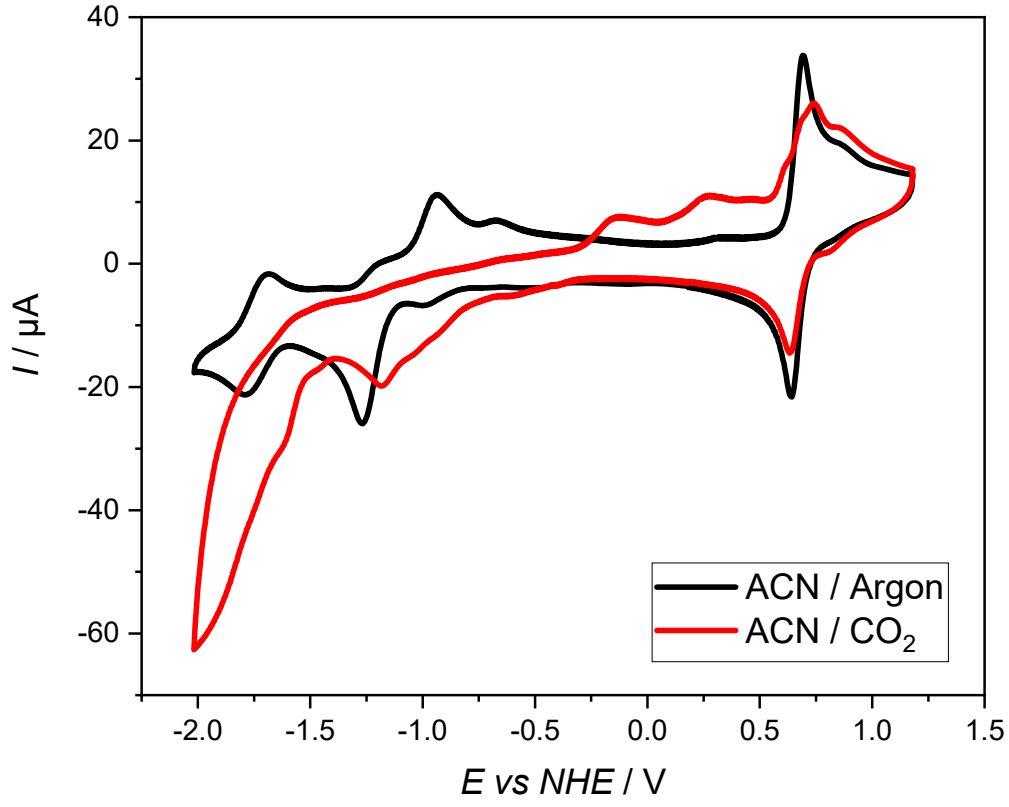


**Figure S67:** Comparison of cyclic voltammograms of 4-diethylamino-BIAN **L6** in acetonitrile under argon and $CO_2$.

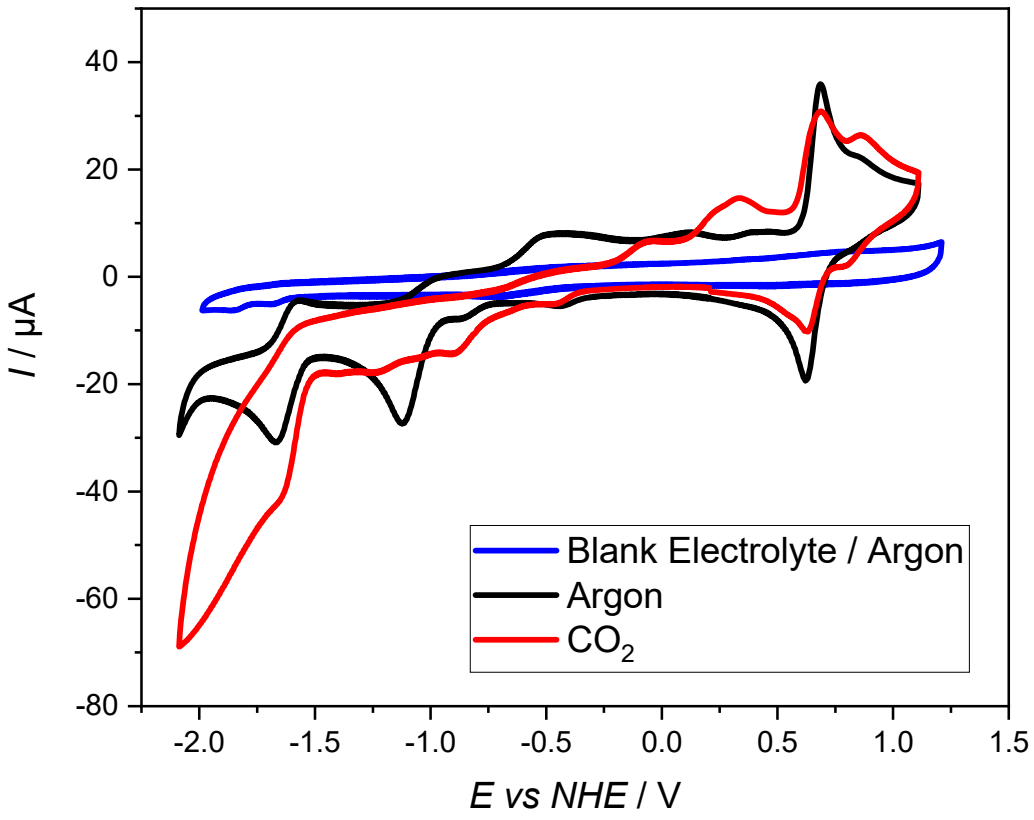


**Figure S68:** Comparison of cyclic voltammograms of 4-diethylamino-BIAN **L6** in acetonitrile with 2% $H_2O$ under argon and $CO_2$ and the blank electrolyte.

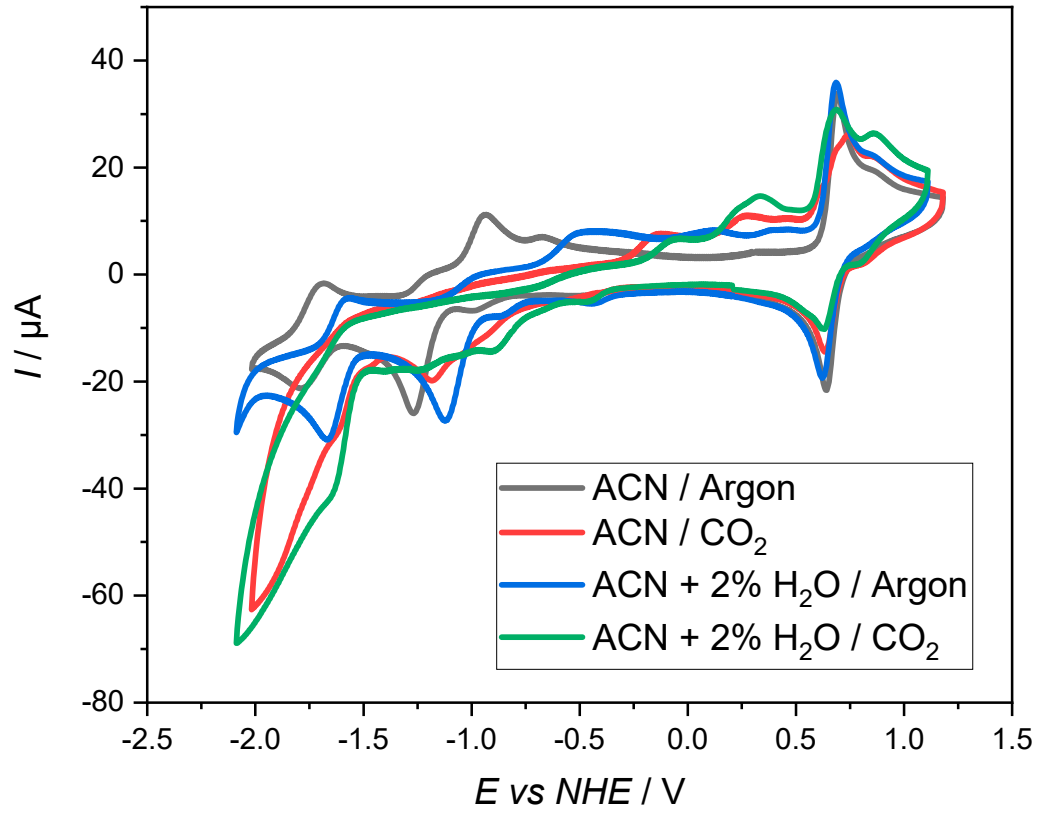


**Figure S69:** Comparison of cyclic voltammograms of 4-diethylamino-BIAN **L6** in acetonitrile and acetonitrile with 2% $H_2O$ under argon and $CO_2$.

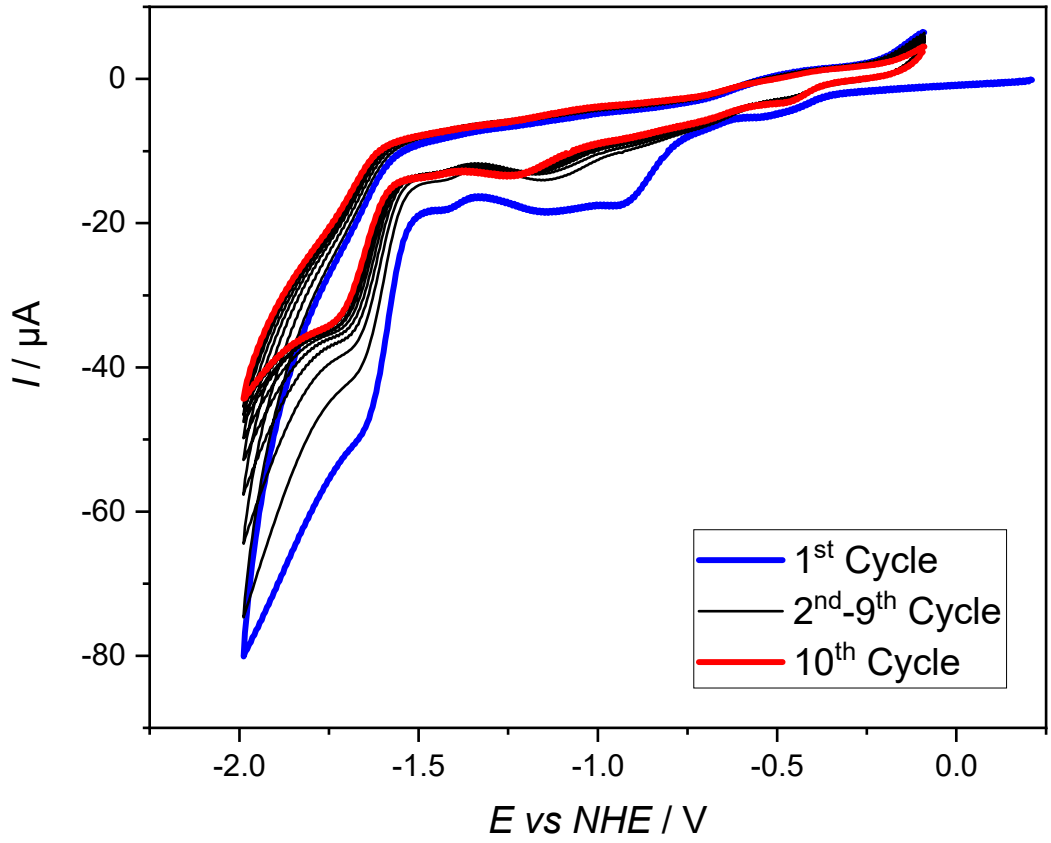


**Figure S70:** Catalytic stability test of the reductive section of 4-diethylamino-BIAN **L6** in acetonitrile with 2% $H_2O$ under $CO_2$ indicating a rapid decrease in cathodic current.

**[Ag(ACN)$_4$]BF$_4$**

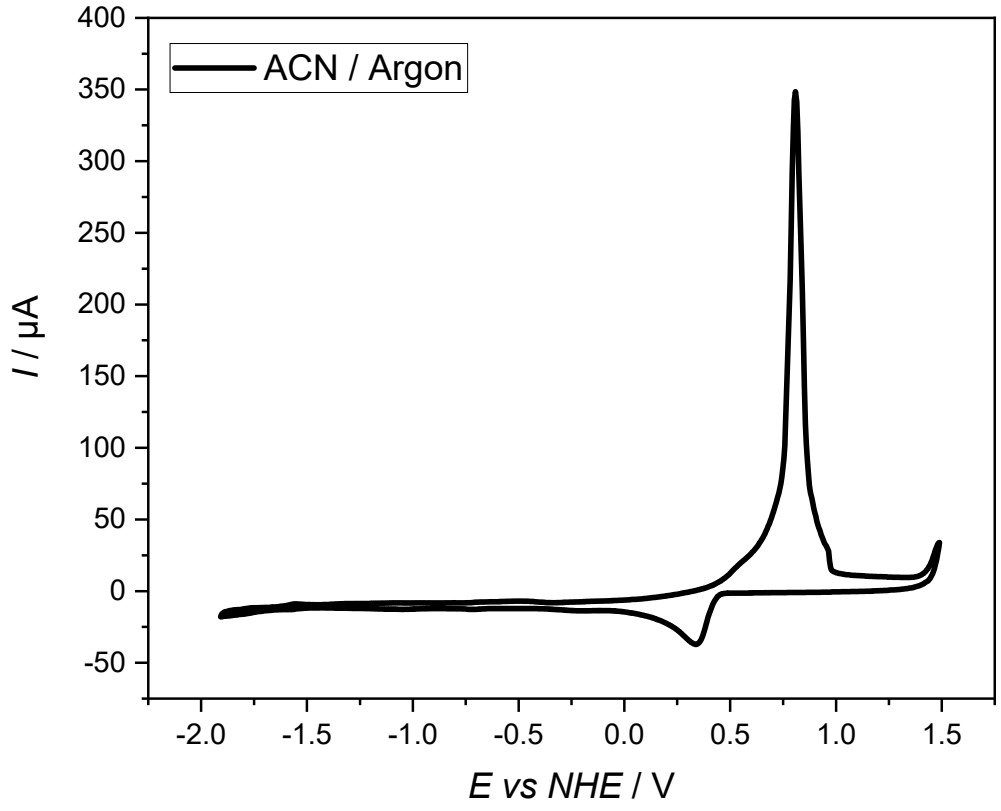


**Figure S71:** Cyclic voltammogram of [Ag(ACN)$_4$]BF$_4$ in acetonitrile under argon.

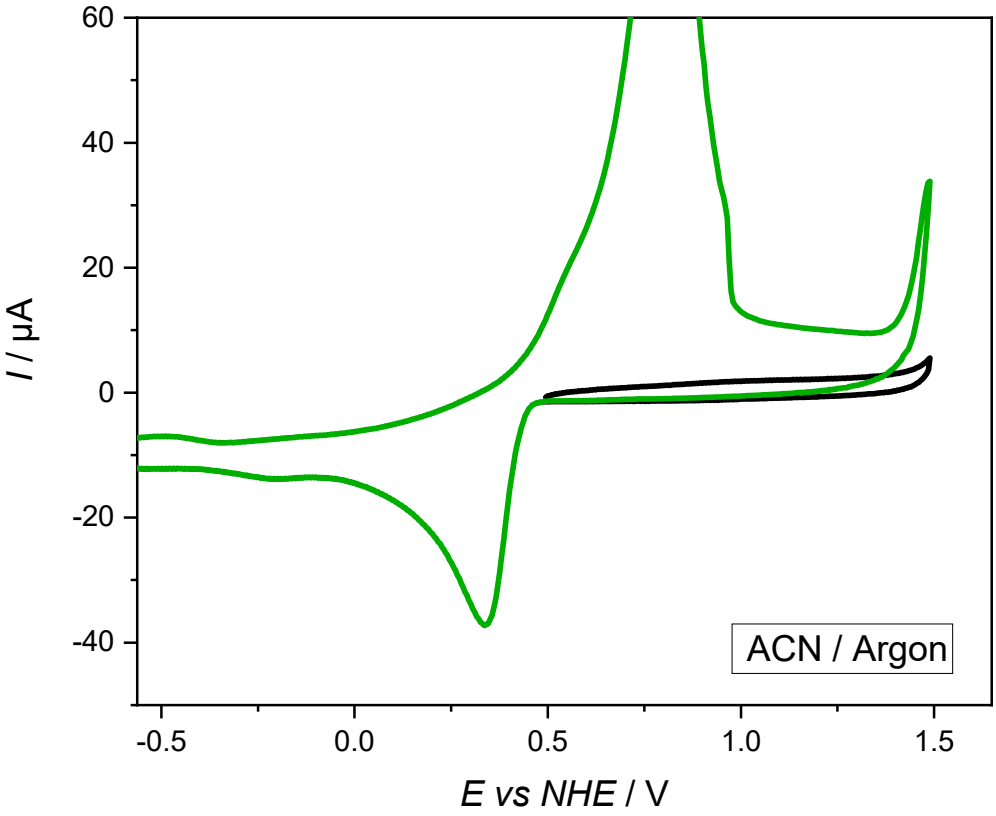


**Figure S72:** Comparison of different scan ranges of [Ag(ACN)$_4$]BF$_4$ in acetonitrile under argon illustrating the absence of an oxidative current for a limited scan range of +0.5 to +1.5V (black line).

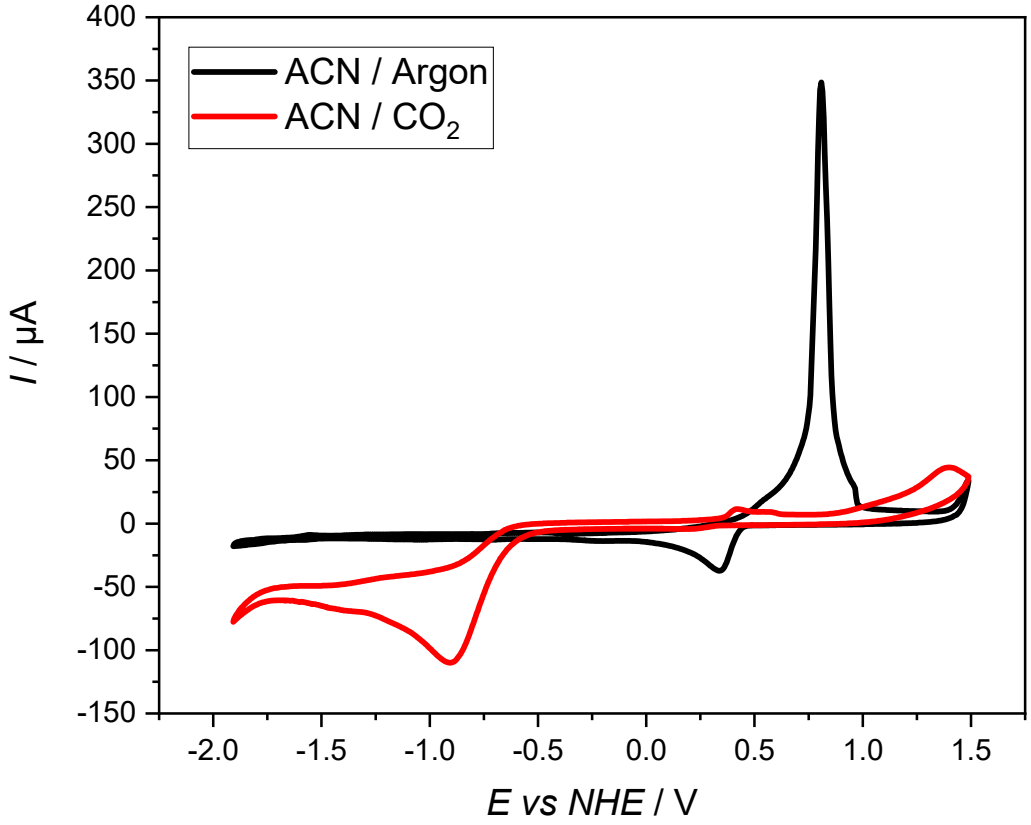


**Figure S73:** Comparison of cyclic voltammograms of $[Ag(ACN)_4]BF_4$ in acetonitrile under argon and $CO_2$.

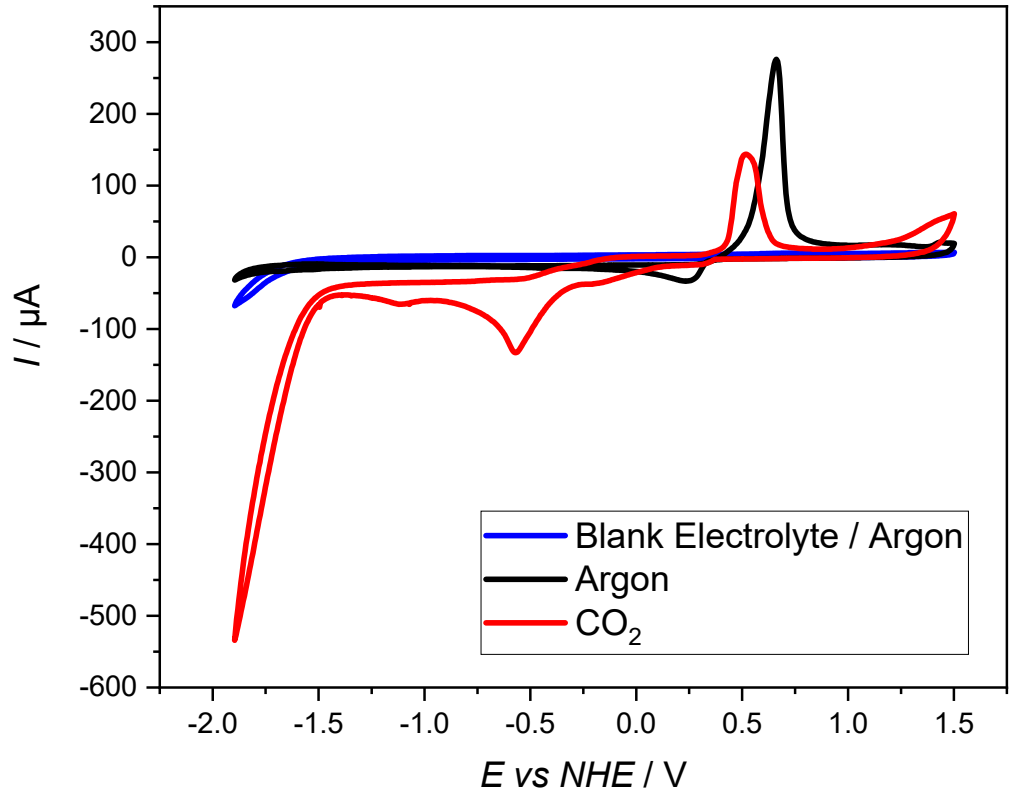


**Figure S74:** Comparison of cyclic voltammograms of $[Ag(ACN)_4]BF_4$ in acetonitrile with 2% $H_2O$ under argon and $CO_2$ and the blank electrolyte.

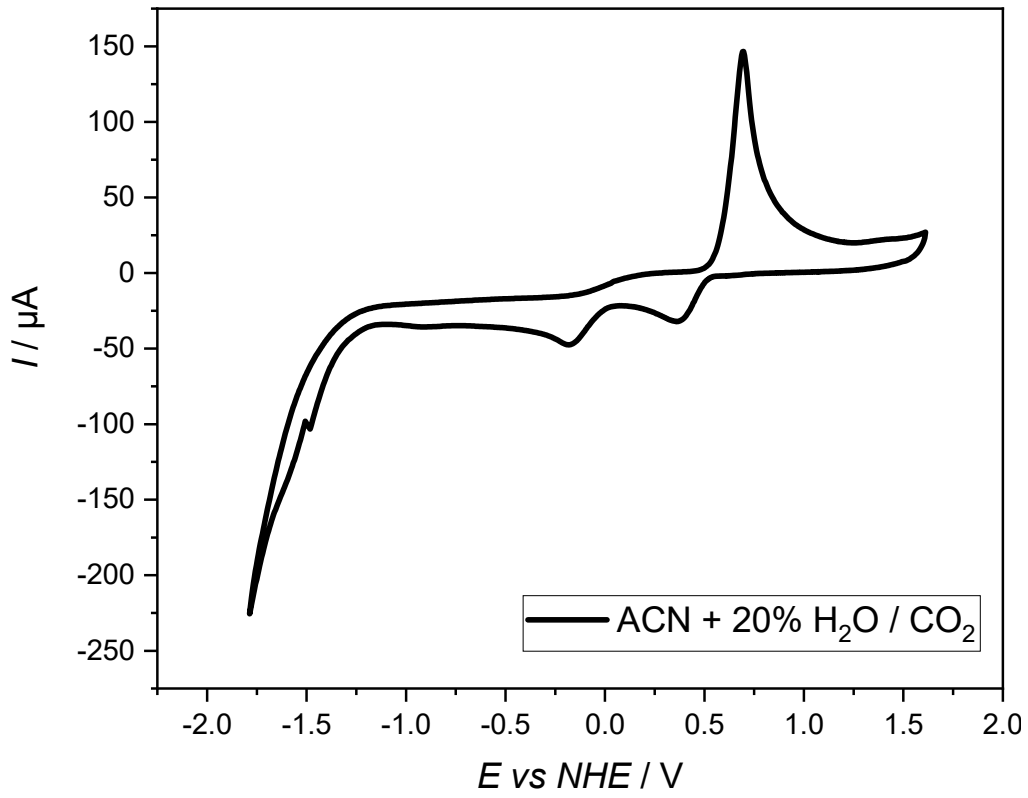


**Figure S75:** Cyclic voltammogram of $[Ag(ACN)_4]BF_4$ in acetonitrile with 20% $H_2O$ under $CO_2$.

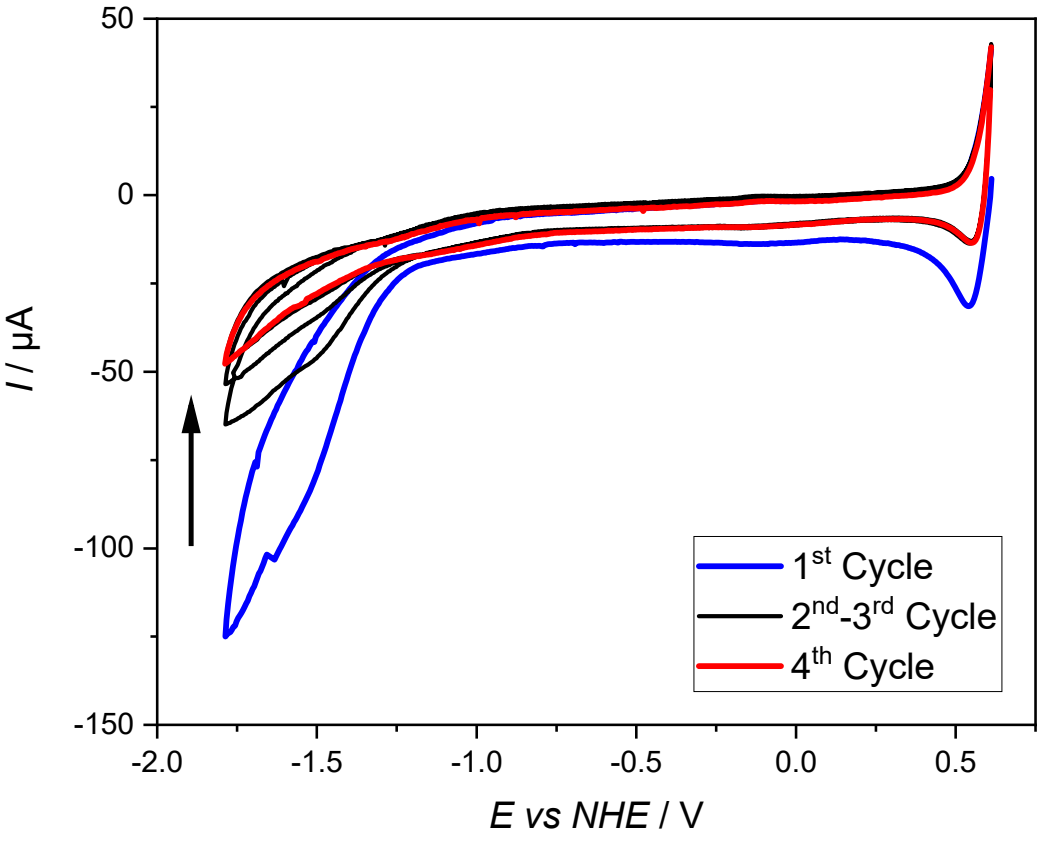


**Figure S76:** Catalytic stability test of the reductive section of $[Ag(ACN)_4]BF_4$ in acetonitrile with 20% $H_2O$ under $CO_2$ indicating a rapid decrease in cathodic current.

**[Ag(3,5-bis-$CF_3$-BIAN)$_2$]$BF_4$ (Ag1)**

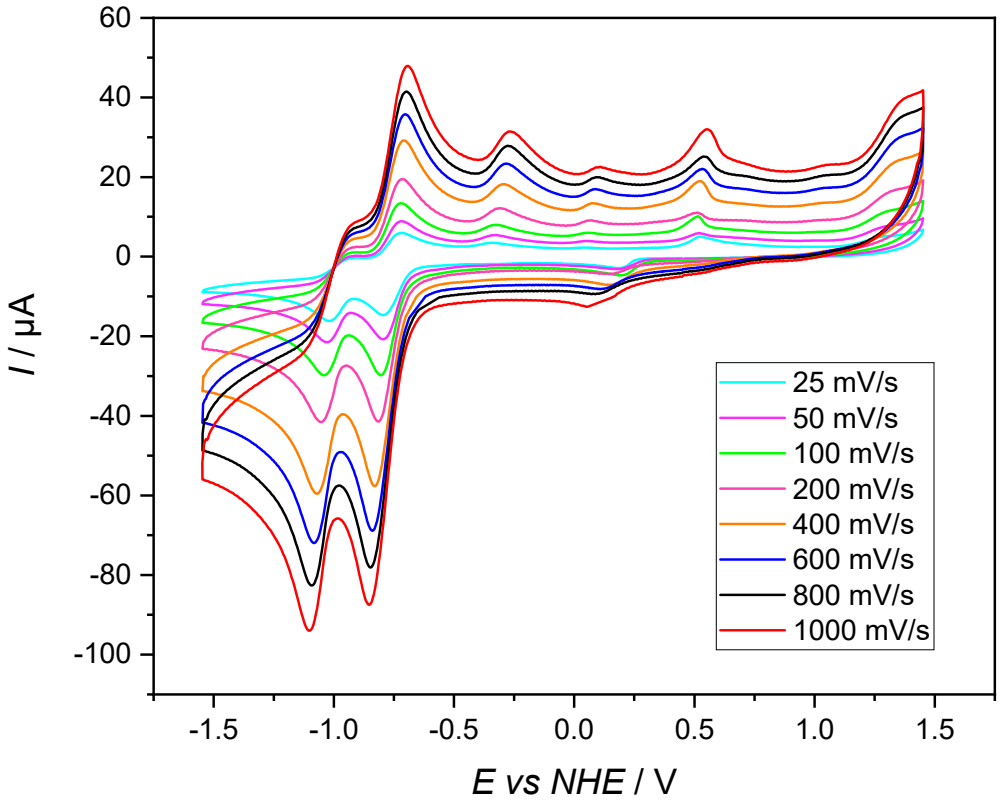


**Figure S77:** Scan rate dependency of [Ag(3,5-bis-CF3-BIAN)$_2$]$BF_4$ **Ag1** in DMF under argon.

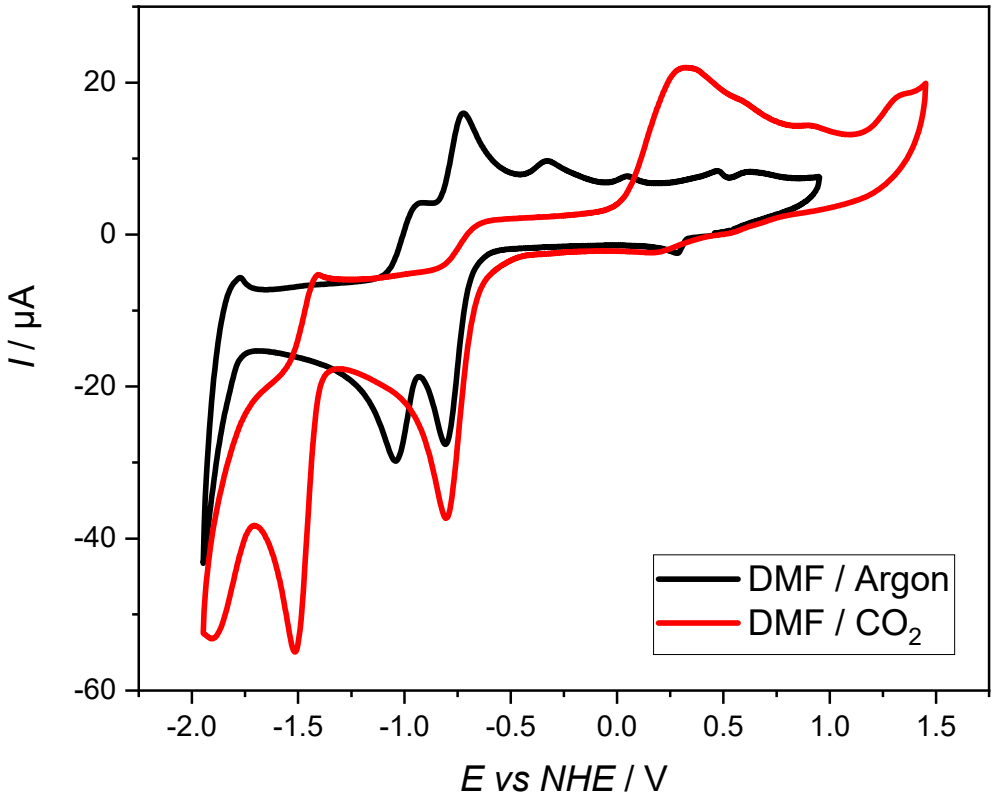


**Figure S78:** Comparison of cyclic voltammograms of [Ag(3,5-bis-CF3-BIAN)$_2$]$BF_4$ **Ag1** in DMF under argon and $CO_2$.

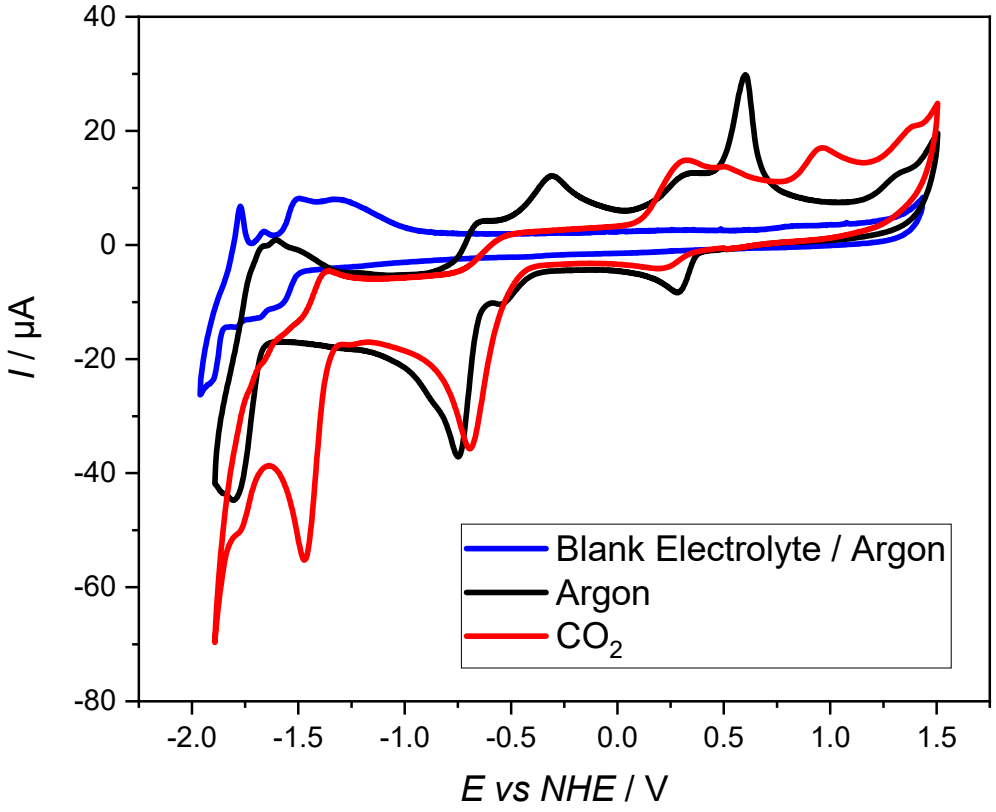


**Figure S79:** Comparison of cyclic voltammograms of $[Ag(3,5\text{-bis-CF3-BIAN})_2]BF_4$ **Ag1** in DMF with 2% $H_2O$ under argon and $CO_2$ and the blank electrolyte.

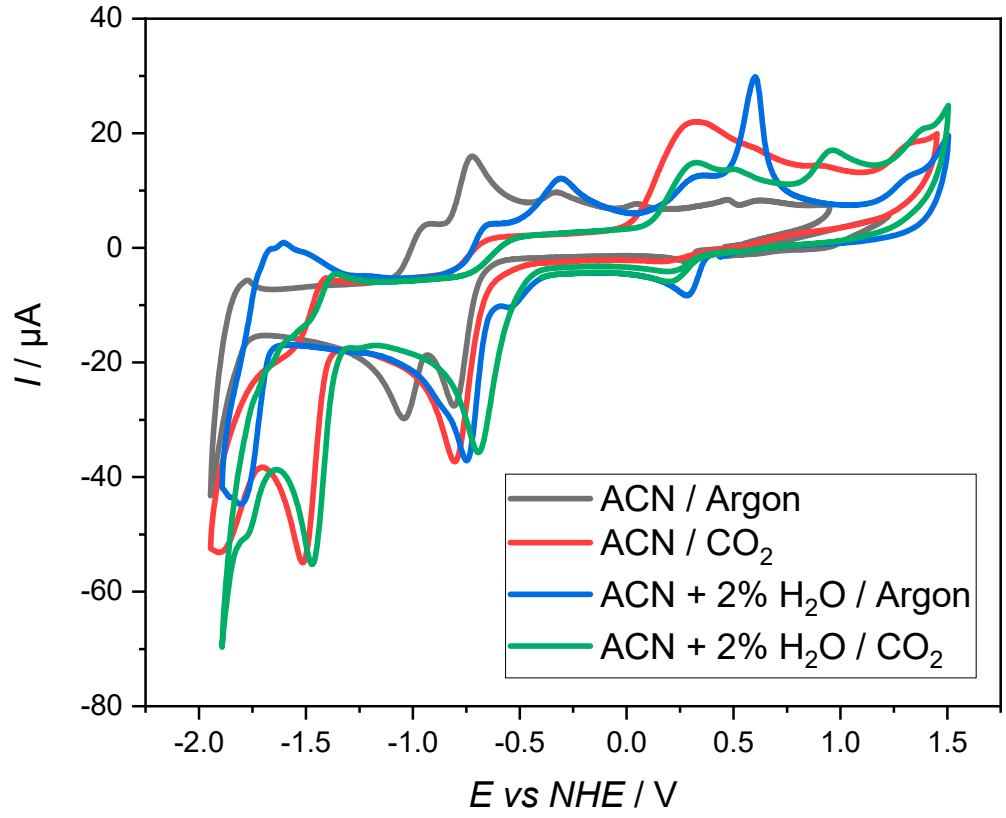


**Figure S80:** Comparison of cyclic voltammograms of $[Ag(3,5\text{-bis-CF3-BIAN})_2]BF_4$ **Ag1** in DMF and DMF with 2% $H_2O$ under argon and $CO_2$.

**[Ag(2,6-dipp-BIAN)$_2$]BF$_4$ (Ag2)**

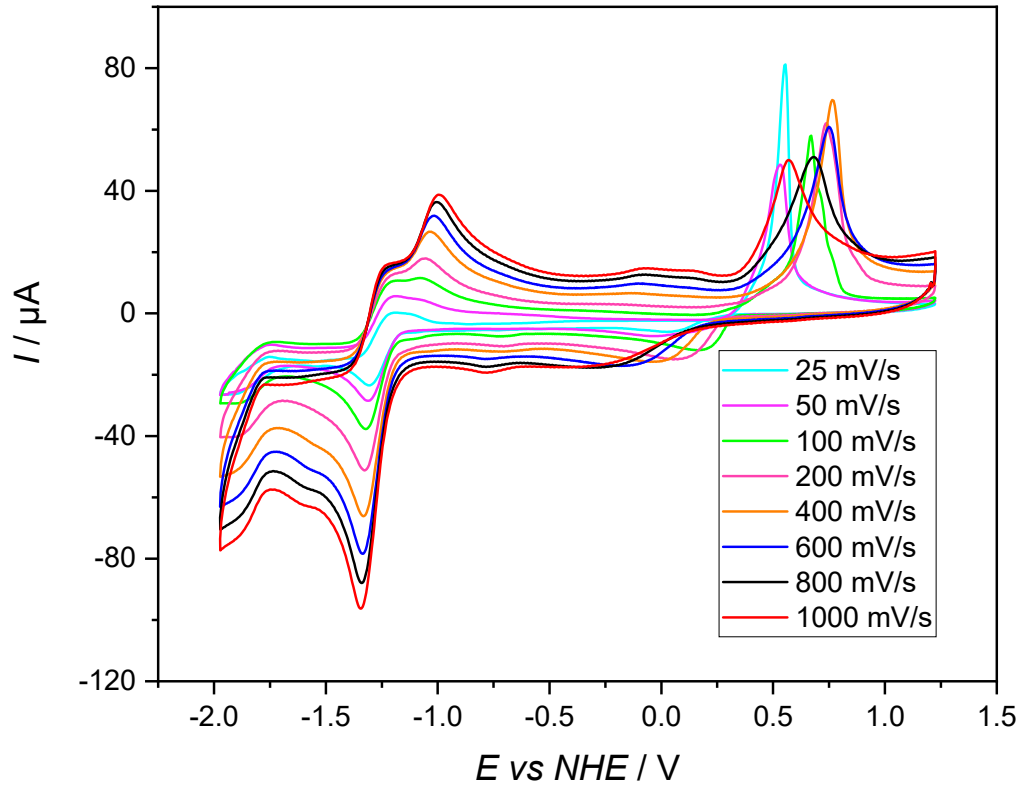


**Figure S81:** Scan rate dependency of 0.5mM [Ag(2,6-dipp-BIAN)$_2$]BF$_4$ **Ag2** in acetonitrile under argon.

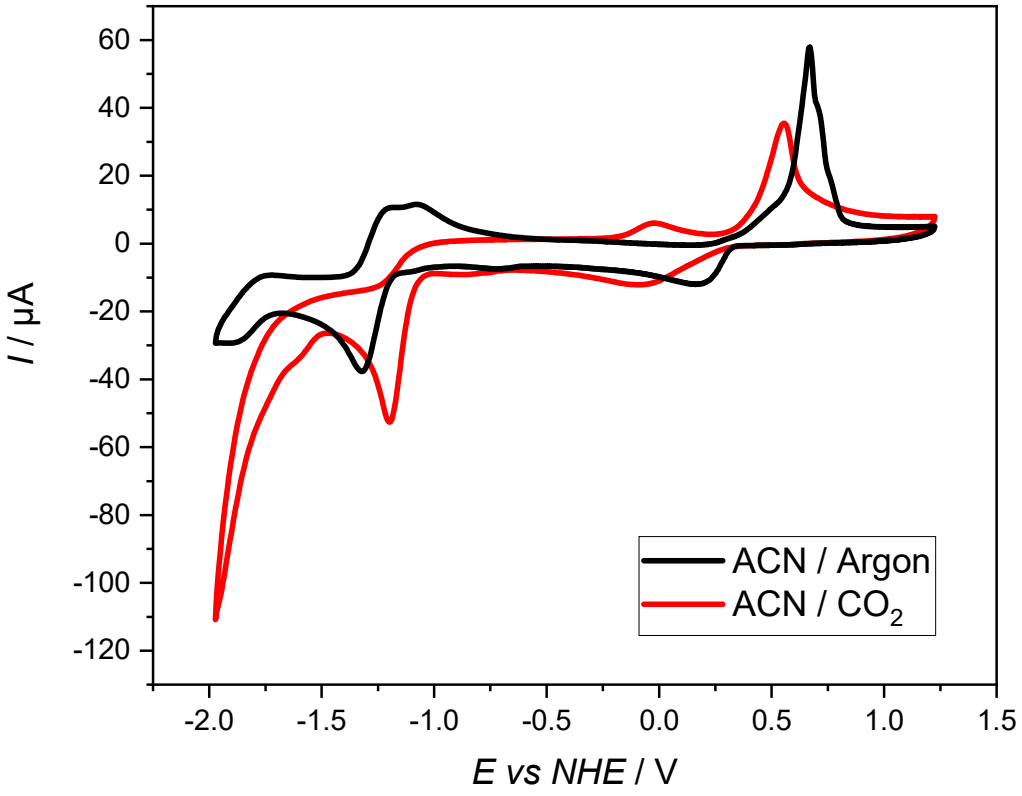


**Figure S82:** Comparison of cyclic voltammograms of 0.5mM [Ag(2,6-dipp-BIAN)$_2$]BF$_4$ **Ag2** in acetonitrile under argon and $CO_2$.

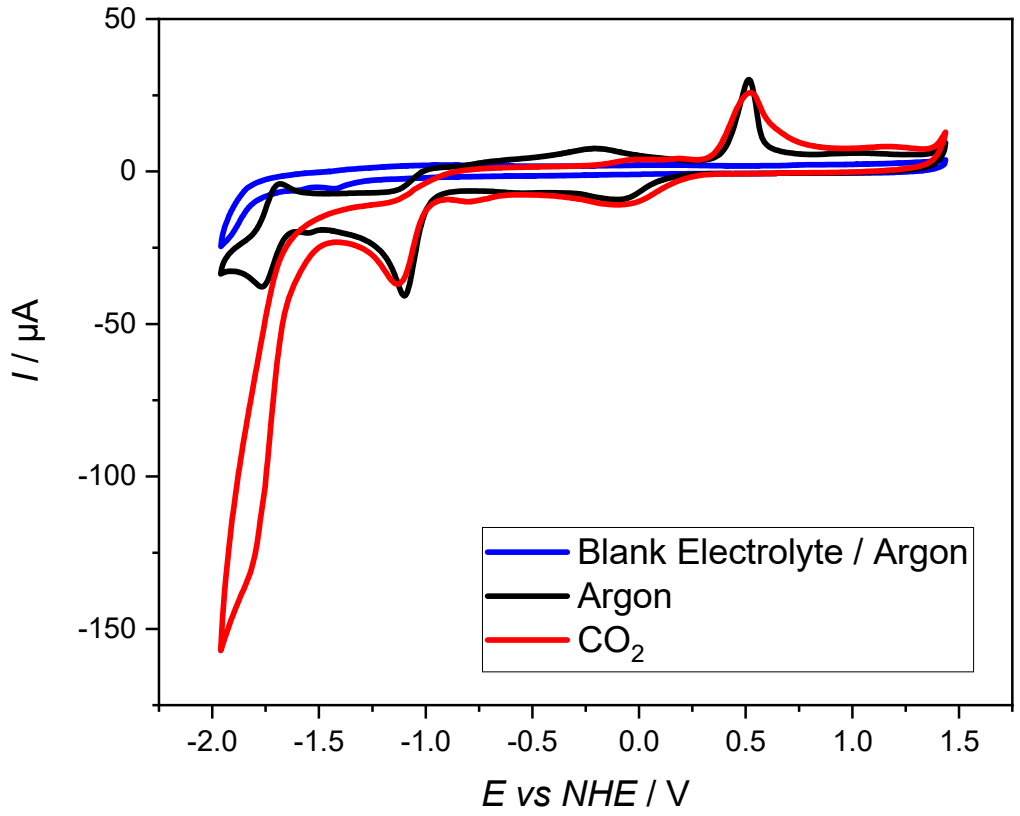


**Figure S83:** Comparison of cyclic voltammograms of 0.5mM $[Ag(2,6\text{-dipp-BIAN})_2]BF_4$ **Ag2** in acetonitrile with 2% $H_2O$ under argon and $CO_2$ and the blank electrolyte.

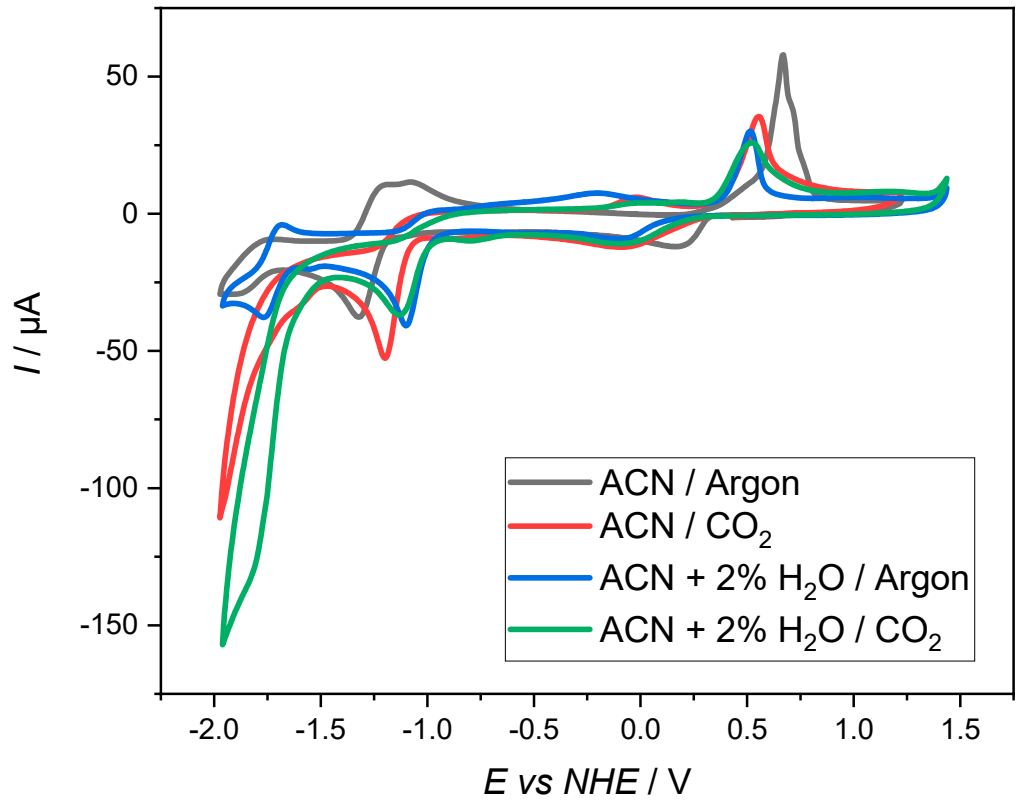


**Figure S84:** Comparison of cyclic voltammograms of 0.5mM $[Ag(2,6\text{-dipp-BIAN})_2]BF_4$ **Ag2** in acetonitrile and acetonitrile with 2% $H_2O$ under argon and $CO_2$.

**[Ag(1-pyrene-BIAN)$_2$]BF$_4$ (Ag3)**

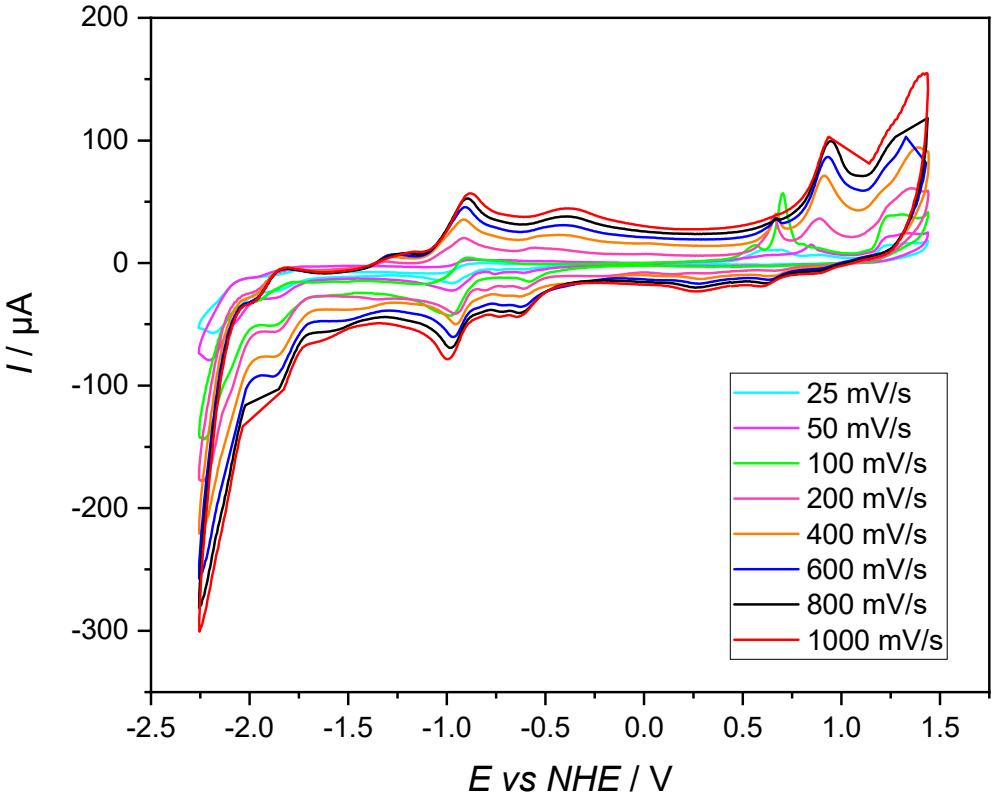


**Figure S85:** Scan rate dependency of [Ag(1-pyrene-BIAN)$_2$]BF$_4$ **Ag3** in acetonitrile under argon. Cut off peaks at high scan rates are caused by limitations of the employed potentiostat.

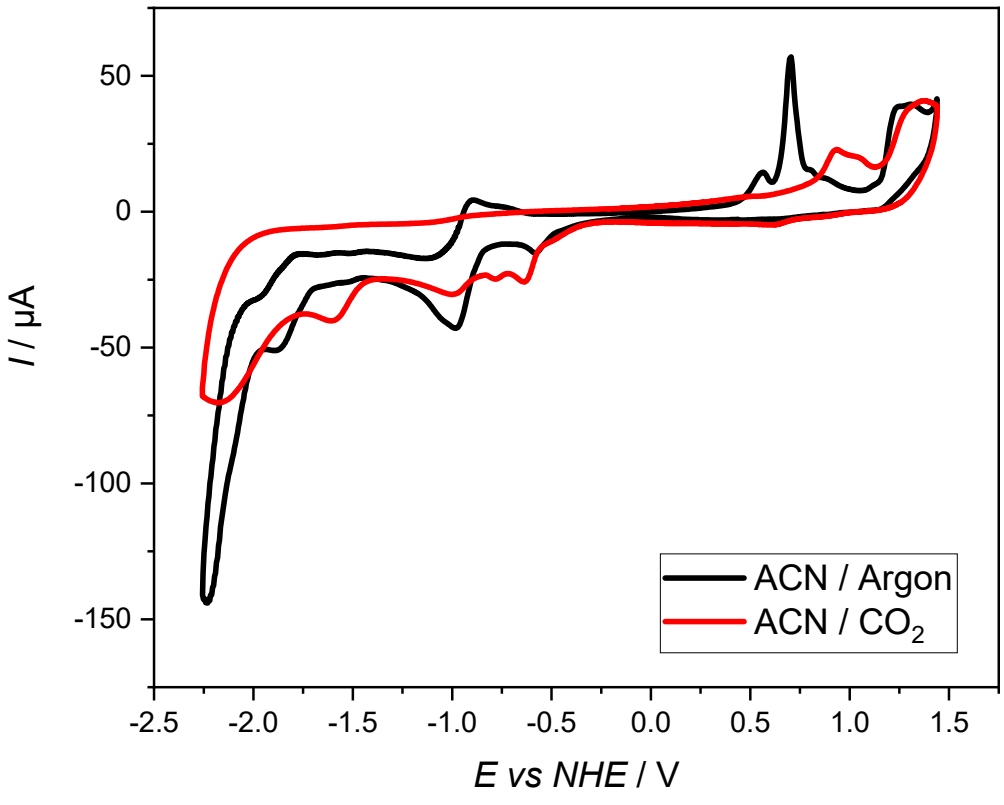


**Figure S86:** Comparison of cyclic voltammograms of [Ag(1-pyrene-BIAN)$_2$]BF$_4$ **Ag3** in acetonitrile under argon and $CO_2$.

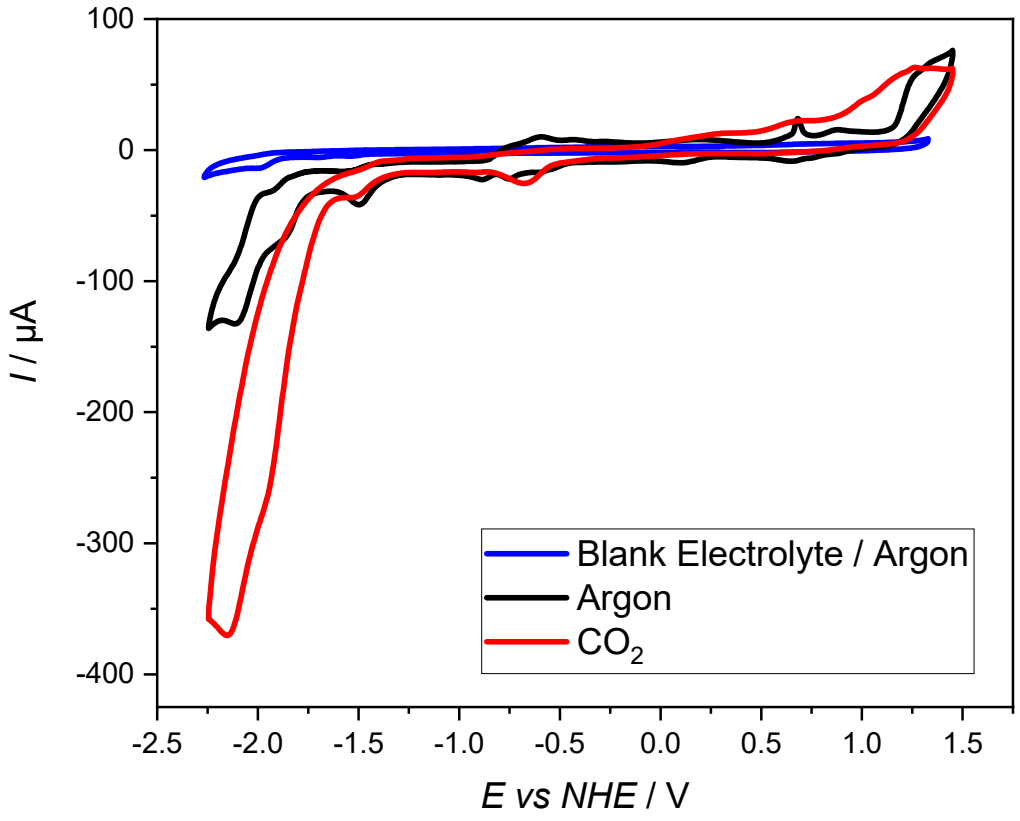


**Figure S87:** Comparison of cyclic voltammograms of $[Ag(1\text{-pyrene-BIAN})_2]BF_4$ **Ag3** in acetonitrile with 2% $H_2O$ under argon and $CO_2$ and the blank electrolyte.

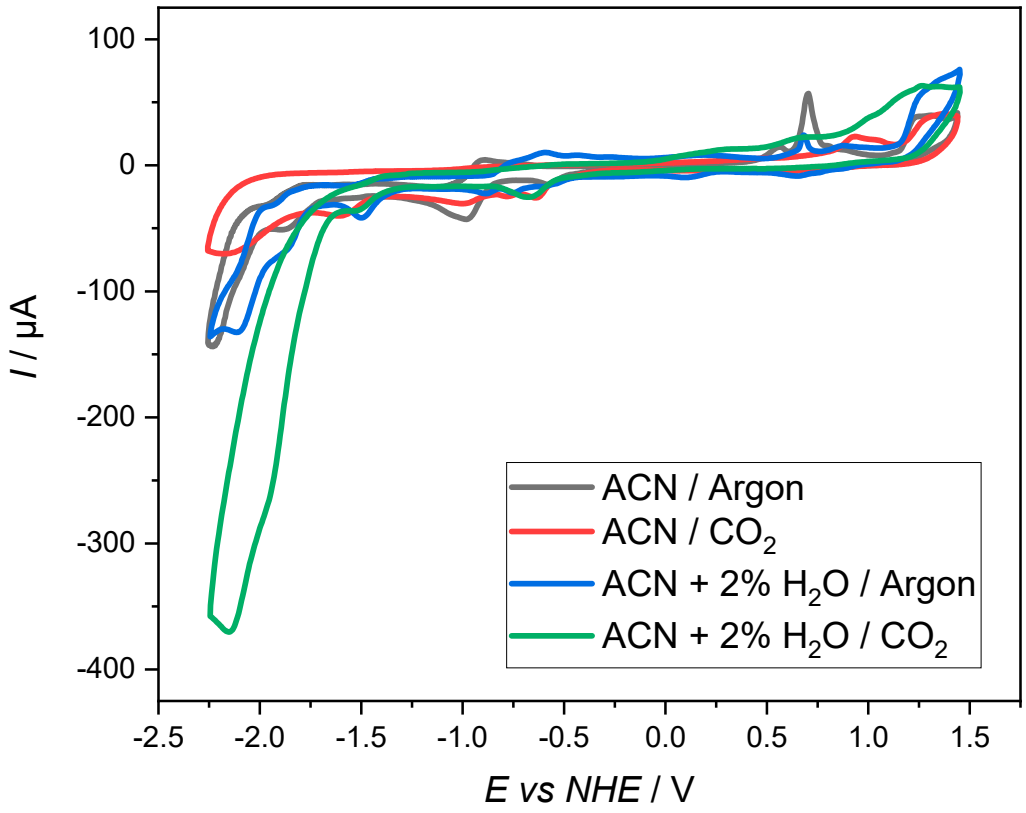


**Figure S88:** Comparison of cyclic voltammograms of $[Ag(1\text{-pyrene-BIAN})_2]BF_4$ **Ag3** in acetonitrile and acetonitrile with 2% $H_2O$ under argon and $CO_2$.

**[Ag(4-OMe-BIAN)$_2$]BF$_4$ (Ag4)**

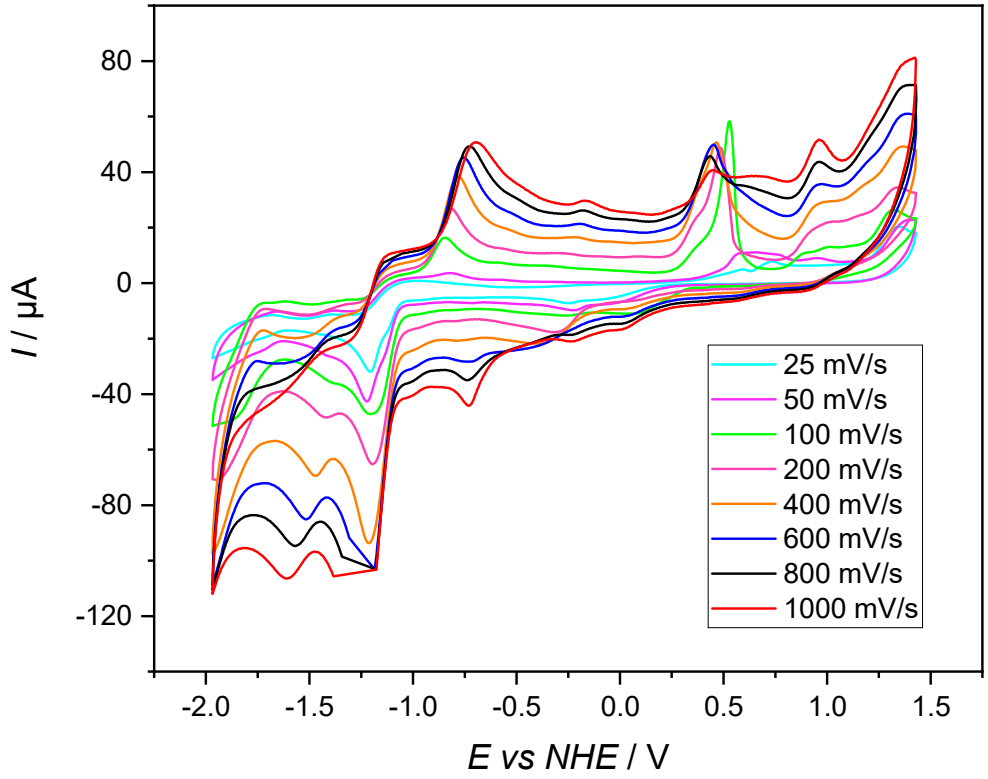


**Figure S89:** Scan rate dependency of [Ag(4-OMe-BIAN)$_2$]BF$_4$ **Ag4** in acetonitrile under argon. Cut off peaks at high scan rates are caused by limitations of the employed potentiostat.

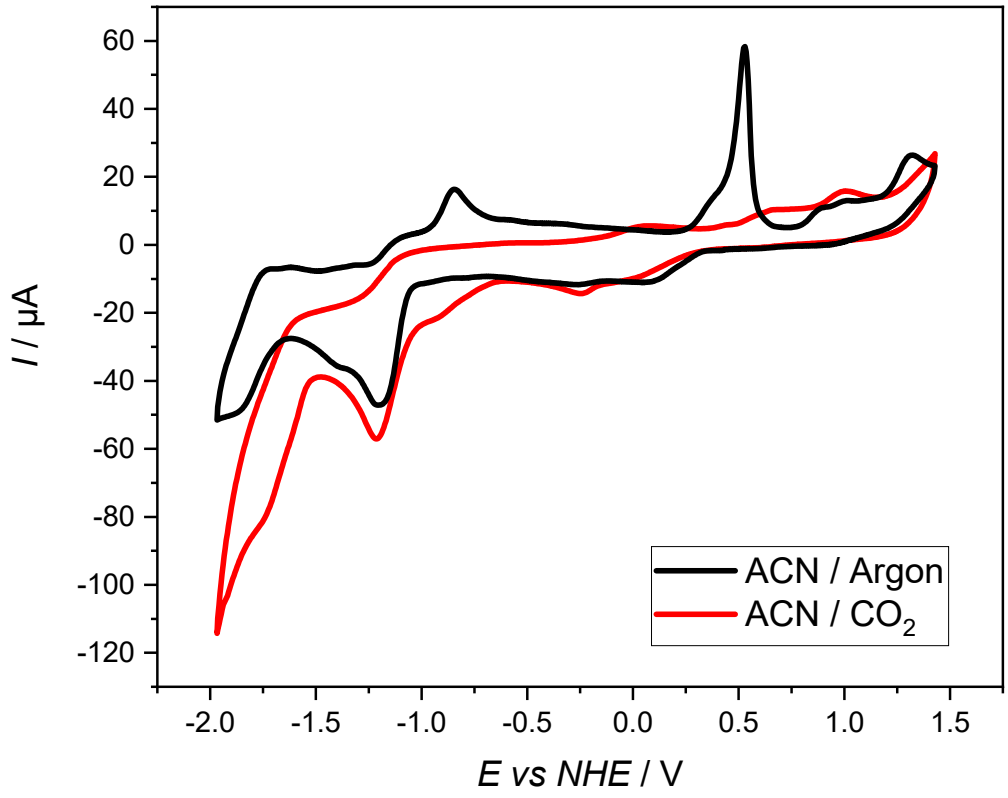


**Figure S90:** Comparison of cyclic voltammograms of [Ag(4-OMe-BIAN)$_2$]BF$_4$ **Ag4** in acetonitrile under argon and $CO_2$.

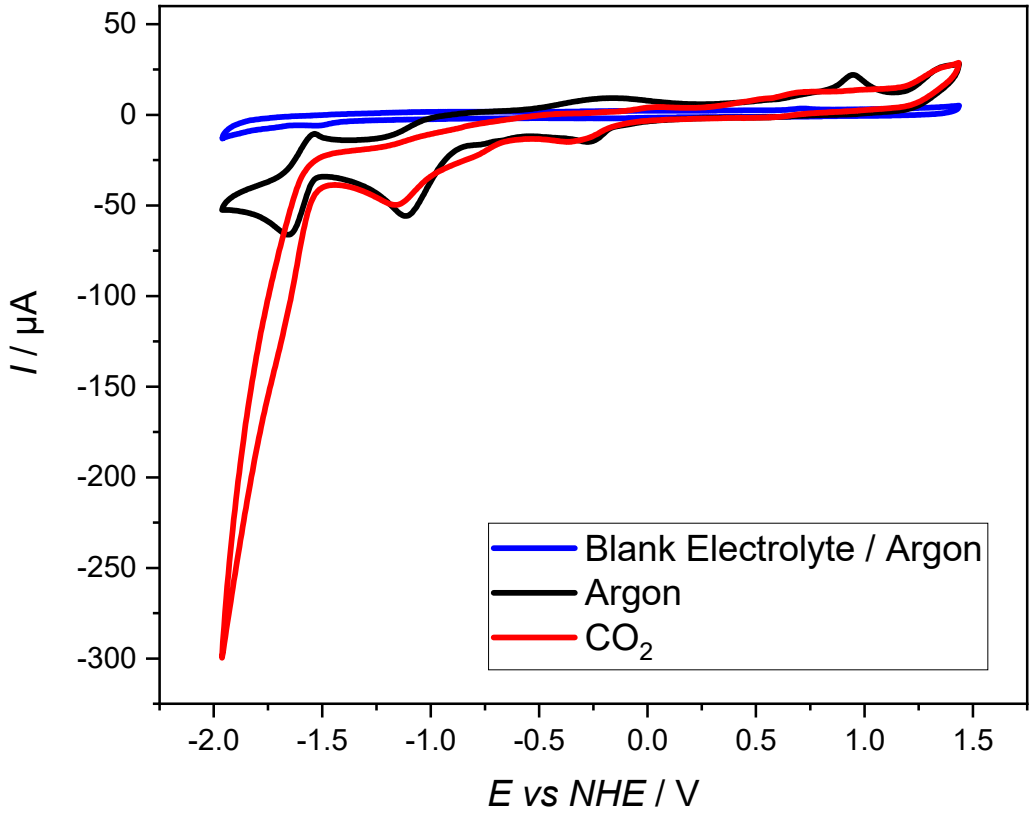


**Figure S91:** Comparison of cyclic voltammograms of $[Ag(4\text{-OMe-BIAN})_2]BF_4$ **Ag4** in acetonitrile with 2% $H_2O$ under argon and $CO_2$ and the blank electrolyte.

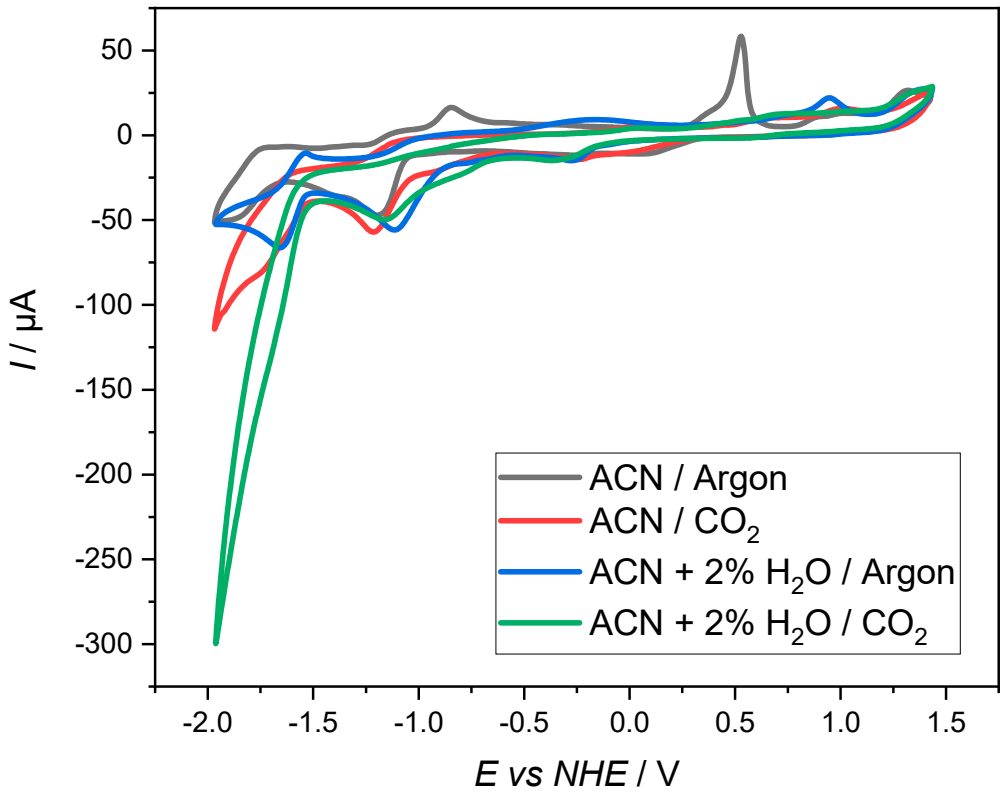


**Figure S92:** Comparison of cyclic voltammograms of $[Ag(4\text{-OMe-BIAN})_2]BF_4$ **Ag4** in acetonitrile and acetonitrile with 2% $H_2O$ under argon and $CO_2$.

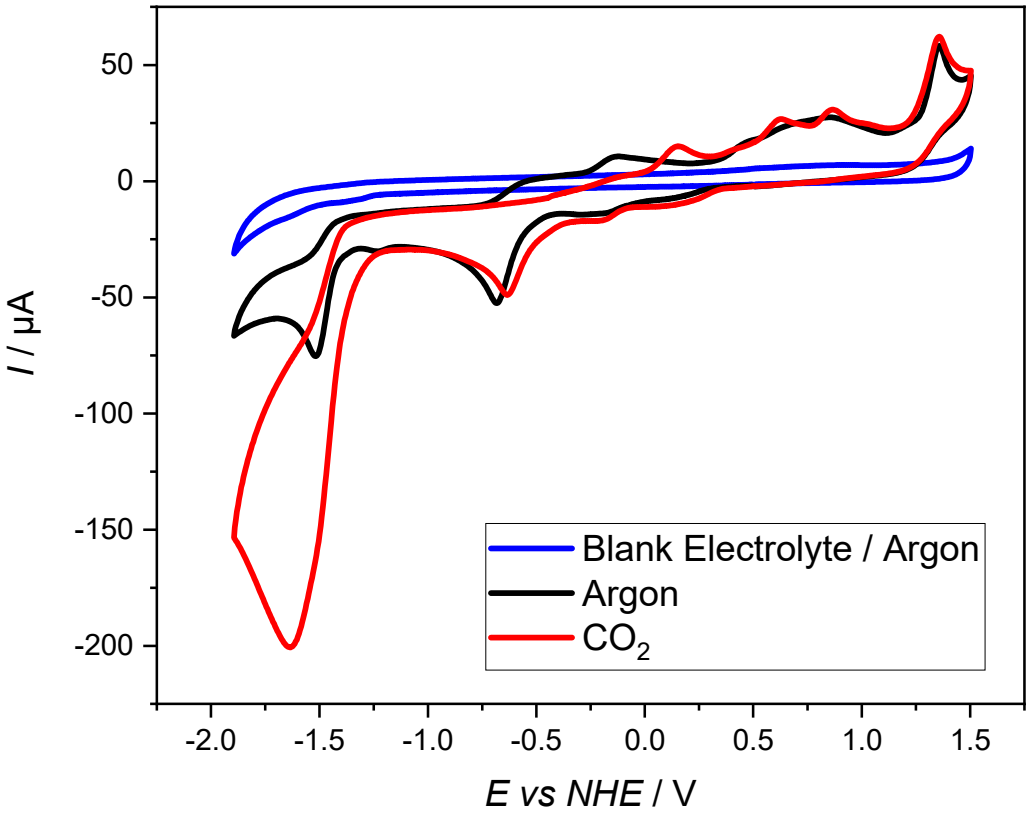


**Figure S93:** Comparison of cyclic voltammograms of $[Ag(4\text{-OMe-BIAN})_2]BF_4$ **Ag4** in acetonitrile with 20% $H_2O$ under argon and $CO_2$ and the blank electrolyte.

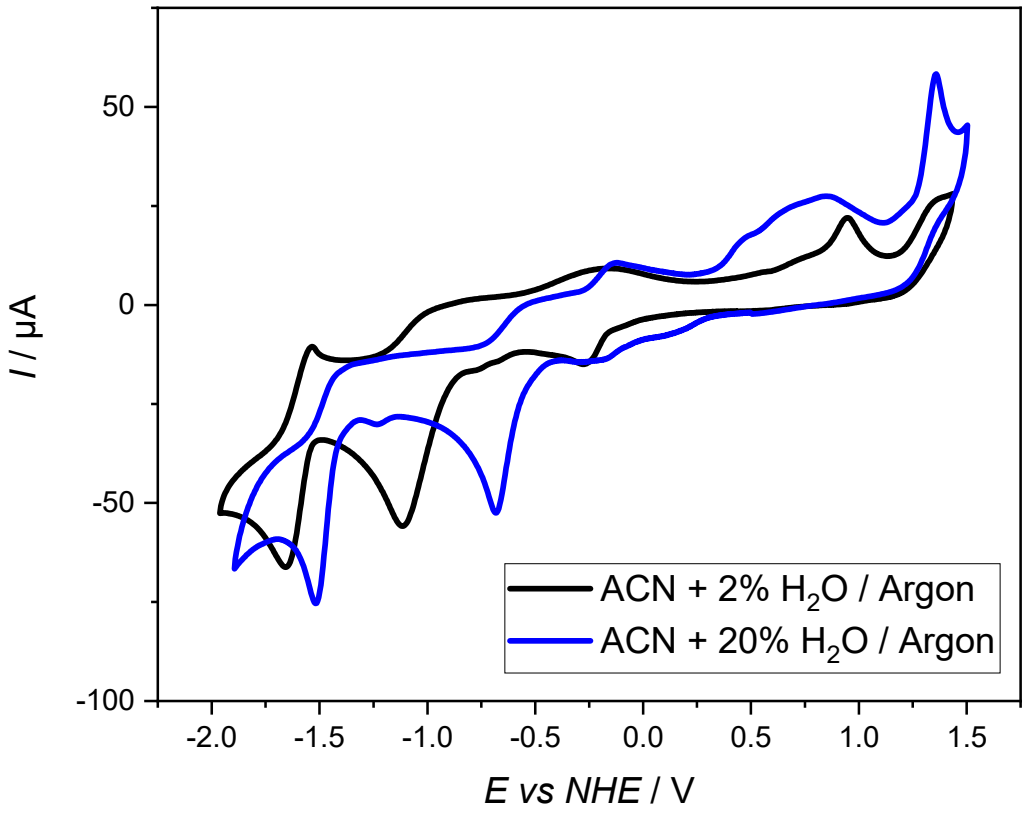


**Figure S94:** Comparison of cyclic voltammograms of $[Ag(4\text{-OMe-BIAN})_2]BF_4$ **Ag4** in acetonitrile with 2% and 20% $H_2O$ under argon.

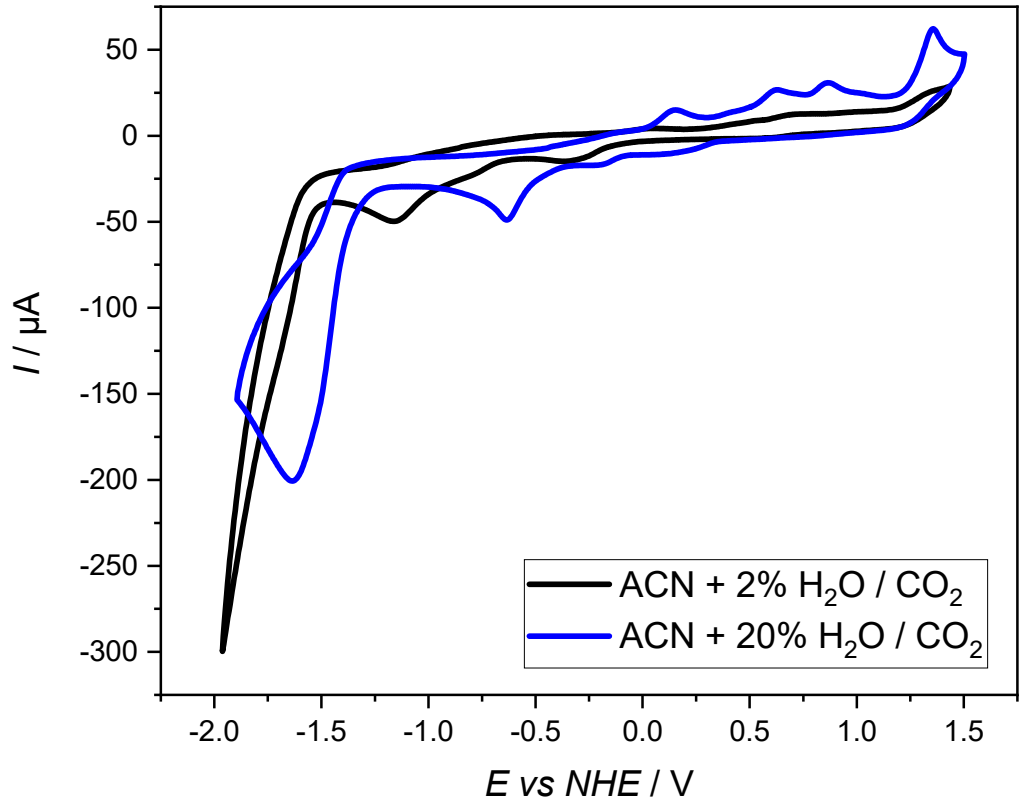


**Figure S95:** Comparison of cyclic voltammograms of $[Ag(4\text{-OMe-BIAN})_2]BF_4$ **Ag4** in acetonitrile with 2% and 20% $H_2O$ under $CO_2$.

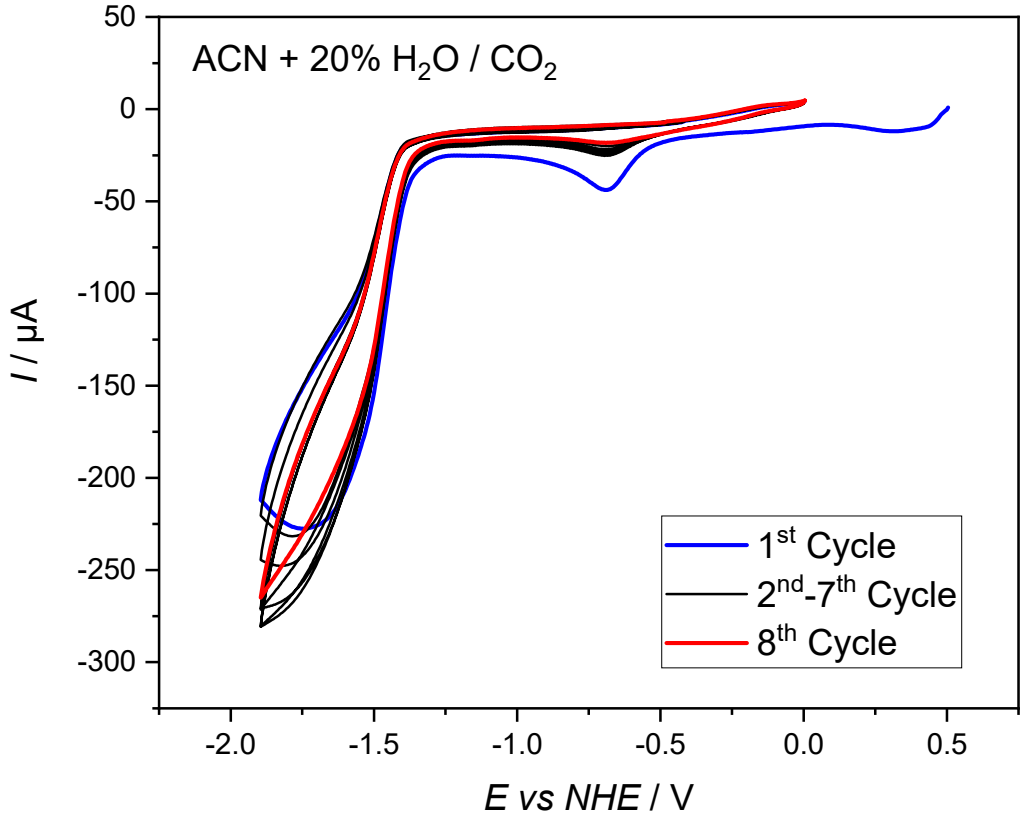


**Figure S96:** Catalytic stability test of the reductive section of $[Ag(4\text{-OMe-BIAN})_2]BF_4$ **Ag4** in acetonitrile with 20% $H_2O$ under $CO_2$.

**[Ag(3,4,5-trimethoxy-BIAN)$_2$]BF$_4$ (Ag5)**

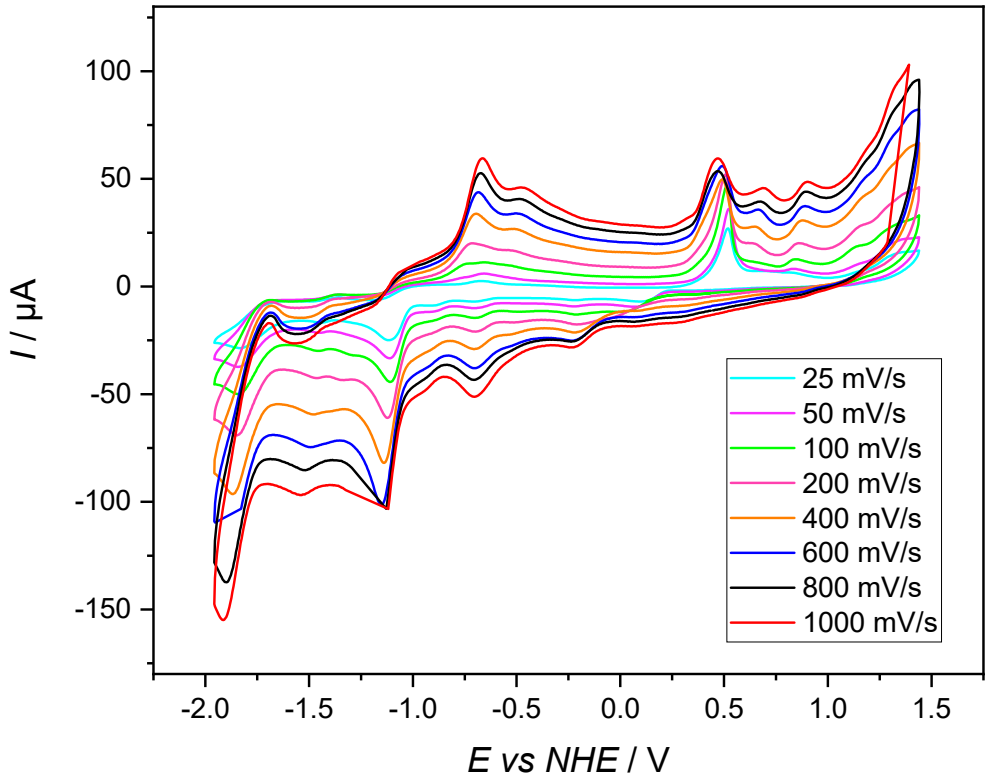


**Figure S97:** Scan rate dependency of [Ag(3,4,5-trimethoxy-BIAN)$_2$]BF$_4$ **Ag5** in acetonitrile under argon. Cut off peaks at high scan rates are caused by limitations of the employed potentiostat.

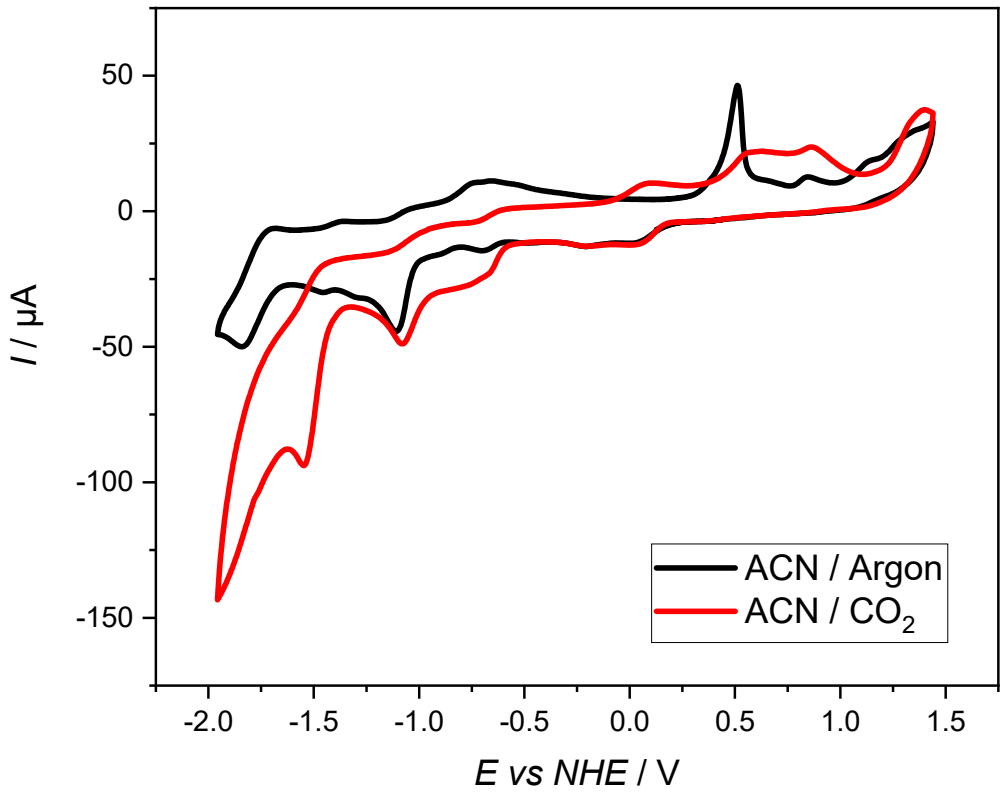


**Figure S98:** Comparison of cyclic voltammograms of [Ag(3,4,5-trimethoxy-BIAN)$_2$]BF$_4$ **Ag5** in acetonitrile under argon and $CO_2$.

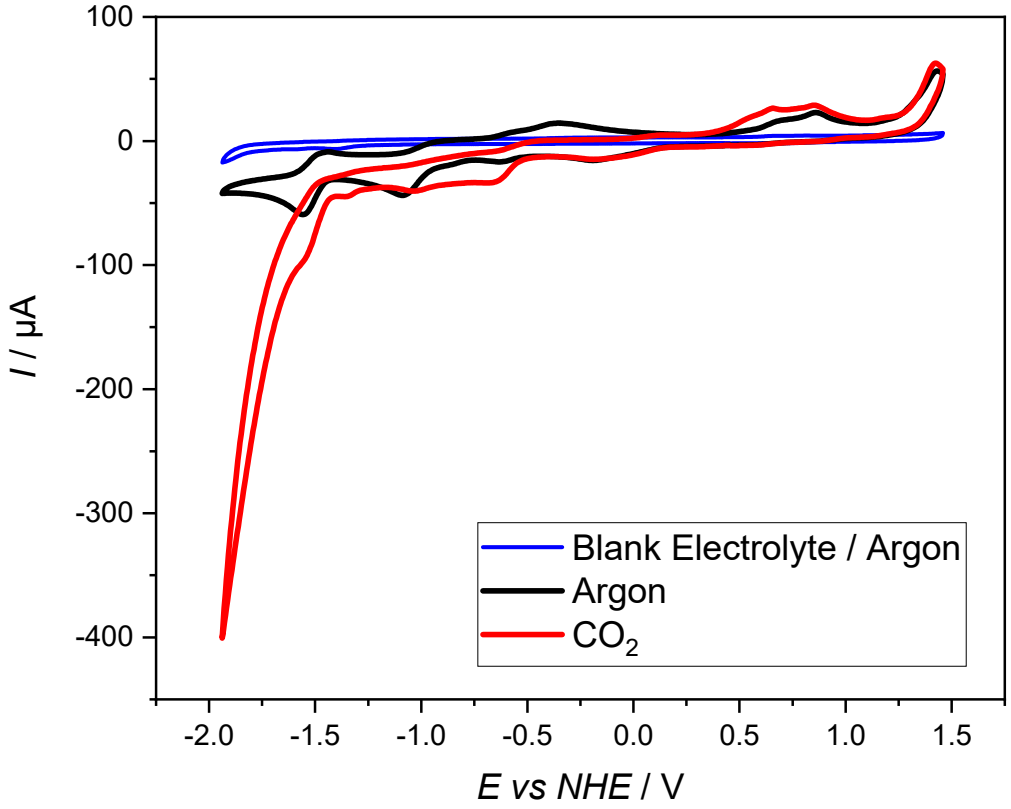


**Figure S99:** Comparison of cyclic voltammograms of $[Ag(3,4,5\text{-trimethoxy-BIAN})_2]BF_4$ **Ag5** in acetonitrile with 2% $H_2O$ under argon and $CO_2$ and the blank electrolyte.

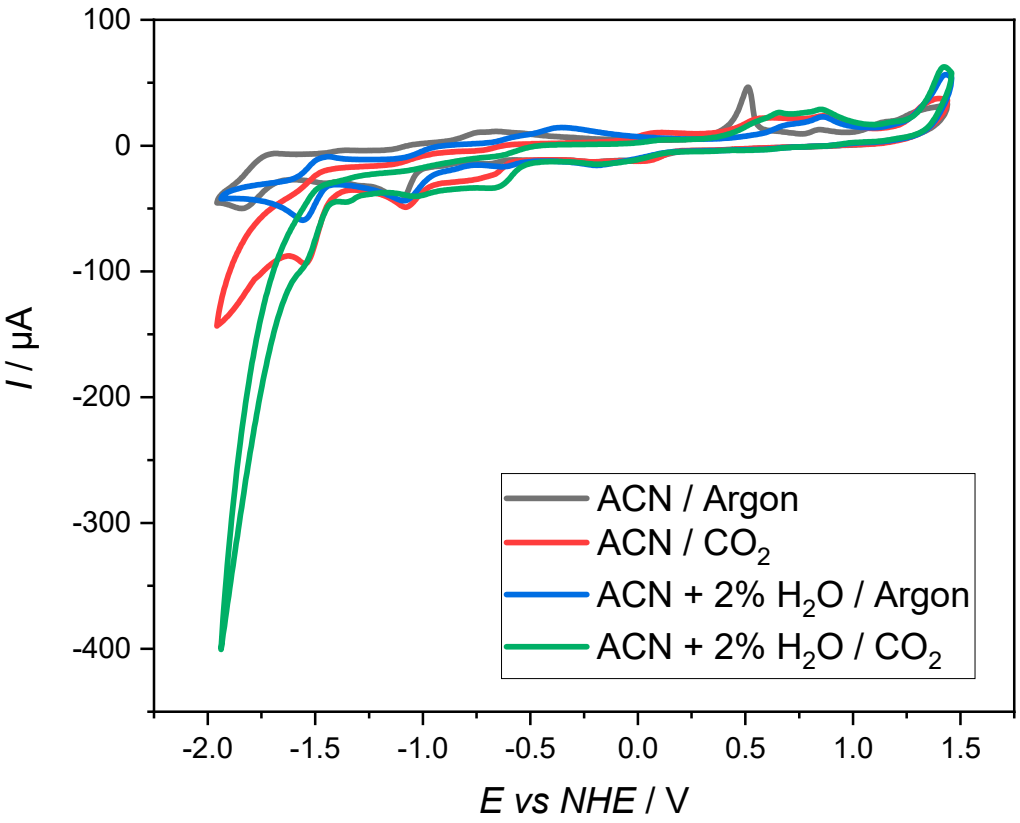


**Figure S100:** Comparison of cyclic voltammograms of $[Ag(3,4,5\text{-trimethoxy-BIAN})_2]BF_4$ **Ag5** in acetonitrile and acetonitrile with 2% $H_2O$ under argon and $CO_2$.

**[Ag(4-diethylamino-BIAN)$_2$]BF$_4$ (Ag6)**

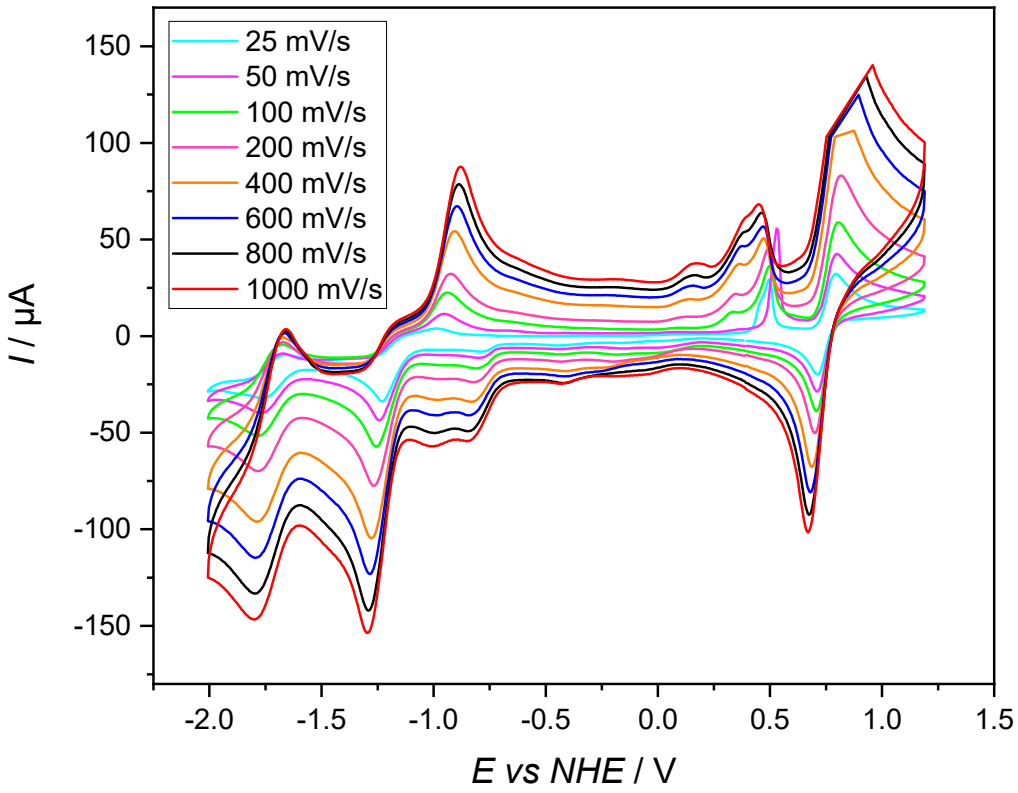


**Figure S101:** Scan rate dependency of [Ag(4-diethylamino-BIAN)$_2$]BF$_4$ **Ag6** in acetonitrile under argon. Cut off peaks at high scan rates are caused by limitations of the employed potentiostat.

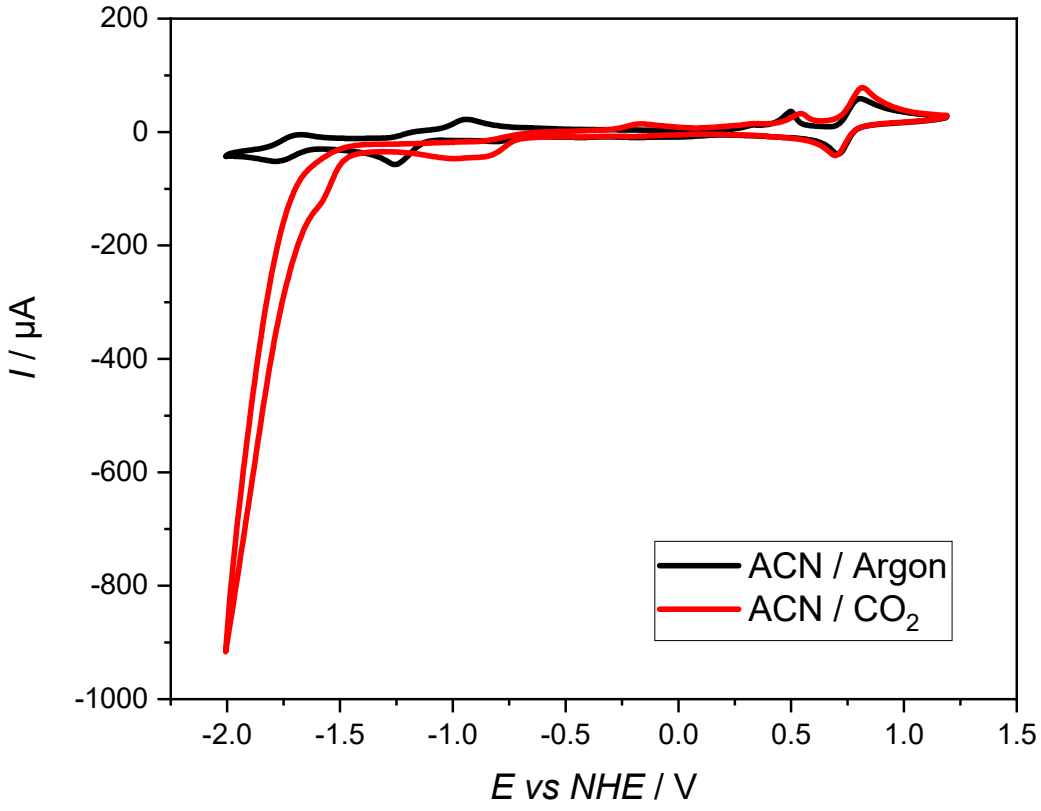


**Figure S102:** Comparison of cyclic voltammograms of [Ag(4-diethylamino-BIAN)$_2$]BF$_4$ **Ag6** in acetonitrile under argon and $CO_2$.

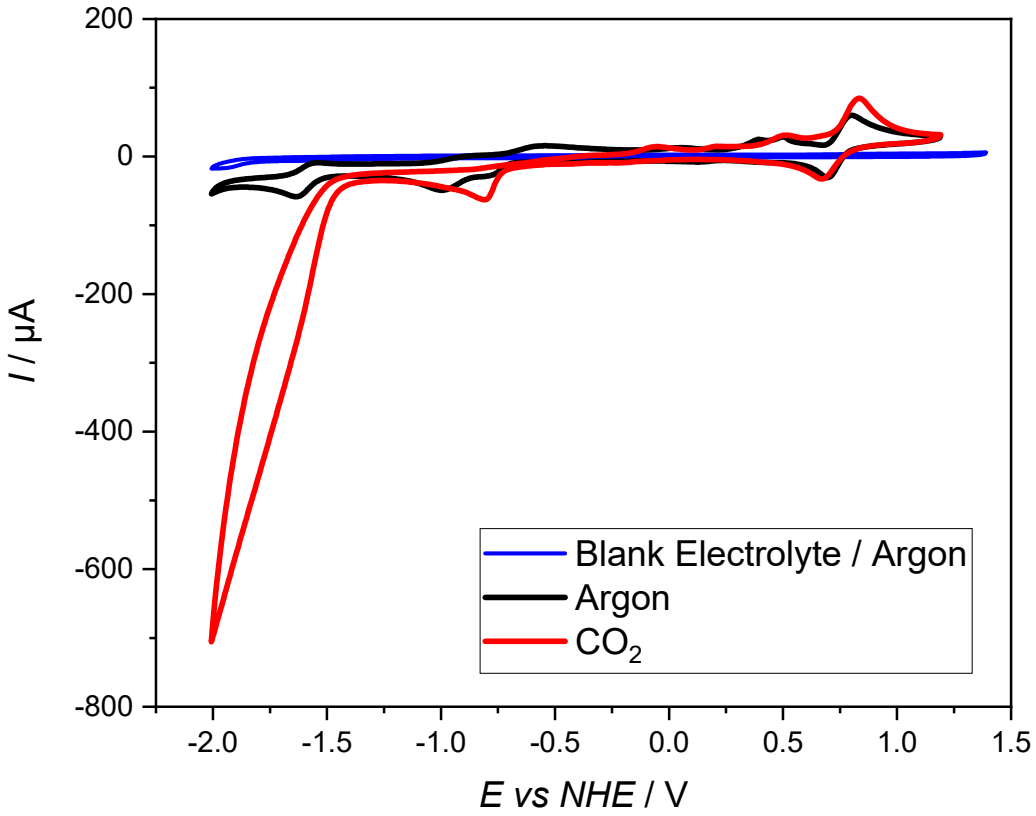


**Figure S103:** Comparison of cyclic voltammograms of $[Ag(4\text{-diethylamino-BIAN})_2]BF_4$ **Ag6** in acetonitrile with 2% $H_2O$ under argon and $CO_2$ and the blank electrolyte.

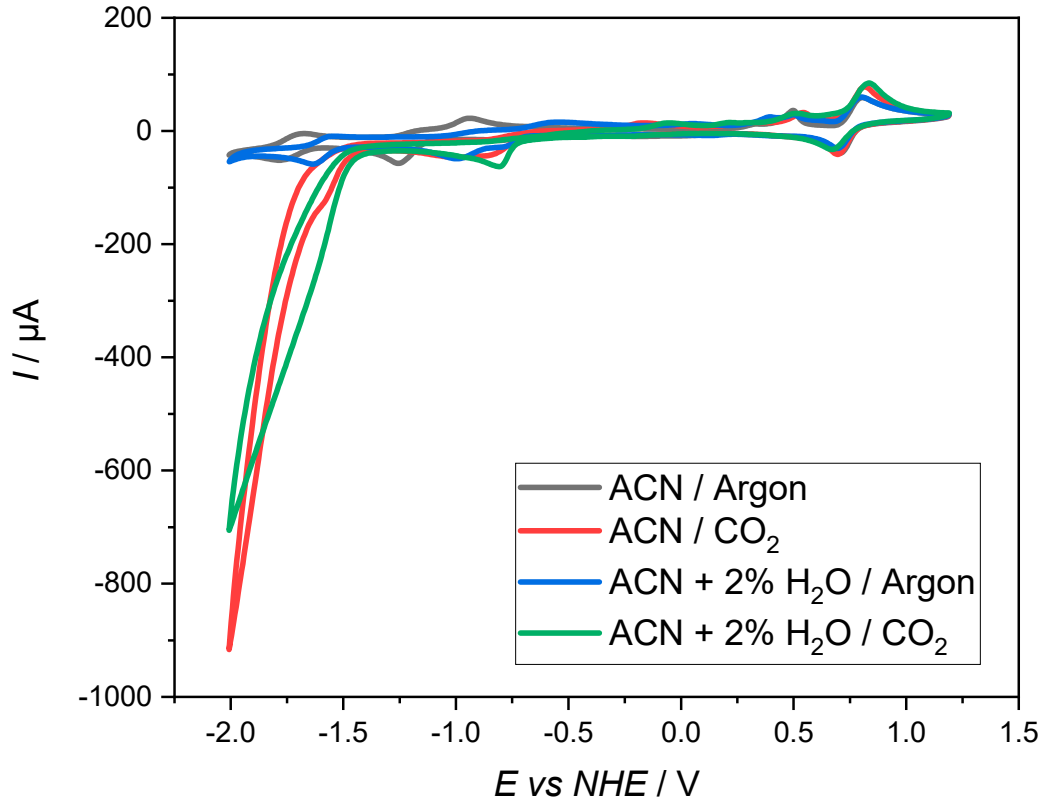


**Figure S104:** Comparison of cyclic voltammograms of $[Ag(4\text{-diethylamino-BIAN})_2]BF_4$ **Ag6** in acetonitrile and acetonitrile with 2% $H_2O$ under argon and $CO_2$.

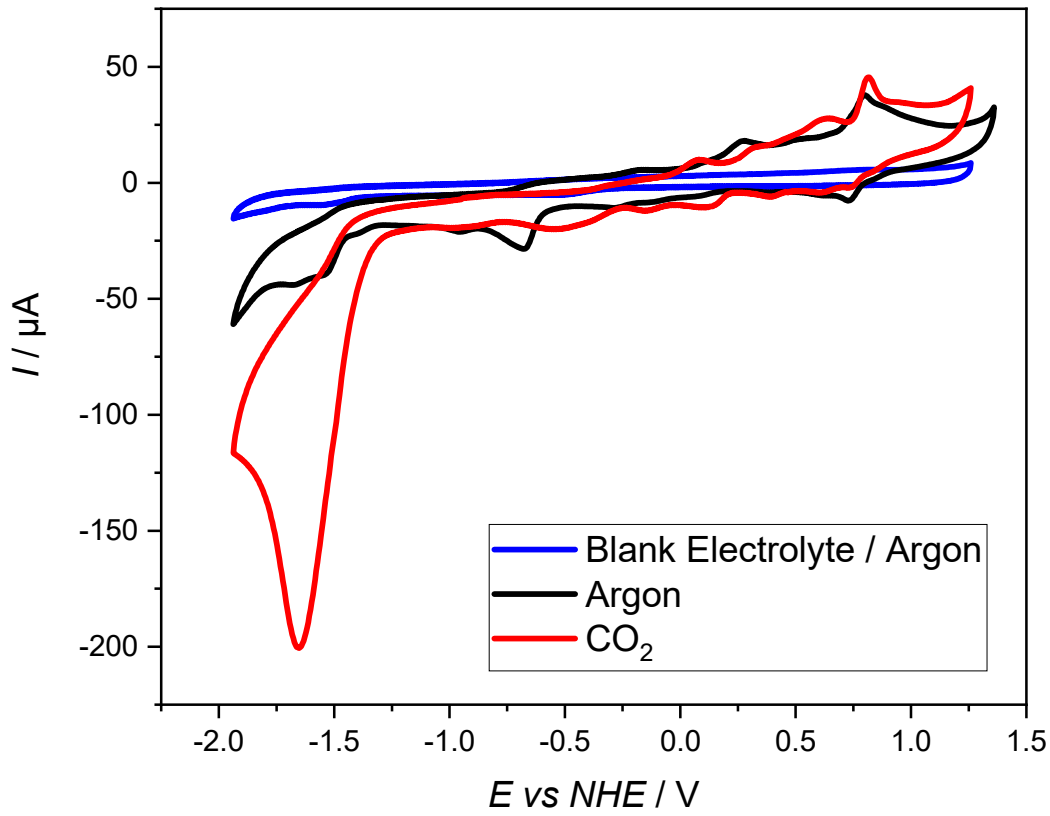


**Figure S105:** Comparison of cyclic voltammograms of $[Ag(4\text{-diethylamino-BIAN})_2]BF_4$ **Ag6** in acetonitrile with 20% $H_2O$ under argon and $CO_2$ and the blank electrolyte.

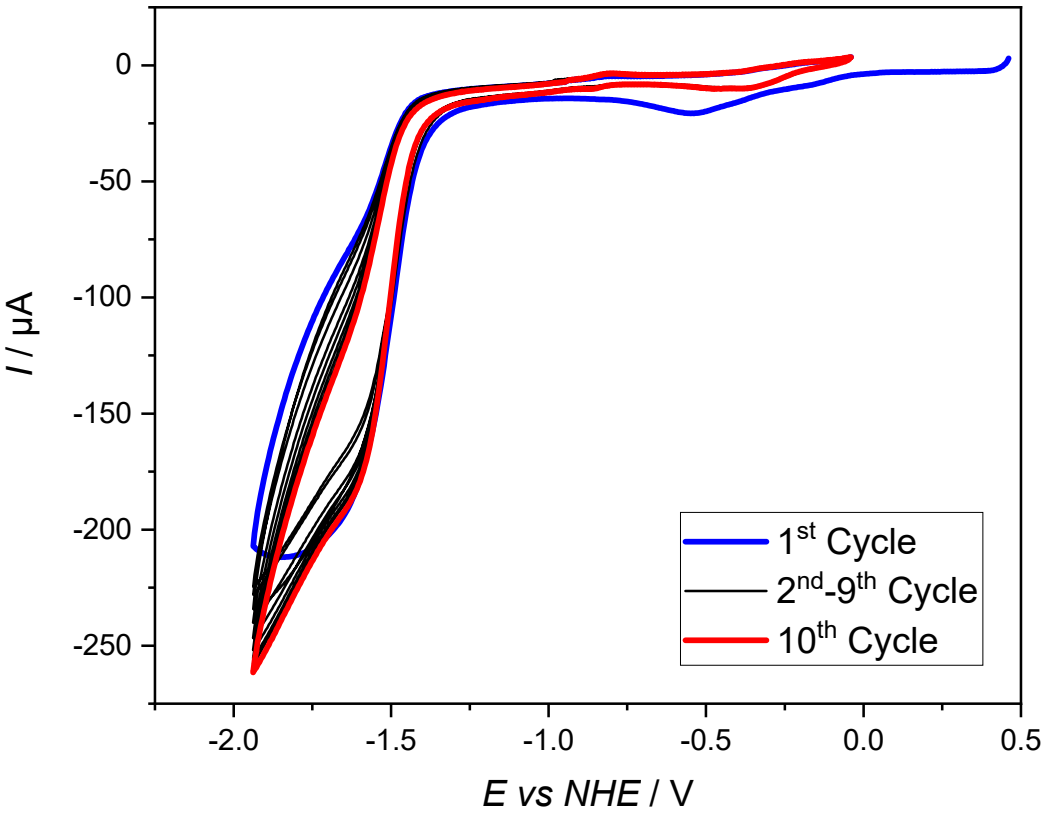


**Figure S106:** Catalytic stability test of the reductive section of $[Ag(4\text{-diethylamino-BIAN})_2]BF_4$ **Ag6** in acetonitrile with 20% $H_2O$ under $CO_2$.

# Heterogeneous Electrochemistry

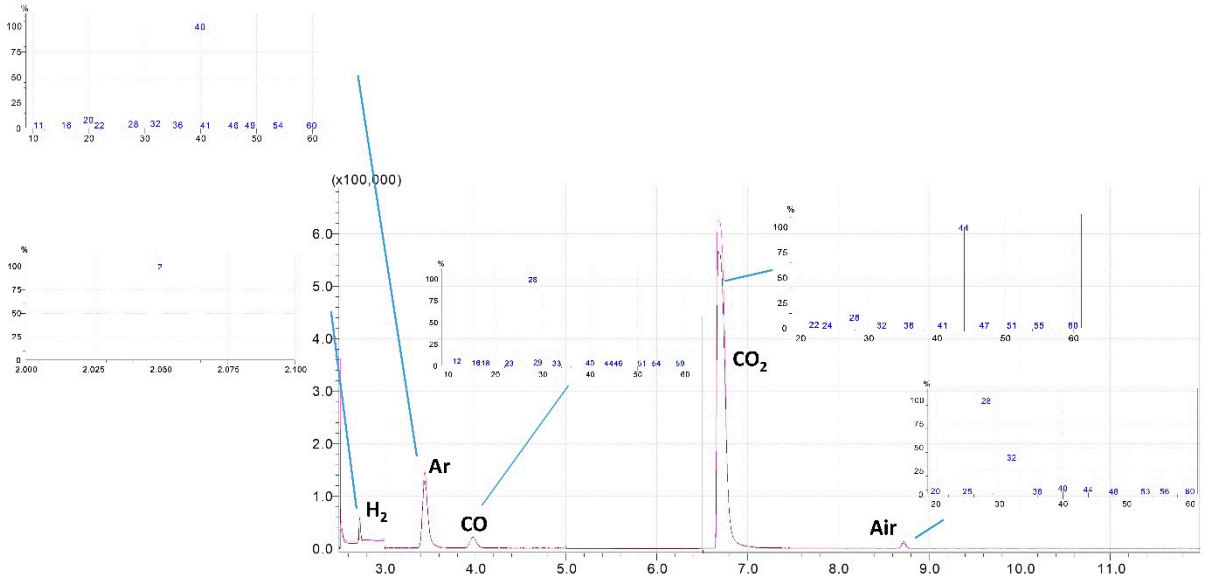


**Figure S107:** Product analysis overlay of the heterogeneous electrochemical measurements at 50 mA $cm^{-2}$. GC chromatogram and corresponding MS spectra.

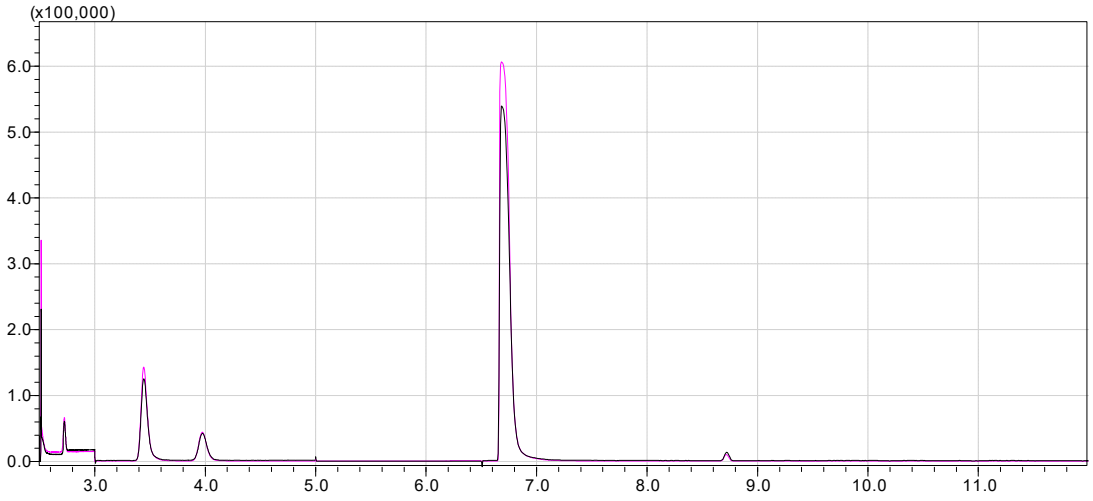


**Figure S108:** Product analysis overlay of the heterogeneous electrochemical measurements at 100 mA $cm^{-2}$. GC chromatogram with peak assignment as displayed in Figure S105.

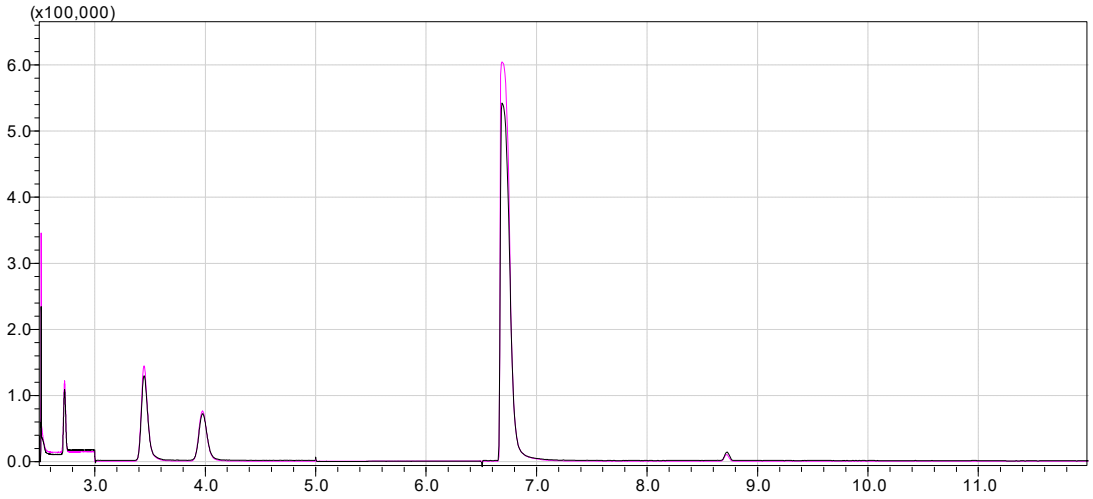


**Figure S109:** Product analysis overlay of the heterogeneous electrochemical measurements at 200 mA $cm^{-2}$. GC chromatogram with peak assignment as displayed in Figure S105.